Electrostatic Lattice Energy of $PbSO_4$, $BaSO_4$, $SrSO_4$ and $CaSO_4$[1]

By Yosio SAKAMOTO

(Received March 1, 1952)

§ 1. Lattice-Energy Problem on the Complex Ionic Crystal

The lattice energy of ionic crystals of simple composition and structure has been studied fairly completely, though this subject still leaves room for more thorough consideration at least in some particular aspects, for instance, in the strict application of thermodynamics. On the contrary, few researches have been made into ionic crystals of so complex a structure that the degree of their symmetry is small or their atoms form into partial groupings. One of the chief purposes of the author is to study these complex ionic crystals, especially to elucidate[2] physicochemical properties of radical ions, the properties not a few of which (e. g., the energies fo hydration) have remained quite obscure.

Among the ionic crystals whose lattice energies have so far been evaluated by means of computing lattice sums,[3] those which belong to the rhombic system have the smallest degree of symmetry. No more than two studies[4][5] have been made on these rhombic crystals, which, moreover, contain radical ions. In the one case,[4] however, the treatment seems to be unsatisfactory, and in the latter[5] the spatial arrangement of the ions is orderly enough.

On the other hand, the ionic arrangement in the rhombic crystals of lead sulfate, in which Dr. Kobayashi[2] was interested, and of the alkaline earth sulfates is relatively irregular and complex. So, first, for the rectangular crystal lattice of any complexity a set of expressions of Madelung's coefficient[6] is derived, and then verified in two simple cases by means of numerical application. The mode of calculation based on this set of expressions will produce effectually an exact and precise result with minimum effort, even for the cases considerably complicated.

§ 2. A Set of Expressions for the Calculation of Madelung's Coefficient M_d

2.1) The crystal lattice in general.[7]—The electrostatic potential energy per mol., Φ_1, of a crystal lattice is expressed by

$$\Phi_1 = -Ne^2 M_d / d \tag{1}$$

where d is a quantity proportional to length, and M_d Madelung's coefficient[6] referred to d. M_d may be represented, through Ewald's method,[8] by a set of expressions suitable for the calculation of its value, thus:

$$M_d = -\{(d/\delta)^3 L/\pi + \bar{Y} + Y/s - \varepsilon d/\sqrt{\pi}\} \sum_h z_h^2;$$

$$L = \mathop{\mathrm{S}'}_{\bar{l}} w_l L_l,\ L_l = e^{-\kappa\lambda_l}/\lambda_l,\ \kappa = (\pi/\varepsilon d)^2,$$

$$\lambda_1 = |\vec{q}^1 d/2\pi|^2,\ w_l = 1 + (2/s)\bar{X}_l,$$

$$\bar{X}_l = (\nu/\sum_h z_h^2) \sum_{(kk')}' z_k z_{k'} \cos(\vec{q}^l \vec{r}_{kk'});$$

$$\bar{Y} = \mathop{\mathrm{S}'}_{\bar{l}} \bar{Y}_l,\ \bar{Y}_l = G(\varepsilon d\bar{\eta}_l)/\bar{\eta}_l,\ \bar{\eta} = |\vec{r}^l|/d;$$

$$Y = (\nu/\sum_h z_h^2) \mathop{\mathrm{S}}_{l} \sum_{(kk')}' z_k z_{k'} Y^l_{kk'},$$

$$Y^l_{kk'} = G(\varepsilon d\eta^l_{kk'})/\eta^l_{kk'},\ \eta^l_{kk'} = |\vec{r}^l_{kk'}|/d;$$

$$s = \sum_k 1 = \sigma \sum_h 1 = \sigma\nu,\ h = 1, 2, \cdots\cdots, \nu;$$

$$\bar{l} = (\bar{l}_1, \bar{l}_2, \bar{l}_3),\ \bar{l}_i = -l_i;$$

$$i = 1, 2, 3; \tag{2}$$

(1) (a) "Lattice Energy of $PbSO_4$, $BaSO_4$, $SrSO_4$ and $CaSO_4$." Unpublished thesis, Hirosima Univ., 1942; revised and enlarged, 1946—51, ("Physical Chemistry of a Radical Ion SO_4^{--},") Jan. 1951—; (b) "Lattice Energy..... I. Electrostatic Potential Energy." Oral report, *Nippon-Buturi-Gakkai.Si* **4**, 64 (1949).

(2) This intention was suggested to me in 1942 by the late Prof. Yozo Kobayashi (1895—1945).

(3) In regard to ionic crystals with radical ions several reports have been issued since 1926 on the (electrostatic) lattice energy whose values were obtained by means of computing lattice sums; these radical ions are: CO_3^{--}, NO_3^-, BO_3^{---}, HF_2^-, N_3^-, BF_4^-, NH_4^+, CN^-, OH^-, SH^-, SeH^-, C_2^{--}, O_2^-, and O_3^-. On the other hand, Kapustinskiĭ (1933, 1943) offered a general expression that gives, without performance of lattice summations, a rough value of the lattice energy, and for radical ions it has been utilized since 1935 by several Soviet investigators; above all, extensively by Yatsimirskiĭ since 1947.

(4) B. Y. Oke: (a) *Proc. Indian Acad. Sci.*, **4A**, 1 (1936); (b) ibid., **5A**, 326 (1937).

(5) T. Matsuhara [-bara] and T. Nagamiya, *Sci. Papers Osaka Univ.*, No. 14, pp. 17 (1949).

(6) As for a crystal with the structure of small degree of symmetry the constancy of the so-called Madelung's constant is not perfect; accordingly, it might be proper to adopt the term "coefficient" (or "factor") in general as a substitute for the term "constant."

(7) Cf.: M. Born, "Atomtheorie des festen Zustandes," 1923, from which are taken several symbols used here: δ, a_l, s, $\vec{r}^l_{kk'}$ etc., l_i etc., S, Σ, S′ etc., $\vec{q}^l$, — on Y, ε, and $G(x)$. Notice: C. N. Wall, *Phys. Rev.*, **36**, 1243 (1930); R. H. Canfield, ibid., **40**, 1034 (1932); W. J. Taylor, *ibid.*, **77**, 763 (1950); G. Molière, *Z. Krist.*, **101**, 383 (1939).

(8) P. P. Ewald, *Ann. Physik.* [4] **64**, 253 (1921).

CHEMISTRY HALL LIBRARY

where h ("intramolecular index") and ν correspond to k and s, resp., σ is the number of the "molecules" in a cell, z_h the valency of an ion as particle h, and S with $\bar{l}$ and $\sum$ with (kk') denote such a summation that a pair of indices l & $\bar{l}$ and a pair of permutations of indices kk' & $k'k$, resp., be counted once only.

In the case of a z-z-valent compound it is suitable for comparison to introduce a derived quantity M_d/z^2. The linear size, χ, of a molecule may be defined by

$$\chi = (V/N)^{1/3} = \delta/\sigma^{1/3} \tag{3}$$

where V is the molal volume; and the adoption of $M\chi$ as M_d is also valuable in some cases.

2.2) The rectangular crystal lattice.—The preceding set of expressions of M_d may be specified so as to fit to the rectangular crystal lattice in the following form:

$$\delta^2 = \prod_l a_l;\quad L = \frac{1}{2}\mathop{\mathrm{S}'}_{\mathring{l}} c_l L_l + (2/\delta)\mathop{\mathrm{S}'}_{\bar{l}} X_l L_l,$$

$$\lambda_l = (d/a_1)^2 \sum_l (a_1/a_l)^2 l_l^2,$$

$$X_l = (\nu/\sum_h z_h^2) \sum_{(kk')}{}' z_k z_{k'} \cos 2\pi \sum_l (k_l - k_l')l_l;$$

$$\bar{Y} = \frac{1}{2}\mathop{\mathrm{S}'}_{\mathring{l}} c_l \bar{Y},\quad \bar{\eta} = (a_1/d)\{\sum_l (a_l/a_1)^2 l_l^2\}^{\frac{1}{2}};$$

$$\mathring{\eta}_{kk'} = (a_1/d)\{\sum_l (a_l/a_1)^2 (k_l - k_l' + l_l)^2\}^{\frac{1}{2}};$$

$$\mathring{l} = (\mathring{l}_1, \mathring{l}_2, \mathring{l}_3),\ \mathring{l}_l = |l_l|;$$

$$c_l = 2^\mu,\ \mu = 0, 1, 2, 3; \tag{4}$$

where S with $\mathring{l}$ denotes such a summation that a set of like cells with one and the same value of $\mathring{l}$ be counted once only, c_l is the number of these like cells in a set, and μ the number of the non-zero components of $\mathring{l}$.

In case that X_l depends solely on the absolute values (regardless of the signs) of the components of l, i. e.,

$$X_l = X_l(\mathring{l}) \tag{5}$$

further simplification may be brought about, thus

$$L = \frac{1}{2}\mathop{\mathrm{S}'}_{\mathring{l}} c_l w_l L_l \tag{6}$$

In § 3.2 and 4 the numerical calculation of $M_\delta (= Ma_1\delta/a_1)$ is made in the two selected cases:

$$(1)\quad \varepsilon = \varepsilon^0 = \pi/d \qquad (2)\quad \varepsilon = \varepsilon' = \pi/d\sqrt{2}$$
$$\text{with } d = a_1 \text{ (but finally } d = \delta) \tag{7}$$

§ 3. Verification of the Expressions of M_δ

3.1) The cubic case NaCl.[9a]—After the expressions of M_δ for the cubic crystal lattice had been derived from those given in § 2, they were applied to the case of NaCl, the numerical calculations with the three selected values of ε producing for M_δ the values $3.495129189266_{48\pm17}$, $\cdots\underline{6}3_{24\pm48}$, and $\cdots\underline{6}3643_{25\pm17}$ molec^{-1}. cell$^{-1/3}$. These values coincide not only with each other perfectly but also with Emersleben's corresponding one practically. This fact seems to support the reliability of all the above-mentioned expressions for M_d or M_δ and of the mode of handling them.

3.2) The rhombic case $CaCO_3$.[9b]—The expressions of M_δ given in § 2 were applied to the rhombic case of $CaCO_3$, and the numerical calculations (cf. Eq. 7), being carried out by use of the same data for the crystal structure as used by Oke[4] but in a fashion somewhat different from his, produced for M_δ the values 12.84723_9 and $\cdots\underline{3}_3$ molec^{-1}. cell$^{-1/3}$. The fact that they perfectly coincide will be satisfactory. While, on the other hand, the agreement between each of them and Oke's corresponding one is not satisfactory, since there is a discrepancy of 11% between them. This poor agreement, however, was found[9c] to be caused by the inaccurateness in the value of Oke.

§ 4. Calculation[10] of Madelung's Coefficient M_δ

With the two applications in § 3 as preliminary, the set of expressions of M_δ is now applied to the crystals of the four sulfates in which the author has become interested. These four cases shown in the title are designated by a', a'', a''', and b, resp.

4.1) Data for the crystal structure[11][12]—

State: 0—30° C, 1 atm. Rhombic; a: $BaSO_4$ type, b: $CaSO_4$ type; $\sigma = 4$ molec. cell^{-1};

$\nu = 2$ part. molec^{-1}—$Me^{++} + SO_4^{--}$[13] (8)

In Case a, an approximate fraction is selected for the value of each parameter, and the adopted values are:[14]

$$v \approx \frac{24}{72},\quad u \approx \frac{23}{72},\quad v' \approx \frac{50}{72},\quad u' \approx \frac{68}{72} \tag{9a}$$

(9) For details, see the three papers (a, b, and c) in *J. Sci. Hiroshima Univ.*, Ser. A, **16**, No. 3 (1953), where (a) Emersleben's and (c) Oke's works are touched upon with comment.

(10) For details, see *J. Sci. Hiroshima Univ.*, Ser. A, **16**, No. 3 (1953).

(11) Mainly, R. W. G. Wyckoff: (a) "The Structure of Crystals," 2. ed., 1931—see also (b) "Crystal Structures," Vol. II, 1951.

(12) The values of $a:b:c$ are taken from: "J. D. Dana: The System of Mineralogy," 6th ed., 1915. For its 7th ed., Vol. II, 1951, see Note 4b of Ref. 10.

(13) Here, the electricity is assumed to be located at the center of SO_4^{--} (i. e., of its S) as well as of Me^{++} as a point charge.

(14) The magnitudes of the error thereby caused are: -42, 36, -3, 14; -55, 14, -3 124; and -55, -14, -3, 14 (resp.) $\times 10^{-4}$. If we adopt $u' \approx 67/72$ instead, each last number becomes -124, -14, or -124, resp.

Table 1

i					1, +2					2, −2
ii	1		2		3		4			5–8
iiia	$\frac{1}{4}$, v, u		$\frac{3}{4}$, $\bar{v}$, $\bar{u}$		$\frac{1}{4}$, $\frac{1}{2}-v$, $\frac{1}{2}+u$		$\frac{3}{4}$, $\frac{1}{2}+v$, $\frac{1}{2}-u$			(v', u')
iiib	u, $\frac{1}{4}$, 0		$\bar{u}$, $\frac{3}{4}$, 0		$\frac{1}{2}+u$, $\frac{1}{4}$, $\frac{1}{2}$		$\frac{1}{2}-u$, $\frac{3}{4}$, $\frac{1}{2}$			(u')
Case	a′		a″		a‴				b	
iv	1:1.28939:1.57032		1:1.31359:1.63040		1:1.28005:1.55790				0.89325:1:1.0008	
v	0.33_{75} 0.31_{56}	0.69_{47} 0.94_{70}	0.33_{88} 0.31_{50}	0.69_{47} 0.93_{20}	0.33_{88} 0.32_{68}	0.69_{47} 0.94_{80}			0.65	0.15

i: h, z_b. ii: k. iii: Atomic positions. iv: $a_1{:}a_2{:}a_3$ (a:) $= b^*{:}c^*{:}a^* = b{:}c{:}2a$ or (b:) $= a^*{:}b^*{:}c^* = a{:}b{:}c$, where a^*, b^*, c^* are the (röntgenoscopical) lattice constants and $a{:}b{:}c$ is the (morphometrical) axial ratio. v: Parameters (a:) $\frac{vv'}{uu'}$ or (b:) uu'.

In Case b, without artificial approximation,

$$u=\frac{13}{20},\quad u'=\frac{3}{20} \tag{9b}$$

4.2) Calculated values of M_δ (to be amended in §6).—Each couple (cf. Eq. 7) of numerical values for M_δ obtained by calculation is given in Table 2. The coincidence between them seems

Table 2

M_δ	$PbSO_4$	$BaSO_4$	$SrSO_4$	$CaSO_4$
Case 1	13.16377_8	13.18779_4	13.15651_2	13.50363_5
〃 2	$\ldots75_8$	$\ldots78_5$	$\ldots51_0$	$\ldots62_7$

so perfect that they conform to the verification of accounts in Ewald's method. Every one of these four values might be acceptable, from the standpoint assumed in the author's other paper,[15] as of reasonable magnitude.

§5. Estimation of the Uncertainty in the Calculated Value of M_δ

5.1) General remark.—The error with which the value of M_δ calculated in this mode is expected to be accompanied may be analyzed—as mentioned in Ref. 9b, §2.3—into three sorts of errors, which are to be discussed in some detail.

5.2) The error from computation.—The main error (i) of computation comes from that reduction of the decimal to its approximate fraction which is done in Eq. 9a concerning the parameters of atomic positions. A rough value for it has been merely indirectly estimated to be 0.2%.[16] On the other hand, the ordinary computational error (ii) must be only subordinate, because the two calculated values for M_δ coincide to the extent of 10^{-4}%.

5.3) The error from theory.—Several assumptions underlying the method of this calculation are to be mentioned here. The matters concerning the grain size, the imperfection of a crystal (such as the mosaic structure and the lattice defect), and the thermal motion of the constituent particles may be insignificant in ordinary cases; the question of chemical purity of the material will rather be regarded as a matter of experiment.

On the other hand, several difficulties are encountered when we consider the following aspects peculiar to our subject. The character of the bonds between ions in these crystals is—though mainly ionic—in a fair measure, covalent owing to the small degree of symmetry in the crystal structure and of uniformity in the ionic distribution, not a little polarizability of the radical (sulfate) ion in particular, the bivalency of the ions, and the great polarizing influence by lead ion and that by calcium ion. Yet, this crystal system retains rectangular symmetry, the distribution of the neighboring anions around a cation (or the reverse) is passably uniform and the coordination number[17] of an ion is no less than some value between 5 and 7, the deformability of sulfate ion is by no means great,[18] and the shape of sulfate ion is of regular tetrahedron, though slightly distorted. Consequently, the assumption[15] made about the distribution of electric charges, i. e., the purely ionic bonding between point charges (with certain integral multiples of the electric elementary quantum) at the assigned sites, will be practically not far from reality. Furthermore, it is to be noticed that the electrostatic potential energy of a crystal lattice may be regarded as a quantity *defined*, in a

(15) Ref. 9c, Art. V.

(16) In Case b, which is free from this error and in which the crystal structure bears a close resemblance to that in Case a, another calculation has been executed with the values $u-\frac{1}{2}=u'=0.1$ (besides, 0, 0.05, 0.2, and 0.25), producing for M_δ the numerical value 12.9941_1. Certain considerations have then been made with such materials as Eq. 9b, Note 14, and Table 7 of Ref. 10 (including the sub-table for $CaSO_4$ with $u'=0.1$) and with a certain possible supplementary assumption.

(17) In these crystals we cannot definitely assign to this quantity any discrete number. Cf. Table 6 of Ref. 10, where γ_p is proportional to the interionic distance and (a) the five or (b) the three $-\frac{1}{2}d_{\nu\nu'}{}_{p'}$'s are, so to speak, the "components" of the coordination number.

(18) "[Geiger-Scheel.] Handbuch der Physik," Bd. XXIV/2 (2. Aufl.), 1933, Kap. 6 (by H. G. Grimm and H. Wolff), Ziffn. 61, 64—66, esp. Tab. 62.

certain sense (so far as the present state of our knowledge is concerned), on the basis of an assumption such as mentioned above, the possibility[19] of the subsequent step to approximation being left to a later estimation of the whole potential energy (or, further, the total energy in the thermodynamic signification).

The magnitude of the error originating from theory is, accordingly, somewhat indefinite, and so it is difficult to be estimated; still the author will give it a value 0.5%, if necessary.

5.4) The error from experiment.—M_δ depends upon the axial ratio (a:b:c) and the parameters of atomic positions (briefly, parameters). These quantities vary with temperature and pressure and, from a practical viewpoint, with chemical purity (and certain physical matters mentioned in Art. 3). The error due to these variations and that due to measurement constitute together the total experimental error.

In regard to variation in the magnitudes of the parameters we have as yet no information, while the magnitudes of the variabilities of a:b:c are known for some of these crystals and are shown in Table 3.[20]~[25] It will be seen from this table that any datum with such specification as "at some ordinary temperature and pressure" suffices for our present purpose and, at the same time, that the experimental error in a:b:c of No. 1 is less than 0.3%. The effect of uncertainty in a:b:c upon M_δ is not simple in nature and might scarcely be estimated exactly unless we execute several sets of calculations. Nevertheless, the author will try to form a very rough estimate of it.

Now the three crystals of the barite type have been considered, in Eq. 9a, to have the same value for each parameter, and so the distinction between these crystals will remain solely in a:b:c. These calculations may, therefore, be regarded as having been made on such a crystal of one and the same compound as with three different experimental values for a:b:c. There is then constructed a table (Table 4a) that shows the relation between M_δ and a:b:c. It is seen from this table that, for this special case (in which a/b and c/b alter alike in both magnitude and sign), the quotient $2M_\delta/\{(b/a)\Delta(a/b)+(b/c)\Delta(c/b)\}$ is at most $ca.$ 0.07.[24]

Table 3

No.	a′	b
1	0.78516:1:1.28939	0.89325:1:1.0008
2	0.7852 (−62°) 1.2891	0.8911 (−64°) 0.9996
3	0.7894 (514°) 1.2870	0.8996 (500°) 1.0025
4	7.3 −3.6	15.1 5.5
	a″	a‴
1	0.81520:1:1.31359	0.77895:1:1.28005
2	0.8161 (−60°) 1.3121	0.7785 (−62°) 1.2821
3	0.8124 (570°) 7.3047	0.7794 (550°) 1.2780
4	−5.9 −11.7	1.5 −6.7
5	1.431 2.252 1.490†	1.920 1.851 1.490
6	−6.7 −10.0	0.54 −6.4
7	5.221 6.757 5.194	6.222 4.406 4.462
8	1.25 2.05	−1.41 −0.072
9	$0.81\frac{6}{2}$:1:1.31$\frac{5}{0}$	$0.7\frac{9717}{6964}$:1:1.$\frac{30010}{25506}$
10	0.8146 :1:1.3119	0.78093:1:1.28324††
11	0.81439:1:1.31223	——

1: Axial ratio (a. r.) adopted in Table 1. 2, 3: A. r. at the temp. indicated. 4, 6: Mean increments per deg. in a. r., in 10^{-6} deg.$^{-1}$. 5: Coeffs. of linear thermal expansion at 0—100° C, in 10^{-5} deg^{-1}. 7: Linear compressibilities at 23—26° C, 0 atm., in 10^{-7} bar^{-1}. 8: Increments per bar in a. r., in 10^{-7} bar^{-1}. 9: A. r. of various minerals. 10: A. r. of a pure mineral. 11: A. r. from a^*, b^*, c^* adopted by Wyckoff. † For the new data, see S. S. Sharma, *Proc. Indian Acad. Sci.*, **33A**, 283 (1951). †† See also Note 4b of Ref. 10.

Table 4a

No.	(1)	(2)	(3)	(4)	(5)	(6)	(7)	(8)
$BaSO_4$ ···					···			
B—P	300, 242		376, 186	281		240	18.2	0.065
$PbSO_4$ ···					···			
P—S	62, 93		80, 73	76		73	5.5	0.072
$SrSO_4$ ···					···			

1: A. r. in Table 3, No. 1. 2: Differences in a. r. between the crystals, as indicated by B—P or P—S. 3: Quotients (2)÷(1). 4: Arithmetical mean of the quotients in (3). 5: M_δ in Table 2. 6: Difference in M_δ similar to (2). 7: Quotient (6)÷(5). 8: Quotient (7)÷(4). In Nos. 2-4, 6, and 7 the unit is 10^{-4}.

(19) E. g., the mode of treatment in Ref. 5.

(20) Nos. 2, 3. R. Kolb's, through *Chem. Zentr.*, **1911**, I, 1317.

(21) Nos. 5, 9, 10. "Gmelins Handbuch," 8. Aufl. The values for a^*, b^*, c^* recommended in this book give 0.81342 : 1 : 1.31066.

(22) No. 7. Values calculated by the present author from: P. W. Bridgman, *Proc. Am. Acad. Arts Sci.*, **77**, 187 (1949).

(23) No. 11. Ref. 11b. In this book Walton and Walden's work is cited; their values for a^*, b^*, c^* of a pure artificial crystal at 24—30°C give 0.81326 : 1 : 1.31124.

(24) In a preliminary calculation (Case α) I adopted for a:b:c the values derived from those of the lattice constants quoted in Ref. 11a. The values (Case α) that correspond to those (Case β) in Table 4a are: No. 1—0.816630 : 1 : 1.316079, 0.785316 : 1 : 1.288104, 0.779851 : 1 : 1.276119; No. 5—13.188$0_8$, 13.1637$_7$, 13.1572$_8$; No. 8—0.063, 0.061; and for $CaSO_4$ No. 1—0.893525 : 1 : 1.001439; No. 5—13.50251. If we construct a table which is similar to Table 4a and in which a combination $\beta\alpha$ is taken for each crystal, the values corresponding to those in Table 4a, No. 8, in the order of B, P, S, and C, are: 0.049, −0.00$_9$, −0.059, and −0.175. If such a weighted mean as $\{10(b/a)\Delta(a/b)+(b/c)\Delta(c/b)\}/11$ is taken instead of the arithmetical mean in No. 4, the above-mentioned eight values for No. 8 become: 51, 70; 51, 69; 50, 02±20, 74, and −246 (resp.) $\times 10^{-8}$. After such complementary considerations it will be found admissible to adopt the magnitude $ca.$ 0.07 for Case a or $ca.$ −0.2 for Case b.

After all, the error (i) in M_δ due to uncertainty in $a:b:c$ will not exceed ($0.3\% \times 0.07 \approx$) 0.02% in Case a, while in Case b,[24] possibly, 0.05%. On the other hand, the error (ii) due to uncertainty in the parameters does not, presumably, differ much from the amount 0.2% mentioned in Art. 2 in Case a, and in Case b this error is estimated[25] to be *ca.* 0.4%.

§ 6. Values of M_δ with Their Probable Errors

The purity of the materials whose values of the axial ratio are adopted in these calculations (§ 4) is unknown to the present author. With respect to $BaSO_4$ and $SrSO_4$, however, certain reported values are for chemically pure crystals or are designated as recommended ones.[26] They are now adopted and the values of M_δ in Table 2 are amended by utilizing the consideration made in § 5.4. In Table 5 each final value of M_δ is given, to which both its probable error, estimated[27] in § 5, and its corresponding axial ratio

Table 5

Madelung's Coefficients (M_δ) of the Sulfates at 0—30°C

(δ: Mean lattice constant. Unit: molec^{-1},cell$^{-1/3}$)

	$PbSO_4$	$BaSO_4$
M_δ	13.164±0.7%	13.187±0.7%
$a:b:c$	0.78_{52}:1:1.28_{94}	0.814:1:1.312
	$SrSO_4$	$CaSO_4$
M_δ	13.159±0.7%	13.504±0.9%
$a:b:c$	0.78_{69}:1:1.28_{32}	0.89_{32}:1:1.00_{08}

are appended. The corresponding values of M_χ/z^2 are: 2.0_{73}, 2.0_{77}, 2.0_{72}, and 2.1_{27} (resp.) molec$^{-4/3}$.-valency^{-2}.

§ 7. Rates of Variation in M_δ with Temperature and Pressure

By utilizing the consideration made in § 5.4 a rough estimation of the variability of (viz. the rate of variation in) M_δ with temperature or pressure has been made,[28] producing the results: $-(\partial M_\delta/\partial T)_P^*/M_\delta$, in 10^{-7} deg^{-1}: 5, −4 or −4,[29] 0.9 or 0.1, and −20; $(\partial M_\delta/\partial P)_T^*/M_\delta$, in 10^{-9}-bar^{-1}: —, 8, −7, and —; for Cases a′, ...b, resp.; where * means that the parameters of atomic positions are assumed to be kept constant. Thence it is seen that the (absolute) magnitudes of these two quantities are 10^{-2} of those of the mean linear thermal expansibility and of the mean linear compressibility, respectively.

§ 8. Values of the Electrostatic Lattice Energy Φ_1

The molal electrostatic potential energy, Φ_1, of a crystal lattice may be computed by use of Eq. 1 with $d=\delta$; while (cf. Eqs. 3, 4)

$$\delta^3 = a_1 a_2 a_3 = \sigma V/N = \sigma M/\rho N \qquad (10)$$

where M is the gram-formula mass and ρ the density. The values of Φ_1 thus computed[30] are shown in Table 6.[31] Every one of them is accurate to *ca.* 1%, but the relative error, viz. the

Table 6

Electrostatic Lattice Energies (Φ_1) of the Sulfates, with their corresponding quantities of ρ and δ, at 25° C

		$PbSO_4$	$BaSO_4$
i	ρ	6.37±0.02	4.49±0.01
ii	δ	6.812±0.007	7.015±0.005
iii	$-\Phi_1$	641.6±5.1	624.1±4.8
		$SrSO_4$	$CaSO_4$
i	ρ	3.97±0.01	2.98±0.02
ii	δ	6.748±0.006	6.719±0.015
iii	$-\Phi_1$	647.5±5.1	667.3±7.5

Unit. i: g. cm^{-3} ii: Å. cell$^{-1/3}$
iii: kcal. mol^{-1}

error in each difference between them, may probably be much less than (possibly, *ca.* 1/6 of) the corresponding sum of their independent errors. (This statement is valid also for M_δ in § 6.)

The rate of variation in Φ_1 with temperature or pressure will be approximately equal to the minus mean linear thermal expansibility or the mean linear compressibility, resp., if we refer to § 7 and assume that the corresponding rate of variation in M_δ due to the parameters of atomic positions may be small enough.

Summary

A plan for investigation of the physical chemistry of radical ions is stated with especial reference to the strict treatment of the lattice-energy problem and the treatment of complex ionic crystals. First, the expressions suitable for the practical numerical calculation of

(25) The experimental error in u or w being supposed to be 0.005, an interpolation is made between the values 13.50 and 12.99—refer to Note 16 and Tables 1 (v) and 2.

(26) Cf. Table 3 (Nos. 10, 11) and Notes 21, 23.

(27) In Case a the errors 2-i and 4-ii are counted once collectively.

(28) The materials in Tables 3 (Nos. 2—8) and 4a (No. 8) and in Note 24 have been used.

(29) A set of the data in Ref. † of Table 3 leads to −5 for both 25° and 0—100° C.

(30) The values adopted are: M's, and N, e, and cal in *J. Am. Chem. Soc.*, **74**, 2447, 2699 (1952); σ in Eq. 8; and ρ's selected from various sources, esp. from Liter. 4b of Ref. 10.

(31) The corresponding values of the lattice constants a^*, b^*, c^*, in kx. cell$^{-1/3}$, computed by use of the values of $a:b:c$ in Table 5 and of λ_Q/λ_x (1.00202 kx. Å^{-1}), are: 8.439, 5.374, 6.929; 8.850, 5.436, 7.132; 8.342, 5.341, 6.851; and 6.218, 6.961, 6.967; resp.

Madelung's coefficient of the general and the rectangular crystal lattice are derived from Ewald's original general expressions. Next, they are verified in the two simple cases, NaCl and the rhombic $CaCO_3$, by means of numerical application. Then, they are applied to the more complex cases, i. e., the rhombic crystals of $PbSO_4$, $BaSO_4$, $SrSO_4$, and $CaSO_4$, with SO_4^{--} which is assumed to be a point charge. The degree of accuracy of the calculated values is further discussed; and, in connection with it, an attempt is made to estimate the extent of variability of Madelung's "coefficient" (or "constant," as it is called). Finally, the electrostatic lattice energy is evaluated.

I express my sincere thanks to the late Dr. Y. Kobayashi, who introduced me to this problem. I am grateful to Professor Tamamushi for his encouragement and kindness in reading my original manuscript. I am also indebted to Assist. Prof. M. Miura, who has afforded facilities for continuing my work, and to Assist. Prof. E. Hirahara for his valuable advice.

Department of Chemistry, Hirosima University of Literature and Science, Hirosima

---

The Separation of Isotopes by Countercurrent Gaseous Exchange Column. I. Transport Equation and Over-All Separation

By Kunihiko KIGOSHI

(Received August 1, 1952)

Introduction

Taylor and others[1][2] have observed a very efficient isotope separation with experiments on the countercurrent gaseous exchange column. Bernstein and Taylor[2] have used a hot wire type thermal diffusion column with a top reservoir filled with carbon dioxide and a bottom reservoir in which a chemical converter reduces carbon dioxide to carbon monoxide. The column consisted of a water-jacketed glass tube 1.0 cm. in diameter and 110 cm. long. When it ran two or three days with hot wire temperature 1150°C., the heavy isotope C^{13} was concentrated 1.5 times to the initial concentration at the bottom reservoir. This overall separation is much greater than that of ordinary thermal diffusion.

To account for its high efficiency, Bernstein and Taylor[2] have treated the problem with the simplified flow pattern and idealized two cases; diffusion rate limited case and exchange rate limited case. However, the treatment of this problem is so simplified that it cannot explain the mechanism of isotope separation by this column. The exchange reaction between carbon dioxide and monoxide had been studied by Brandner and Urey,[3] and recently Norris and Ruben[4] reexamined this problem. Though their results are not entirely conclusive it may be said that the reaction velocity is very slow at the temperature below 700°K., and at the higher temperature the reaction velocity increases as the ordinary chemical reactions. Since the diffusion rate is proportional to the square of temperature, it may be reasonable to assume that above the certain temperature T_b the reaction is very rapid compared with the diffusion process. At the region where temperature is below T_b the exchange reaction may be considered very slow compared with the diffusion process, therefore we may treat the behavior of heavy isotope C^{13} in carbon dioxide and carbon monoxide separately. In the region where the temperature is higher than T_b, the equilibrium of the isotopic exchange reaction,

$$C^{12}O_2+C^{13}O \rightleftarrows C^{13}O_2+C^{12}O$$

holds with the equilibrium constant $\alpha(T)$ of this temperature. Under these situations the mechanism of the isotope enrichment by countercurrent gaseous exchange column can

(1) T. I. Taylor and R. B. Bernstein, *J. Am. Chem. Soc.*, **69**, 2076 (1947); T. I. Taylor and W. Spindel, *J. Chem. Phys.*, **16**, 635 (1948).
(2) R. B. Bernstein and T. I. Taylor, *J. Chem. Phys.*, **16**, 903 (1948).
(3) J. Brandner and H. C. Urey, *ibid.*, **13**, 351 (1945).
(4) T. H. Norris and S. Ruben, *ibid.*, **18**, 1595 (1950).

be solved using no more serious assumptions and simplified cases.

Descriptions of Experimental Conditions and Notations

Suppose two different gases of species 1 and 2 each has the same element A, and there are two isotopes A^i and A^j. When we write AB for the gas molecule of species 1 and AC for species 2, the chemical exchange reaction,

$$A^iB+A^jC \rightleftarrows A^jB+A^iC \qquad (1)$$

takes place very rapidly compared with the diffusion process at the temperature higher than T_b and slowly enough at the temperature below T_b.

The apparatus is supposed to be an ordinary hot wire type thermal duffusion column, and its dimensions are as follows; r_1, r_2=radius of cooled cylinder and hot wire, Z=length of column, T_1 and T_2 are absolute temperatures of cooled cylinder and hot wire respectively. r and z are radial and vertical (along the column) coordinates; $r_2 \leq r \leq r_1$, $0 \leq z \leq Z$.

The gas in the apparatus is a mixture of AB and AC. c_1, c_2=fractional molar concentration of species 1(AB) and 2(AC); $c_1+c_2=1$. ν_1, ν_2= fractional molar concentration of isotope A^i of the species 1 and of species 2. ν=fractional molar concentration of isotope A^i as a whole; $\nu=c_1\nu_1+c_2\nu_2$. D_1, D_2=self diffusion coefficient of species 1 and 2. λ=thermal conductivity, η=viscosity, ρ=density of gas mixture. M_1, M_2=molecular weight of AB and AC, $\bar{M}$=mean molecular weight; $\bar{M}=c_1M_1+c_2M_2$.

Isotopic Transport

The consideration about the distribution of different gases in the thermal diffusion column treated here is based on the theory which had been developed by Furry, Jones and Onsager.[5] Suppose species 1 concentrates to the hot part of the column by thermal diffusion, the transport τ_1 (mol./sec.) of species 1 along the column is given by Furry and Jones[6][7] as follows,

$$\bar{M}\tau_1 = Hc_1c_2-(K_c+K_d)(dc_1/dz) \qquad (2)$$

where H, K_c and K_d are given by expressions (52), (40) and (47). Regarding the flow of gas, the equation of flux (mol./sec. cm.) of species 1 was given by Furry, Jones and Onsager[5] as follows,

$$\boldsymbol{J}_1=(\rho/\bar{M})[\boldsymbol{v}c_1+D'_1(-\operatorname{grad} c_1 + \alpha_t c_1c_2 \operatorname{grad} \ln T)] \qquad (3)$$

and a corresponding equation holds for $\boldsymbol{J}_2$. Where $\boldsymbol{v}$ is velocity vector of convective flow, D'_1 is diffusion coefficient of species 1 in the gas mixture and α_t is thermal diffusion constant for the mixture of two different gases. The isotopic exchange reaction and the separation of isotope in the column are treated here at the situation in which the steady state was attained about the distribution of two gases of species 1 and 2. Then we have

$$\operatorname{div} \boldsymbol{J}_1 = \operatorname{div} \boldsymbol{J}_2 = 0 \qquad (4)$$

Regarding the flow of isotope in the gas of species 1, the equation of flux of A^i is

$$\boldsymbol{I}_1=\nu_1\boldsymbol{J}_1-(\rho D_1c_1/\bar{M})(\operatorname{grad}\nu_1 - \alpha_1(1-\nu_1)\nu_1 \operatorname{grad}\ln T) \qquad (5)$$

and the flux of A^i in the gas of species 2 is

$$\boldsymbol{I}_2=\nu_2\boldsymbol{J}_2-(\rho D_2c_2/\bar{M})(\operatorname{grad}\nu_2 - \alpha_2(1-\nu_2)\nu_2 \operatorname{grad}\ln T) \qquad (6)$$

where α_1 and α_2 are isotopic thermal diffusion constants for gases of species 1 and 2 respectively. We assume that the time variation of ν_1 and ν_2 at each point in the tube is negligible, i. e. stationary or quasistationary state with respect to the isotopic distribution in the column. This assumption holds not only at the final equilibrium but also during the approach to equilibrium when both reservoirs are sufficiently large. From these conditions we have

$$\operatorname{div} \boldsymbol{I}_1 = \operatorname{div} \boldsymbol{I}_2 = 0 \quad (T<T_b) \qquad (7)$$

at the point where the temperature is below T_b. In the region where the temperature is higher than T_b, the exchange reaction (1) takes place. Then in this region we have only one equation,

$$\operatorname{div}(\boldsymbol{I}_1+\boldsymbol{I}_2)=0 \quad (T \geq T_b) \qquad (8)$$

and in this region ν_1 and ν_2 are related by equilibrium canstant

$$\nu_2/\nu_1=\alpha(T) \quad (T \geq T_b) \qquad (9)$$

The application of equations (5), (6) and (2) on equation (7) gives

(5) W. H. Furry, R. C. Jones and L. Onsager, *Phys. Rev.*, **55**, 1083 (1939).
(6) R. C. Jones and W. H. Furry, *Rev. Mod. Phys.*, **18**, 151 (1946).
(7) W. H. Furry and R. C. Jones, *Phys. Rev.*, **69**, 459 (1946).

$$\boldsymbol{J}_1 \operatorname{grad} \nu_1 - \operatorname{div}(\rho D_1 c_1 \operatorname{grad} \nu_1)/\bar{M} = 0 \quad (T < T_b) \tag{10}$$

$$\boldsymbol{J}_2 \operatorname{grad} \nu_2 - \operatorname{div}(\rho D_2 c_2 \operatorname{grad} \nu_2)/\bar{M} = 0 \quad (T < T_b) \tag{11}$$

in the same way we have from equations (8) and (9)

$$\boldsymbol{J}_1 \operatorname{grad} \nu_1 + \boldsymbol{J}_2 \operatorname{grad}(\alpha\nu_1) - \operatorname{div}(\rho D_1 c_1 \operatorname{grad} \nu_1 + \rho D_2 c_2 \operatorname{grad}(\alpha\nu_1))/\bar{M} = 0 \quad (T \geq T_b) \tag{12}$$

where we neglected the third terms of equations (5) and (6) which are derived from thermal diffusion of isotope in each of two gases. Because we are now interested in the case having a large separation factor which would never be explained by thermal diffusion. We can see from equation (3) that the z-component j_{iz} of the vector $\boldsymbol{J}_i$ $(i=1, 2)$ is sufficiently large compared with other components except the small region where v_z becomes zero. Then from equations (10), (11) and (12), neglecting the radial components of $\boldsymbol{J}_i$ we have

$$j_{iz}(\partial\nu_1/\partial z) - r^{-1}(\partial/\partial r)\rho D_i c_i r(\partial\nu_i/\partial r)/\bar{M} = 0 \quad (i=1, 2)\ (T < T_b) \tag{13}$$

$$j_{1z}(\partial\nu_1/\partial z) + j_{2z}(\partial\nu_2/\partial z) - r^{-1}(\partial/\partial r)\rho r[D_1 c_1(\partial\nu_1/\partial r) + D_2 c_2(\partial\nu_2/\partial r)]/\bar{M} = 0 \quad (T \geq T_b) \tag{14}$$

In the above equations the terms containing $(\partial^2\nu_1/\partial z^2)$ and $(\partial^2\nu_2/\partial z^2)$ are omitted. These terms represent the effects of diffusion of isotope along the column which are separately treated in the equation of isotopic transport. The term $D_1\rho(\partial c_1/\partial z)(\partial\nu_1/\partial z)\bar{M}$ and corresponding term of species 2 are also omitted in (13) and (14), since the diffusion along the column is small enough compared with the convective flow. The neglect of these terms in equations (13) and (14) gives only a slight effect as much as the neglect of radial components of $\boldsymbol{J}_i$ in equations (10) and (11).

Now we introduce the functions L_i and L which are defined as follows,

$$\int_{r_1}^{r} 2\pi r j_{iz} dr = L_i(r) \quad (i=1, 2) \tag{15}$$

$$L_1(r) + L_2(r) = L(r) \tag{16}$$

Using the above equations we can integrate (13) and (14),

$$(\partial\nu_1/\partial z)L_i(r) = 2\pi\rho D_i c_i r(\partial\nu_i/\partial r)/\bar{M} \quad (i=1, 2)\ (T < T_b) \tag{17}$$

$$(\partial\nu_1/\partial z)L_1(r) + (\partial\nu_1/\partial z)L_2(r) = 2\pi\rho r[D_1 c_1(\partial\nu_1/\partial r) + D_2 c_2(\partial\nu_1\alpha/\partial r)]/\bar{M} \quad (T \geq T_b) \tag{18}$$

since $\partial\nu_1/\partial r$ and $\partial\nu_2/\partial r$ must vanish at the walls and we neglect small differences between $\partial\nu_1/\partial z$ and $\partial\nu_2/\partial z$, and their dependence on radial coordinate. By means of equation (15) the total flow of gases of species 1 and 2 are given by

$$-\tau_i = L_i(r_2) \quad (i=1, 2) \tag{19}$$

As the total flow of gas as a whole is zero, we get

$$\tau_1 + \tau_2 = 0 \tag{20}$$

At any point $\operatorname{div}(\boldsymbol{I}_1 + \boldsymbol{I}_2)$ is zero then, total transport (τ = mol./sec.) of isotope A^i along the tube is independent of z, i.e.,

$$\tau = \int_{r_2}^{r_1} 2\pi r(j_{1z}\nu_1 + j_{2z}\nu_2)dr - (\partial\nu_1/\partial z)\int_{r_2}^{r_1} 2\pi\rho r(D_1 c_1 + D_2 c_2)dr/M = \text{const.} \tag{21}$$

The first term of equation (21) represents the transport of isotope by the convective flow of gases and the second term is derived from the vertical diffusion of isotope. When the small radial variations of c_1 and c_2 are neglected, the second term becomes the same as the case of thermal diffusion column, and we can use the results of Furry and Jones[6,7] as follows,

$$(\partial\nu_1/\partial z)\int_{r_2}^{r_1} 2\pi\rho r(D_1 c_1 + D_2 c_2)dr/\bar{M} = [c_1(K_d)_1/\bar{M} + c_2(K_d)_2/\bar{M}](\partial\nu_1/\partial z) \tag{22}$$

where $$(K_d)_i = 2\pi(\rho D_i)_1 r_1^2 k_d \quad (i=1, 2) \tag{23}$$

They tabulated the numerical values of k_d for the different values of (T_2/T_1) and (r_1/r_2) in the case of a Maxwellian gas. The subscript 1 of (ρD_i) emphasizes that the quantity in parethesis is to be evaluated at T_1. Using equation (15), partial integration of the first term of equation (21), gives

$$\int_{r_2}^{r_1} 2\pi r(j_{1z}\nu_1 + j_{2z}\nu_2)dr = \int_{r_2}^{r_b} 2\pi r\nu_1(j_{1z} + \alpha j_{2z})dr - \int_{r_1}^{r_b} 2\pi r(\nu_1 j_{1z} + \nu_2 j_{2z})dr$$

$$= \tau_1\nu_1(r_b) + \tau_2\nu_2(r_b) - \int_{r_2}^{r_b}[(\partial\nu_1/\partial r)(\tau_1 + L_1)$$

$$+(\partial\nu_2/\partial r)(\tau_2+L_2)\}]dr$$
$$+\int_{r_1}^{r_b}((\partial\nu_1/\partial r)L_1+(\partial\nu_2/\partial r)L_2)dr$$

where r_b is radial coordinate, the temperature of which is T_b. According to (15), (9), (20), (17) and (18) the above expression becomes

$$\nu_1\tau_1(1-\alpha(T_b))$$
$$+\int_{r_2}^{r_b}\frac{D_2c_2(\tau_1+L_1)-D_1c_1(\tau_2+L_2)}{D_1c_1+D_2c_2}\nu_1\frac{d\alpha}{dr}dr$$
$$+\int_{r_1}^{r_b}\frac{\bar{M}}{2\pi\rho r}\left(\frac{L^2_1}{D_1c_1}+\frac{L^2_2}{D_2c_2}\right)\frac{\partial\nu_1}{\partial z}dr$$
$$+\int_{r_b}^{r_2}\frac{\bar{M}}{2\pi\rho r}\left(\frac{L^2}{D_1c_1+D_2c_2}\right)\frac{\partial\nu_1}{\partial z}dr \quad (24)$$

We may regard in expression (24) the functions ν_1 and $\partial\nu_1/\partial z$ depend only on z. By expressions (22) and (24), the isotopic transport given by (21) becomes as follows,

$$\tau=A\nu_1-(B_c+B_d)\partial\nu_1/\partial z \quad (25)$$

where

$$A=\tau_1(1-\alpha(T_b))$$
$$+\int_{r_2}^{r_b}\frac{D_2c_2(\tau_1+L_1)-D_1c_1(\tau_2+L_2)}{D_1c_1+D_2c_2}\frac{d\alpha}{dr}dr \quad (26)$$

$$-B_c=\frac{\bar{M}}{2\pi}\left[\int_{r_1}^{r_b}\left(\frac{L_1^2}{D_1c_1}+\frac{L_2^2}{D_2c_2}\right)\frac{dr}{\rho r}+\int_{r_b}^{r_2}\frac{L^2}{D_1c_1+D_2c_2}\cdot\frac{dr}{\rho r}\right] \quad (27)$$

$$B_d=(c_1(K_d)_1+c_2(K_d)_2)/\bar{M} \quad (28)$$

Evaluation of integrals in B_c is simply performed when some approximations are introduced for L_1, L_2 and diffusion coefficients. In expression (27) diffusion coefficients D_1 and D_2 are contained in positive terms, therefore we can substitute these coefficients by mean value $\bar{D}$ without great error.

The main part of j_{iz} is convective flow along the tube. Then we may put

$$j_{iz}=\rho c_i v/\bar{M} \quad (i=1,2) \quad (29)$$

in equation (15), where v is z-component of convective flow $\boldsymbol{v}$. This is very close approximation since the effects of diffusion are small enough compared with convective flow. We can remove c_i from under the integral sign of (15), because c_i varies only slightly with T. Then we may substitute L_i by c_iL. Using above approximation we obtain

$$-B_c=\frac{\bar{M}}{2\pi}\int_{r_1}^{r_2}\frac{L^2}{\rho Dr}dr \quad (30)$$

In order to evaluate the second term of expression (26) we use the following approximation which is similar to one applied to L_i in the above case;

$$\tau_i+L_i=\int_{r_2}^{r}2\pi rj_{iz}dr\cong c_iL$$

By this approximation we can rewrite equation (26) as follows,

$$A=\tau_1(1-\alpha(T_b))+\frac{c_1c_2(D_2-D_1)}{c_1D_1+c_2D_2}\int_{r_2}^{r_b}L\frac{d\alpha}{dr}dr \quad (31)$$

Convective Flow

Except the both ends of the tube, temperature gradient is determined by conduction alone, and in this region we have

$$2\pi Q=2\pi r\lambda(-dT/dr) \quad (32)$$

where $2\pi Q$ is heat flow by conduction per unit length of the tube, in cal./cm. sec.

The hydrodynamical equation of steady viscous flow in cylindrical coordinates is

$$r^{-1}(\partial/\partial r)r\eta(\partial v/\partial r)=dp/dz+\rho g \quad (33)$$

where p is pressure and g is acceleration of gravity. We assume that the velocity is entirely in z direction, and it is independent of z. Using equation (33) we have

$$Q^2(d/dT)\lambda^{-1}r^{-2}(d/dT)\eta\lambda^{-1}(dv/dT)=g(d\rho/dT) \quad (34)$$

Convective flow v must vanish at the walls;

$$v(T_1)=v(T_1)=0 \quad (35)$$

We have from equations (15), (16) and (29),

$$L=\int_{r_1}^{r}2\pi r\rho vdr/\bar{M} \quad (36)$$

From this equation we can see that L is the total flow of convection at the outside of the cylindrical part of radius r. Then we have

$$L(r_1)=L(r_2)=0 \quad (37)$$

Differentiate equation (36) with respect to r, and using equation (32) we have

$$v=-(\bar{M}Q/2\pi\lambda r^2)(dL/dT) \quad (38)$$

Substitution of equation (38) in (34) gives a differetial equation for L,

$$\frac{\bar{M}\zeta^3}{2\pi}\frac{d}{dT}\frac{1}{r^3\lambda}\frac{d}{dT}\frac{\eta}{\lambda}\frac{d}{dT}\frac{1}{r\lambda\rho}\frac{dL}{dT}=g\frac{d\rho}{dT} \tag{39}$$

From (35), (37) and (38) the boundary conditions are

$$L(r_1)=L(r_2)=L'(r_1)=L'(r_2)=0 \tag{39}'$$

The function L obtained from (39) and (39)' is identical to

$$(2\pi\rho\bar{D}/\lambda\zeta^3\bar{M})G$$

where G is the function used by Furry and Jones[6][7]. Therefore we can use their results of calculation about the integral contained in equation (30), and we have

$$B_c=K_c/\bar{M}=(2\pi/9!)(\rho^3g^2/\eta^2\bar{D})_1\cdot r^8{}_1k_c/\bar{M} \tag{40}$$

where values of k_c are tabulated for Maxwellian gases by Furry and Jones[6] for various combinations of (T_2/T_1) and (r_1/r_2). In order to evaluate the integral in equation (31), we have to solve the differential equation (39). Using the assumption that the quantities λ, η and ρD are proportional to T, an assymptotic solution of equation (39) for extreme cylindrical case $(r_2/r_1\to 0)$ has been given by Furry and Jones[7];

$$L(T)=2\pi\bar{M}(\rho g/\eta)_1\cdot r^4{}_1t^3{}_1\exp(2t^2{}_1)\gamma(t) \tag{41}$$

$$\gamma(t)\cong\frac{\gamma_\infty-(\gamma''/t_2)}{1-(\delta''/t_2)},$$

$$\delta''=\left[\exp(-t^2{}_1)\Big/\int_{t_1}^{\infty}\exp(-x^2)dx\right]-t_1$$

Where variable t is defined by

$$t=(\lambda/QT)^{1/2}T \tag{42}$$

and t_1 and t_2 are values of t at $T=T_1$ and T_2 respectively. The numerical values of γ_∞ and γ'' as the functions of t were tabulated by Furry and Jones.[7] Using these results we obtain the expression for the integral in (31) in terms of known functions as follows,

$$H_b=\int_{r_2}^{r_1}L(d\alpha/dr)dr$$

$$=(2\pi/\bar{M})(\rho g/\eta)_1r^4{}_1t^3{}_1\exp(2t^2{}_1)\times[h_b-(h''{}_b/t_2)]/[1-(\delta''/t_2)] \tag{43}$$

$$h_b=-\int_{t_b}^{\infty}\gamma_\infty(d\alpha/dt)dt \tag{44}$$

$$h''{}_b=-\int_{t_b}^{\infty}\gamma''(d\alpha/dt)dt$$

Equilibrium Separation Factor

We proceed from the equation for transport of isotope A up to the tube:

$$\tau=A\nu_1-(B_c+B_d)(d\nu_1/dz) \tag{45}$$

where A is given by (31) and (43);

$$A=\tau_1[1-\alpha(T_b)]+[c_1c_2(D_2-D_1)/\bar{D}]H_b \tag{46}$$

B_c is given by equation (40), and B_d is given by equation (28);

$$B_d=K_d/\bar{M}=2\pi(\rho\bar{D})_1r^2{}_1k_d/\bar{M} \tag{47}$$

The approximation was used to derive above equations that we put D_1 and D_2 are equal to $\bar{D}$ except the case which contains their difference.

In the final equilibrium state τ is zero all along the tube. Putting $\tau=0$ in (45) we obtain

$$A\nu=(B_c+B_d)(d\nu/dz) \tag{48}$$

The integral of (48) gives a ratio of the concentration of isotope A in the top and the bottom reservoirs. In general case the distinction between ν_1 and ν_2 is not necessary when we consider the large separation of isotope in both reservoirs. The functions of z in equation (48) are ν and A which depends z through c_1c_2 in (46). Then integral of (48) is

$$(1-\alpha(T_b))Z+\frac{D_2-D_1}{\bar{D}}H_b\int_0^Z c_1c_2dz=(B_c+B_d)\ln\left(\frac{\nu(Z)}{\nu(0)}\right) \tag{49}$$

where $\nu(0)$ and $\nu(Z)$ are values of ν at the bottom and the top reservoirs respectively.

By the similar way we obtain from equation(2)

$$(H/\bar{M})\int_0^Z c_1c_2dz=\tau_1Z+(K_c+K_d)(c_1(Z)-c_1(0))/\bar{M} \tag{50}$$

where $c_1(Z)$ and $c_1(0)$ are c_1 at the bottom and the top reservoirs. Substitution of (50), (40) and (47) into (49) leads to the expression for over-all separation S as follows,

$$\ln S=\ln\left(\frac{\nu(Z)}{\nu(0)}\right)=\left[(1-\alpha(T_b))+\frac{D_2-D_1}{\bar{D}}\frac{H_b}{H/\bar{M}}\right]\frac{\tau_1Z}{B_c+B_d}+\frac{D_2-D_1}{\bar{D}}\frac{H_b}{H/\bar{M}}(c_1(Z)-c_1(0)) \tag{51}$$

When we use the approximate formula (41), H becomes

$$H=2\pi(\rho^2 g/\eta)_1 r^4{}_1 t^3{}_1 \exp(2t^2{}_1)\frac{h_\infty-(h''/t_2)}{1-(\delta''/t_2)} \tag{52}$$

where $$h_\infty=\int_{t_1}^{\infty}\alpha_t(\gamma_\infty/t)dt$$

$$h''=\int_{t_1}^{\infty}\alpha_t(\gamma''/t)dt \tag{53}$$

The expressions (53) and (43) give

$$\frac{H_b}{H/\bar{M}}=\frac{h_b-(h_b''/t_2)}{h_\infty-(h''/t_2)} \tag{54}$$

Discussion

From rather surprisingly simple results given by equation (51) we can easily calculate overall separation $\mathcal{S}$, since B_c, B_d and $(c_1(Z)-c_1(0))$ may be determined from experimental conditions, and H_b/H may be numerically calculated by expression (54) when we know the temperature T_b.

The details of experimental verification of equation (51) will be reported in part 2 on this Bulletin.

We shall now discuss the functioning of gaseous exchange column. The remixing effects of the diffusion of isotope along the tube and of the countercurrent in the tube are represented by $B_d d\nu_1/dz$ and $B_c d\nu_1/dz$ respectively in the transport equation (45). It is reasonable that an appropriate approximation leads these terms to the expressions which are identical for the ordinary thermal diffusion as shown by equation (40) and (47). The initial isotopic transport obtained by putting $d\nu_1/dz=0$ in equation (45) is rather complicated, but its meaning is clear. When the ratio ν_2/ν_1 is $\alpha(T_b)$ at any point in the tube,

$$\nu_1\tau_1(1-\alpha(T_b))=\tau_1\nu_1+\tau_2\nu_1\alpha(T_b)$$

is transport of isotope A along the tube. Whereas in the equilibrium region ($T\geq T_b$) α varies with temperature. If we assume the self diffusion coefficient D_1 is larger than D_2, the radial variation of ν_1 may not be large, but the radial variation of α results in a strong variation of ν_2. The deviation of transport estimated in the first term of the expression (46) is corrected by the second term which is derived from such an asymmetric variation of ν_1 and ν_2 between r_2 and r_b. An application of (46) to the experiments of Bernstein and Taylor[2] shows that the first term is negligibly small compared with the second term. Therefore we may conclude that the transport of isotope in the equilibrium region results in the high efficiency of the gaseous exchange column. Perphaps there is another possibility to obtain the high efficiency by the mode of operation in which τ_1 takes large value by the thermal dissociation with suitable gas. In this case the transport of gases must be recalculated with the equilibrium constant of thermal dissociation.

Summary

The theoretical treatment of the countercurrent gaseous exchange method for the separation of isotopes is developed here. The equation of transport is derived with the assumption that the equilibrium of the isotopic exchange reaction holds only in the sharply defined region in which temperature is higher than T_b. An appropriate approximation leads the transport equation to one which is formally similar to the transport equation of thermal diffusion column. The mechanism of isotope enrichment by countercurrent gaseous exchange method is discussed using the transport equation. The equilibrium separation factor is also derived from the transport equation.

Department of Physics and Chemistry, Gakushuin University, Mejiro Tokyo

Purification and Characterization of Tobacco Mosaic Virus

By Itaru WATANABE and Yoshimi KAWADE

(Received October 13, 1952)

Since the isolation and crystallization of tobacco mosaic virus (TMV), by Stanley[1] studies on physicochemical properties of viruses have greatly advanced, especially by taking advantage of the ultracentrifuge for purification. Ultracentrifugal purification of TMV now seems to be a well-established method; a preparation with high degree of homogeneity is, nevertheless, not easy to obtain. Only a few comprehensive studies on the properties of TMV particles are found in the literature which are based on simultaneous measurements of various physicochemical characteristics of a purified solution. In this paper the results obtained by the authors during the last few years[2] are shown, concerning the ultracentrifugal purification of TMV and characterization of purified preparations, by various means among which a sample of high degree of homogeneity is included.

Experimental

A. Purification of TMV.

1. Ultracentrifuge.—The ultracentrifuge used is an air-driven, vacuum-type one[3] first constructed in Japan at the end of 1948, some details of which were reported previously.[4][5]

2. Materials.—Tobacco leaves infected with tobacco mosaic disease were kindly supplied by Dr. J. Hitaka of the Tobacco Experimental Station at Hatano, Kanagawa Prefecture. Xanthi was used for the starting plant in our earlier experiments, but it was found that brownish pigments were not completely removed even after several cycles of alternate high and low speed centrifugations. In later experiments, therefore, we used mainly the infected leaves of White Burley, for it was found much easier to remove colored materials by centrifugation only.

The virus studied here is believed to be the ordinary strain of tobacco mosaic virus.

3. Purification Procedures.—Of the several preparations obtained, the purification methods of TMV-8 and -9 are described, which follow essentially those of Stanley.[6]

Young White Burley tobacco plants were harvested about two or three weeks after inoculation with TMV. The leaves were frozen in a refrigerator and ground through a meat chopper after three weeks (TMV-8); or they were frozen with solid carbon dioxide and ground the following day (TMV-9). On grinding, solid K_2HPO_4 was added amounting to 2.5% of the fresh weight of the leaves to maintain the *p*H of the expressed juice near neutrality. The juice was clarified by centrifugation and then subjected to three (TMV-8) or five (TMV-9) cycles of alternate high and low speed centrifugations. The high speed runs to obtain the virus pellets were made for one hour at 30,000 R. P. M. (65,000×g) or for half an hour at 36,000 R. P. M. (95,000×g), and those of low speed to remove heavier impurities, at 9,000 to 12,000 R. P. M. (6,000 to 10,000×g) for about 15 minutes. The solvents used to dissolve the pellets of TMV were 0.1M phosphate buffer at *p*H 7.0 for the first two cycles and 0.01M for the others. The final pellets so obtained were practically pigment-free. They were dissolved in 0.01M phosphate buffer at *p*H 7.0 and stored in a cold room near 0°C.

4. Yields.—Biological assays by the half leaf method on *Nicotiana glutinosa* were performed only qualitatively, and it was found that no serious loss or inactivation of TMV had occurred during the isolation processes by comparing the infectivity of purified preparation with that of original juice.

The yields of purified virus were found to be about the same order as that reported by other workers[7][8][9] and are shown in Table 1.

Table 1
Yields of Purified TMV

Sample	Total amount of TMV obtained, g.	Mg. TMV per g. of original plant	Mg. TMV per cc. of plant juice
TMV-8	0.030	1.0	1.2
TMV-9	1.07	1.4	1.8
	(1.5)	(2.0)	(2.5)

( )···Including less pure TMV

(1) W. M. Stanley, *Science* **81**, 644 (1935).
(2) A brief preliminary report, I. Watanabe, Y. Otsuka, and S. Mizushima, *Repts. Radiation Chem. Research Inst., Tokyo Univ.*, No. 5, 10 (1950).
(3) E. G. Pickels, *Rev. Sci. Instruments*, **9**, 358 (1938).
(4) S. Sasaki and O. Taniguchi, *J. Japan Soc. Mech. Eng.*, **54**, 255 (1951).
(5) I. Watanabe and Y. Kawade, *Chemistry and Chem. Industry*, **5**, 585 (1952).
(6) W. M. Stanley, *J. Am. Chem. Soc.*, **64**, 1804 (1942).
(7) W. M. Stanley, in R. Doerr und C. Hallauer, "*Handbuch der Virusforschung*", I, Vienna (1938), pp. 447—546.
(8) H. K. Schachman and W. J. Kauzmann, *J. Phys. Colloid Chem.*, **53**, 150 (1949).
(9) F. C. Bawden, "*Plant Viruses and Virus Diseases*", Waltham (1950).

← Ascending → Descending

Fig. 1.—Electrophoretic pattern of 0.44% solution of TMV-9 in 0.2 ionic strength phosphate buffer at *p*H 7.7[16]

B. Homogeneities and Properties of Purified TMV.

Some chemical and physical properties of purified TMV have been examined to test its homogeneity and to determine size and shape of the virus particles.

1. Chemical Analyses.—An aliquot of the purified stock solution (TMV-9) was dialyzed against distilled water, and precipitated by acidified ethanol. The precipitate, washed and dried, was dissolved in weak alkali and submitted to analyses for nitrogen by the micro Kjeldahl method, phosphorus by King's method,[10] and pentose nucleic acid by the orcinol method.[11] Dische's diphenylamine test[12] for DNA was found entirely negative. The results are shown in Table 2 and are in good agreement with the values reported by previous investigators.[9][13]

Table 2

Chemical Analyses of Purified TMV
(Sample: TMV-9)

	N %	P %	N/P	PNA %	DNA %
	16.6	0.51		6.2$_7$	0.0
	16.7	0.50		5.8	0.0
Average	16.7	0.51	33	6.0	0.0

2. Physical Measurements. — Electrophoretic measurements of purified preparations were carried out in a Tiselius-type[14] apparatus, equipped with a Svensson optical system,[15] in phosphate buffers of various ionic strengths at *p*H 7.7 and the details will be published elsewhere.[16] In all preparations examined, except in the case only a single boundary was found in the electrophoretic pattern of TMV-8, and the boundary remained very sharp during the course of electrophoresis (forexample, see Fig. 1). A small amount of an unidentified slower component was seen in the pattern of TMV-8. The electrophoretic mobilities were calculated from the descending patterns and in Table 3 are shown the representative data of TMV-9 at 0°C.

Diffusion constants were measured refractometrically by the Svensson schlieren method[15] using a Neurath-type[17] diffusion cell under

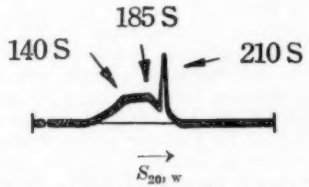

Fig. 2.—Tracing of sedimentation pattern of 0.51% solution of TMV-8 in 0.01M phosphate buffer at *p*H 7.0[18]

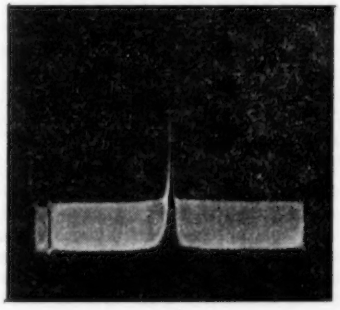

Fig. 3.—Sedimentation pattern of 0.61% solution of TMV-9 in 0.01M phosphate buffer at *p*H 7.0[16]

(10) E. J. King, *Biochem. J.*, **26**, 292 (1932).
(11) S. E. Kerr and K. Seraidarian, *J. Biol. Chem.*, **159**, 211 (1945).
(12) F. Seibert, *J. Biol. Chem.*, **133**, 593 (1940).
(13) W. M. Stanley and M. A. Lauffer, in T. M. Rivers, "*Viral and Rickettsial Infections of Man*", Philadelphia (1948), pp. 18—66.
(14) A. Tiselius, *Trans. Faraday Soc.*, **33**, 524 (1937).
(15) H. Svensson, *Kolloid-Z.*, **87**, 181 (1939).
(16) I. Watanabe and N. Ui, in preparation.
(17) H. Neurath, *Science*, **93**, 431 (1941).
(18) I. Watanabe, Y. Kawade, and S. Mizushima, *J. Chem. Soc. Japan, Pure Chem. Sect.*, **73**, 828 (1952).

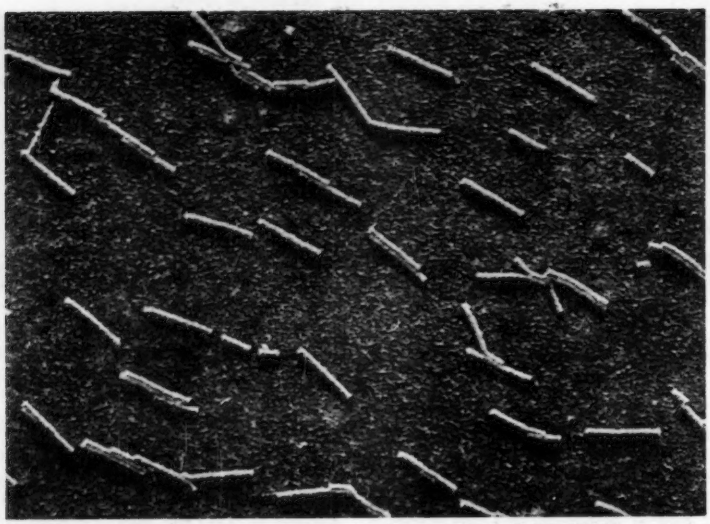

Fig. 4.—Typical electron micrograph of centrifugally purified TMV (TMV-9) photographed by Japan Electron Optics Co., Tokyo. Magnification 35,000 and chromium shadow cast.

various conditions in phosphate buffers. The most reliable value of diffusion constant of the preparation of TMV-9 is shown in Table 3.

Sedimentation studies were carried out in 0.01M phosphate buffer at *p*H 7.0 by using an air-driven analytical ultracentrifuge.[18] TMV-8 proved very inhomogeneous and showed three components in sedimentation pattern (see Fig. 2). The sedimentation constants ($s_{20,w}$) of these three peaks were 210, 185, and 140 S (S: Svedberg unit), when corrected for viscosity of the solution, and would correspond roughly to dimer, monomer, and half-length particle of TMV, respectively. On the other hand, TMV-9 gave a single sharp boundary shown in Fig. 3, suggesting a high degree of homogeneity. It may be stated that such an exceedingly sharp boundary of TMV has not been reported except by Schachman.[19] The sedimentation constant was calculated to be 157S, corrected for viscosity of the solvent, and 185S, corrected for viscosity of the solution according to Lauffer[20] (see Table 3). The latter value is in close agreement with those reported by other workers[5][20][21] for monomeric TMV.

Viscosity was measured in 0.01M phosphate buffer at *p*H 7.0 by an Ostwald-type viscosimeter with low velocity gradient (about 100 sec.$^{-1}$). TMV-8 gave a volume fraction intrinsic viscosity of about 40. This slightly low value of intrinsic viscosity as compared with that of TMV-9 is probably due to the presence of a large amount of shorter (half-length) particles in TMV-8 (see Fig. 2). The viscosity of TMV-9 showed a considerable decrease with time; the intrinsic viscosity at equilibrium state was estimated to be 50 (Table 3).

Electron microscopic observations were made on various samples and in Fig. 4 is shown one of the representative micrographs of purified TMV-9. No extraneous materials have been observed in any. It is apparent that the particles of length about 300 mμ predominate in number in each case. Shorter and longer

Table 3

Physical Data of Purified TMV

(Sample: TMV-9)

Electrophoretic Mobility (at 0°C, in phosphate buffer of ionic strength 0.2 and *p*H 7.7)	$u_D = -7.0_5 \times 10^{-5}$ cm.^{2}/sec. volt
Diffusion Constant	$D_{20,w} = 0.4 \times 10^{-7}$ cm.^{2}/sec.
Sedimentation Constant	$s_{20,w} = 185$ S* (corrected by solution viscosity) $= 157$ S (0.5%) (corrected by solvent viscosity)
Intrinsic Viscosity (Volume Fraction)	$[\eta]_V = 50$
(Partial Specific Volume)	($V = 0.73$)**

* S is a Svedberg unit and a sedimentation rate equal to 10^{-13} cm./sec. in a unit centrifugal field.

** The value obtained by Lauffer.[22]

(19) H. K. Schachman, *J. Am. Chem. Soc.*, **73**, 4808 (1951).

(20) M. A. Lauffer, *J. Am. Chem. Soc.*, **66**, 1195 (1944).

(21) G. Schramm und G. Bergold, *Z. Naturforsch.*, **2b**, 10 (81947).

(22) M. A. Lauffer, *J. Am. Chem. Soc.*, **66**, 1188 (1944).

Table 4
Size and Shape of TMV Particles
(Sample: TMV-9)

Methods	Mol. Wt. (10^6)	Frictional Ratio, f/f_0	Axial Ratio, a/b	Length, a (mμ)	Diameter, b (mμ)
Sedimentation and Viscosity	37	2.2	24	310	13
Sedimentation and Diffuion	42	2.3	28	360	13
Diffusion and Viscositys	53	2.2	24	360	15
Electron Microscope and X-Ray Diffraction	45		20	300	15.2*

* The value obtained by Bernal and Fankuchen from the X-ray diffraction experiments[25]

particles are, however, always present; and even in our most homogeneous preparation, TMV-9, the distribution is broader than reported by American investigators.[22][23][24] Electron micrographs of the original extract for TMV-7 were also taken and it was found that a considerable amount of shorter rods had been already present in plant juice. It might, therefore, be difficult, if not impossible, to ascribe the presence of the short rods entirely to the break-up of the monomer virus rods, due to mechanical stresses during centrifugation.

3. Size and Shape of TMV Particles.—The physical data mentioned above are summarized in Table 3. Size and shape of TMV can be determined by various combinations of viscosity, diffusion, and sedimentation data in conjunction with the partial specific volume.[22] The results of the various methods of determining the dimensions of the particles of TMV-9 are shown in Table 4. In these calculations Lauffer's value[22] of partial specific volume was temporarily adopted. It can be seen that the agreement between the various methods is excellent considering the experimental errors and uncertainties in the calculation methods of determining the size and shape of such highly asymmetric particles. It must be, however, borne in mind that these values are not conclusive, since the concentration dependence of sedimentation constant has not yet been measured exactly in our case and the determinations of various physical constants have not been made at the same time. The latter consideration seems important because of the observed change in the viscosity of solutions of TMV-9 with the lapse of time.

Discussion

In the ultracentrifugal purification of viruses, it seems primarily important to take care of the choice of suitable starting materials. In fact, it was found in our experiments that the leaves of Xanthi contained pigment which was difficult to remove from the virus fraction and that in this respect White Burley was superior to Xanthi. It is also essential to remove heavier materials as completely as possible in the first clarification of the expressed juice. Otherwise, green impurities remaining in the turbid supernatant, once sedimented by high speed centrifugation and redissolved in buffer solution, become somewhat difficult to be removed by subsequent centrifugation and complicate the further purification procedure.

It is clear from the results of chemical and physical measurements on purified TMV that the purity of centrifugally isolated TMV, especially of TMV-9, was very high, so to say, in a chemical sense. The homogeneities of preparations, however, were not always so good. TMV-9 showed a single sharp boundary both in sedimentation and electrophoretic patterns. On the contrary, three peaks appeared in the sedimentation pattern of TMV-8. But this marked heterogeneity was not detected in the electrophoretic measurements, which showed only one main peak except a presence of a small amount of slower component. This apparent discrepancy in sedimentation and electrophoretic patterns of TMV-8 may be ascribed to some difference of sensitivities of sedimentation and electrophoretic analyses in detecting the heterogeneity of length of rod-like particles such as TMV. Another possible explanation, however, cannot be excluded; that is, a certain change in molecular state might have occurred during the preservation, since the electrophoretic measurements were made immediately after the purification of TMV-8 while the ultracentrifugal analysis was performed nearly three months after it. This marked heterogeneity found in sedimentation pattern could not be detected also in diffusion pattern of TMV-8, the measurements of which were made at the same time as the electrophoretic experiments.

TMV-9, on the other hand, showed no evidence of heterogeneity and a single sharp boundary was obtained both in sedimentation and electrophoretic patterns, as mentioned above*; nevertheless, a rather broad distribution was observed in the electron micrographs. In view of the high sensitivity of ultracentrifuge in detecting hetero-

(23) G. Oster, C. A. Knight, and W. M. Stanley, *Arch. Biochem.*, **15** 279 (1947).

(24) R. C. Williams and R. L. Steere, *J. Am. Chem. Soc.*, **73**, 2057 (1951).

(25) J. D. Bernal and I. Fankuchen, *J. Gen. Physiol.*, **25**, 111 (1941).

* Even after storage in a cold room near 0°C. for more than six months, TMV-9 still retained a fairly good homogeneity in sedimentation pattern.[11a]

geneity (presence of short rods) of TMV[19] and a possible change of distribution in length during the preparation of specimen for electron microscopic examination, it might be not unreasonable to conclude that TMV-9 has a high degree of homogeneity and that shorter rods observed in electron micrographs are, at least in part, artefacts. It must be remembered, however, that there still remain other possibilities concerning the origin of these short rods which are seen also in other samples; first, they may be present in the original expressed juice and secondly, they may arise from the break-up of the longer particles as a result of mechanical stresses during the preparation.[26]

It is rather curious that TMV-8, although purified under very similar conditions as TMV-9, showed the marked heterogeneity. In this respect, it would be necessary to point out that in the case of TMV-8, the leaves were frozen in a refrigerator and treated three weeks after the harvest, while in TMV-9, the harvested leaves were frozen with solid carbon dioxide and treated in the following day. These differences in the time of storage of leaves might have caused the unexpected difference in homogeneities of TMV-8 and -9. It seems very desirable, anyway, to start the purification of virus as soon as possible after the harvest of leaves.

Schachman and Kauzmann[6] studied the aggregation effect of phosphate buffer during the purification and storage of TMV and found that isolation of TMV by centrifugation in 0.1M phosphate followed by water leads to the best preparation. Considering their experimental results, however, we used 0.01M phosphate buffer instead of water and the final solution was also stored in the same buffer. Very good results were obtained in this case too. But the solution stored in 0.01M phosphate buffer showed considerable decrease in viscosity with the lapse of time, as mentioned above. This change in viscosity seems very interesting, but other measurements must be performed during storage before a clear explanation can be made about it.

Electrophoretic mobility, diffusion constant, sedimentation constant, and intrinsic viscosity were determined on the most homogeneous preparation, TMV-9. The size and shape of TMV particles were also calculated by various combinations of diffusion constant, sedimentation constant, and intrinsic viscosity and an excellent agreement was found between the results of these indirect physico-chemical procedures and direct observation with the electron microscope.

Since the degree of homogeneity of a purified TMV preparation with respect to the length of the rod-like particle is known to vary various factors, including the purification procedures employed, the nature of the solvent used for preservation, etc.,[27] it is necessary to assess the degree of homogeneity of the specimen when its physicochemical properties are to be studied. Among the numerous investigations on the determination of size and shape of TMV, those of Lauffer[22] and of Schramm and Bergold[21] have been probably the most comprehensive in this respect, but even their samples were apparently inhomogeneous judging from the sedimentation patterns obtained by them. Studies on homogeneous solution of such highly asymmetric particles will be greatly valuable in establishing the hydrodynamic theory underlying the measurements of sedimentation, diffusion, viscosity, etc.

Summary

Tobacco mosaic virus (TMV) was purified by differential centrifugation in a vacuum-type, air-driven ultracentrifuge, first constructed in Japan.

The yield of purified TMV was high and about 2 mg. per cc. of the original plant juice.

Chemical analyses and physico-chemical examinations (including electrophoresis, sedimentation, diffusion, viscosity and electron microscope measurements) were carried out on the purified preparations to test their purities and homogeneities. It was found that the purity of ultracentrifugally isolated TMV was very high in a chemical sense. Although the homogeneity with respect to the length of particles was not always so good, one preparation, TMV-9, was found to have a high degree of homogeneity by the sedimentation and electrophoresis patterns. The size and shape of TMV particles were determined on this preparation by several methods.

The authors wish to express their appreciation of the interest and suggestions of Prof. S. Mizushima of the Department of Chemistry, University of Tokyo, throughout the course of this work. They are also indebted to Prof. S. Sasaki and Prof. O. Taniguchi, Tokyo Institute of Technology, for their kind advices about ultracentrifuge and to Dr. J. Hitaka, Tobacco Experimental Station at Hatano for tobacco leaves. They also wish to acknowledge the technical assistance of Mr. M. Nakamura. Part of the expense of this investigation was defrayed by a Grant in Aid for Scientific Research by the Ministry of Education.

Institute of Science and Technology,
Tokyo University, Tokyo

(26) T. Sigurgeirsson and W. M. Stanley, *Phytopathology*, **37**, 26 (1947).

(27) See, e. g., refs. (26), (24), and (8).

Dosage volumétrique du manganèse et du chrome par le péroxyde d'argent

(Reçu le 18 Novembre, 1952)

Par Motoharu TANAKA

Introduction

Le péroxyde d'argent est un oxydant énergique qui a déjà donné des résultats satisfaisants dans le dosage colorimétrique du manganèse[1] et du chrome[2] et dans le dosage volumétrique du cérium.[3] Ce réactif pourra trouver d'autres applications dans la chimie analytique. Nous présentons l'utilisation possible de ce réactif dans le dosage volumétrique du manganèse et du chrome.

Manganèse[4]

Jusqu'à présent on a employé généralement les trois méthodes suivantes pour le dosage volumétrique du manganèse:

1°)[5] Titrage du permanganate qu'on obtient par l'oxydation d'ion manganeux à l'aide d'un oxydant quelconque.

2°)[6] Titrage direct de l'ion manganeux par une solution titrée de permanganate.

3°)[7] Titrage de l'excès de fer ferreux en traitant le bioxyde de manganèse par une solution titrée de permanganate.

Parmi les trois, la première méthode est la plus ordinaire, et on y emploie divers oxydants comme le persulfate d'ammonium, le bismuthate de sodium et le péroxyde de plomb.

Pour ces deux derniers, il faut filtrer l'excès de l'oxydant après oxydation. Quant au persulfate, l'inhabileté peut provoquer la destruction du permanganate formé dans l'ébullition qui est faite pour éliminer l'excès de l'oxydant. De plus, quand on se sert d'acide arséneux pour le titrage direct du permanganate, on observe parfois au terme de la réaction la recoloration due à la destruction incomplète de l'excès de persulfate.

Les résultats suivants ont prouvé que le péroxyde d'argent est applicable au dosage volumétrique du manganèse avec succès.

Réactifs nécessaires

1°) Péroxyde d'argent (en suspension dans l'eau distillée).

2°) Acide sulfurique (1:1).

3°) Solution titrée de permanganate de potassium.

4°) Solution titrée d'oxalate de sodium.

Mode opératoire

A la solution normale d'acide sulfurique qui contient moins de 2 mg. de manganèse,[8] ajouter en agitant du péroxyde d'argent. Après oxydation complète, ajouter de l'acide sulfurique jusqu'à 3N, chauffer sur le bain-marie pendant 2 minutes pour détruire l'excès d'oxydant. Traiter la solution obtenue avec une quantité connue d'une solution centinormale d'oxalate de sodium, dont l'excès sera titré à l'aide d'une solution centinormale de permanganate.

Exactitude de la méthode

Nous avons répété les titrages sur diverses quantités de manganèse. Les expériences nous révèlent que l'on peut estimer la teneur en manganèse avec un écart absolu inférieur à 0,003 mg. Le tableau 1 reproduit les résultats.

Exemples d'analyse

L'analyse de divers aciers nous permet d'établir le tableau 2. L'emploi des deux méthodes ne garantit pas toujours des résultats identiques. Mais l'inspection précise a prouvé qu'il y a, dans le procédé par le persulfate, un certain point difficile, qui nous amène souvent

(1) Y. Murakami, Ce Bulletin, **22**, 159 (1949); M. Tanaka, *J. Chem. Soc. Japan, Pure Chem. sect.*, **72**, 29 (1950).

(2) M. Tanaka, Ce Bulletin, **23**, 165 (1950).

(3) K. Kimura et Y. Murakami, *Mikrochemie*, **36**, 727 (1950).

(4) Ce rapport a été présenté au "Symposium" de la chimie analytique de la Société chimique du Japon ayant lieu à Sendai, le mois de Nov. 1951.

(5) H. D. Hillson, *Ind. Eng. Chem. Anal. Ed.*, **16**, 560 (1944). H. Marshal, *Chem. News*, **83**, 76 (1901). Fred. C. T. Daniels, *Ind. Eng. Chem.*, **6**, 658 (1914). Z. S. Moukhina et N. V. Zolotareva, *Zab. Lab.*, **3**, 881 (1934); *Ann. chim. analyt. chim. appl.* (3) **17**, 216 (1935).

(6) Luciano Barzaghi, *Anais. assoc. quim. Brasil*, **2**, 187 (1943); *C. A.*, **38**, 4214 (1944); M. Marqueyrol et L. Toquet, *Ann. chim. analyt. chim. appl.*, (2), **9**, 289, 324 (1927); J. Pattinson, *J. Chem. Soc.*, **35**, 365 (1879); J. Majdel, *Z. Anal. Chem.*, **81**, 14 (1930).

(7) P. Nicolardot et al., *Compt. rend.*, **170**, 808 (1920).

(8) Il est nécessaire que la concentration de manganèse soit inférieure à 0,05 mg. par centimètre cube. La présence du phosphate favorise l'oxydation du manganèse et en même temps élimine la teinte jaune du fer.

Tableau 1
Exactitude de la méthode (Manganèse)

Mn présent (mg.)	Mn trouvé (mg.)	Ecart absolu (mg.)	Erreur relative (%)
0.081	0.081	0	0
〃	0.080	−0.001	−1.3
〃	0.082	+0.001	+1.3
0.402	0.404	+0.002	+0.5
〃	0.405	+0.003	+0.7
〃	0.403	+0.001	+0.3
0.558	0.557	−0.001	−0.2
0.810	0.810	0	0
〃	0.812	+0.002	+0.3
〃	0.810	0	0
1.620	1.620	0	0
〃	1.618	−0.002	−0.1
〃	1.618	−0.002	−0.1

Tableau 2
Exemples d'analyse (I)

Echantillon	Mn trouvé (%) Méthode du persulfate	Méthode du péroxide d'argent	Remarque
Acier à la silice	0.79[a]	0.787	Cr 0.07%
Acier au tungstène	0.50[b]	0.498	Cr 0.09%
Acier	0.17[a]	0.171	
Acier	0.47[a]	0.503	
		0.502	
Acier au chrome et manganèse	9.66[a]	9.48	Cr18.06%
		9.48	
		9.45	
Acier rapide[c]	0.078	0.0780	Cr 3.87%
Acier au nickel et chrome[c]	0.45	0.454	Cr 0.78%
Gueuse[c]	0.77	0.776	

a) Résultats obtenus à la Faculté des sciences mécaniques, Université de Nagoya.
b) Résultat obtenu à Daido-Seikô Co.
c) Echantillon d'étalon du Japon. Les résultats de l'analyse donnés dans la première colonne sont donc les moyennes de plusieurs valeurs.

à un mauvais résultat, tandis que notre méthode par le péroxyde d'argent facilement donne les meilleurs resultats.

Influences des divers éléments

Parmi les éléments qui peuvent exister dans les échantillons ordinaires, seule une grande quantité de chrome fait obstacle à la méthode du péroxyde d'argent en rendant difficile la perception du terme du titrage. Mais on peut facilement séparer la plupart du chrome d'avec le fer et le manganèse en employant le péroxyde de sodium ou l'eau oxygénée et la soude caustique. L'emploi de l'oxalate tolère la présence d'une petite quantité de chrome.

On peut facilement neutraliser la gêne du chloride par addition simple de l'ion mercurique.[9]

Chrome[10]

Il y a beaucoup de chimistes qui ont essayé le dosage volumétrique et colorimétrique du chrome en se basant sur le fait qu'on peut oxyder le chrome trivalent en hexavalent. L'oxydation du chrome peut être faite dans le milieu alcalin et dans le milieu acide. Pour cette dernière voie d'analyse on emploie divers oxydants énergiques (bromate de potassium,[11] chlorate de potassium,[12] permanganate de potassium,[13] persulfate de potassium en présence de nitrate d'argent,[14] et acide perchlorique[15] etc.). Mais on y rencontre souvent les difficultés, par exemple nécessité de filtration ou de destruction ennuyeuse de l'excès de l'oxydant.

P. F. Urone et H. K. Anders[16] se sont servis avec succès le bismuthate de sodium dans le dosage colorimétrique de cet élément.

Le péroxyde d'argent a pu trouver une nouvelle application, comme on le verra, dans le dosage volumétrique du chrome. Les résultats obtenus ont été satisfaisants comme dans le cas du dosage volumétrique du manganèse.

Réactifs nécessaires

Acide sulfurique (1:1).
Acide phosphorique à 85%.
Péroxyde d'argent en suspension dans l'eau distillée.
Solution titrée de sulfate ferreux.
Solution titrée de permanganate de potassium.
Solution titrée d'oxalate de sodium.

Mode opératoire

On ajoute du péroxyde d'argent à la solution d'acide sulfurique (environ 1N) contenant le chrome (moins de 2 mg.). On la chauffe sur le bain-marie bouillant pendant deux minutes pour éliminer l'excès du péroxyde, Quand une grande quantité de fer existe, il faut décolorer

(9) M. Tanaka, *J. Chem. Soc. Japan. Pure chem. sect.*, **72**, 136 (1950).
(10) Ce rapport a été déjà présenté à l'assemblée annuelle de la Société analytico-chimique du Japon, a Kyoto, au mois d'Octobre, 1952.
(11) I. M. Kolthoff et E. B. Sandell, *Ind. Eng. Chem., Anal. Ed.*, **2**, 140 (1930).
(12) F. H. Storer, *Amer. J. Science*, (2), **45**, 190 (1868).
(13) W. W. Scott, Standard Methods of Chemical Analysis, 5 th Ed., 495 (1939).
(14) H. Pinsl, Archiv f. Eisenhüttenwesen, **10**, 139 (1936). Fred. C. T. Daniel, op. cit. Willard et Young, *Ind. Eng. Chem.*, **20**, 769 (1928).
(15) L. Bertiaux, R. Chataigner et al., *Chim. anal.*, **33**, 129 (1951); S. Schuldiner et F. B. Clardy, *Ind. Eng. Chem., Anal. Ed.*, **18**, 728 (1946).
(16) P. F. Urone et H. K. Anders. *Anal. Chem.*, **22**, 1317 (1950).

la teinte jaune provenant de cet élément par addition de l'acide phosphorique. Sinon, cette coloration gêne plus ou moins la perception du terme du titrage.

Après refroidissement on verse dans la solution oxydée l'excès de la solution titrée de sulfate ferreux. Puis on le titre avec le permanganate de potassium.

Exactitude de la méthode

Nous avons répété les titrages des solutions dont les teneurs en chrome sont 0.2～1.5 mg. Quand il existe plus de chrome que 2 mg., l'oxydation en est incomplète. Nous donnons ci-dessous les résultats:

Tableau 3

Exactitude de la méthode (Chrome)

Cr présent (mg.)	Cr trouvé (mg.)	Ecart absolu (mg.)
1.580	1.578	−0.002
〃	1.583	+0.003
〃	1.580	±0.000
1.056	1.054	−0.002
〃	1.052	−0.004
〃	1.062	+0.006
0.524	0.526	+0.002
〃	0.509	−0.015
〃	0.516	−0.008
0.208	0.208	±0.000
〃	0.213	+0.005
〃	0.210	+0.002
1.056[a]	1.048	−0.005

a) Nous avons ajouté du manganèse. Cet élément, qui est oxydé par le péroxyde d'argent, est ensuite réduit par les gouttes d'une solution centinormale d'oxalate de sodium.

Influences des éléments étrangers

Si le manganèse existe, cet élément est transformé à l'étape permanganique par le péroxyde d'argent. Mais on peut facilement réduire ce permanganate par introduction de l'acide chlorhydrique ou de l'oxalate sans réduction du chromate formé. Donc dans ce dernier cas il suffit de commencer le titrage du chrome après le dosage volumétrique du manganèse, si l'on emploie la méthode présentée plus haut.

La plus grande partie du fer et du manganèse qui co-existent est facilement séparée d'avec le chrome selon les deux manières suivantes:

1° Après la réduction du fer et du manganèse à l'étape bivalente, on ajoute une solution de bicarbonate de sodium à 8% jusqu'au moment ou l'on observe la précipitation, et on y en verse 4 cc. de plus. On fait bouillir pendant une minute. On filtre le précipité rapidement autant qu'il est possible. On peut reprendre tout le chrome dans le précipité.

2° Quand on verse la solution contenant fer, manganèse, chrome et l'excès du phosphate[9] dans la solution bouillante de péroxyde de sodium, fer et manganèse se précipitent et on reprend le chrome dans le liquide filtré.

La présence du vanadium ne gêne pas le dosage.

Exemples d'analyse

Voici les résultats d'analyse des aciers:

Tableau 4

Exemples d'analyse (II)

Echantillons	Cr trouvé (%) Méthode par péroxyde d'argent	Méthode par permanganate	Remarque
Acier à la silice et manganèse	0.073	0.07[a]	Mn 0.79%
Acier au tungstène	0.094	0.09[b]	Mn 0.50%
Acier au chrome et manganèse	18.05 18.05 18.04	18.06[a]	Mn 9.66%
Acier au nickel, chrome et molybdène	1.23	1.20[a]	Mn 0.81%
Acier au nickel et chrome	1.73	1.68[a]	Mn 1.10%
Acier au nickel et chrome[c]	0.780	0.78	Mn 0.45%
Acier rapide[c]	3.86 3.88 3.88	3.87	Mn 0.078%

a) Résultats obtenus à la faculté des sciences mécaniques, Université de Nagoya.
b) Résultat obtenu à Daidô-Seikô Co.
c) Echantillons d'étalon du Japon. Les resultats de l'analyse donnés dans la deuxième colonne sont donc les moyennes de plusieurs valeurs.

On peut comparer les résultats par le péroxyde d'argent avec ceux par le permanganate de potasse.

Résumé

Nous avons présenté l'utilisation possible du péroxyde d'argent pour le dosage volumétrique du manganèse et du chrome. Nous résumons notre étude:

1°) Même les débutants peuvent employer cette méthode qui assure les résultats exacts.

2°) Le péroxyde d'argent est suffisamment puissant, et l'oxydation par ce réactif et la

(17) Evans, *Analyst*, **46**, 285 (1921). La présence de l'excès du phosphate protège de chrome de co-précipiter avec le fer.

destruction de son excès sont complètes.

3°) Comme il a été déjà indiqué,(1) la durée de conservation du péroxyde d'argent est presque infinie (on peut l'employer sans aucun souci de son changement même un an après la préparation).

4°) Le titrage de l'excès d'oxalate de sodium permet la présence d'une quantité de chrome telle qu'elle ne fait pas obstacle par l'intensité de sa coloration jaune. Aussi, peut-on estimer le manganèse et le chrome simultanément.

Nous ne voulons pas manquer, en terminant, de remercier cordialement Monsieur le Professeur Sugawara qui nous a encouragé pendant cette recherche et Monsieur le Professeur Hirano qui a mis à notre diaposition des échantillons d'acier nécessaires.

Institut de chimie, Faculté des Sciences,
Université de Nagoya

On the Ring-Opening Reactions of the Furan Compounds. I. The Synthesis of 1, 4-Pentadien-3-one-1, 5-dicarboxylic Acid from 2-Furanacrylic Acid

By Hiroshi MIDORIKAWA

(Received January 13, 1953)

In the ring opening of furan compounds by hydrogen peroxide, 2-furanacrylic acid behaved peculiarly, by giving 1,4-pentadien-3-one-1,5-dicarboxylic acid in fairly good yield. This reaction is analogous to the bromine and subsequent silver oxide oxidation(1) by which 2-furanpropionic acid gives furonic acid as illustrated below:

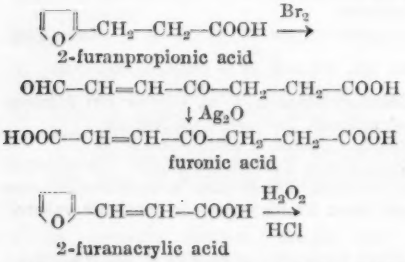

Straus(2) had already synthesized it from 2,4-dibromopentan-3-one-1,5-dicarboxylic acid methyl ester. He reported that the acid decomposes "stürmisch" at 230° and its methyl ester is acted upon by sunlight. In this experiment, the acid decomposed gently at 236°, and pale yellow crystals of the methyl ester were changed to white granular crystals by exposure to direct sunlight. But the photochemical change took place also with the free acid. That is to say, the acid of pale yellow crystals was changed to an acid of hygroscopic white powder by direct sunlight, the methyl ester of which was identified with the 1,4-pentadien-3-one-1,5-dicarboxylic acid methyl ester exposed to direct sunlight. Since it had already been reported that the methyl ester is polymerised to a dimer by direct sunlight,(3) the free acid may be polymerised to a dimer.

On reducing the acid by aluminium amalgam, γ-ketopimelic acid was obtained. By potassium permanganate oxidation, the acid gave oxalic acid and fumaric acid, but no maleic acid. It is assumed, therefore, that two double bonds of the acid have the trans structure as follow:

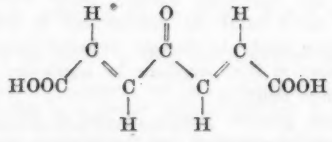

Its carbonyl group reacted upon phenylhydrazine with formation of phenylhydrazone.

α-Methyl-β-(2-furyl)-acrylic-acid, α-phenyl-β-(2-furyl)-acrylic acid and α-cyano-β-(2-furyl)-acrylic acid did not undergo such a furan ring opening by hydrogen peroxide.

(1) A. Baeyer, *Ber.*, **10**, 535 (1877).
(2) F. Straus, *Ber.*, **37**, 3297 (1904).
(3) H. Stobbe and E. Färber, *Ber.*, **58**, 1551 (1925).

Experimental

1,4-Pentadien-3-one-1,5-dicarboxylic acid.—Furanacrylic acid 4.8 g. was suspended in a mixture of 40 cc. 35% aqueous hydrogen peroxide and 5 cc. conc. hydrochloric acid, and the vessel was kept for five days in water at room temperature (about 28°), when orange crystals were formed at the bottom. The cyrstals were filtered and washed with methanol to remove unchanged furanacrylic acid. Yield, 2.2 g. From the filtrate was obtained 0.3 g. of the acid by concentration on the water-bath. The resulting acid was dissolved in boiling water, decolourized by active charcoal and crystallised in pale yellow hexagonal plates on cooling. It melted at 236° with decomposition.

	H	C
Anal. Calcd. for $C_7H_6O_5$:	3.55	49.39
Found:	3.53	49.38

When the acid dissolved in a mixture of phenylhydrazine and acetic acid was left overnight, the phenylhydrazone crystallised out. It formed red needles by recrystallisation from a mixture of methanol and water; m. p. 182-3°.

	H	C	N
Anal. Calcd. for $C_{13}H_{12}O_4N_2$:	4.61	59.97	10.76
Found:	4.52	59.48	10.56

1,4-Pentadien-3-one-1,5-dicarboxylic acid methyl ester.—0.5 g. of the acid was esterified by refluxing for thirty minutes with 3 cc. methanol and 0.2 g. conc. sulfuric acid. On cooling the whole the methyl ester was separated out and recrystallised in pale greenish yellow needles from ethyl acetate; m. p. 171-2°.

	H	C
Anal. Calcd. for $C_9H_{10}O_5$:	5.08	54.52
Found:	5.01	54.57

Its phenylhydrazone was obtained by the same method as the acid, and recrystallised from methanol; lustrous yellow leaflets; m. p. 153-4°.

	H	C	N
Anal. Calcd. for $C_{15}H_{16}O_4N_2$:	5.59	62.45	9.71
Found:	5.25	62.11	9.48

3-Pentanone-1,5-dicarboxylic acid (γ-ketopimelic acid).—To the 20 cc. aqueous solution of the 1 g. acid neutralised by sodium carbonate, was added 0.2 g. aluminium amalgam and left at room temperature for a day. After filtering off aluminium hydroxide, the filtrate was acidified with hydrochloric acid and evaporated to dryness on the water-bath. From the residue, γ-ketopimelic acid was extracted with methanol and recrystallised from a mixture of methanol and chloroform. Yield, about 0.1 g., m. p. 142-3°.

	H	C
Anal. Calcd. for $C_7H_{10}O_5$:	5.79	48.25
Found:	5.57	48.25

Oxidation of 1,4-pentadien-3-one-1,5-dicarboxylic acid.—To 1.7 g. of the acid suspended in 50 cc. water was added drop by drop with stirring at about 15° a potassium permanganate solution which consisted of 5 g. potassium permanganate and 70 cc. water. After about thirty minutes, the reaction was over. The reaction mixture was filtered, neutralised with acid, concentrated on the water-bath and shaken up with ether upon acidification. From the ether solution were obtained two compounds. The one was soluble in water and melted at 100-1°. Yield, 0.1 g.. The mixed melting point of oxalic acid with it showed no depression. The other was insoluble in water and melted at 275° in a sealed tube. Yield, 0.1 g. It was identified with fumaric acid.

	H	C
Anal. Calcd. for $C_4H_4O_4$:	3.47	41.36
Found:	3.73	41.39

Photochemical changes of 1,4-pentadien-3-one-1,5-dicarboxylic acid and its methyl ester.—The methyl ester placed in a covered glass vessel was exposed to direct sunlight for a few hours with frequent stirring. The pale greenish yellow crystals of methyl ester changed into a white powder. It was recrystallised in colourless rhombs from ethyl acetate and melted at 239° with decomposition as reported by Straus. Similarly, the acid changed into a hygroscopic white powder by exposure to direct sunlight. The recrystallisation was unsuccessful. It melted at about 221° with decomposition.

	H	C
Anal. Calcd. for $C_7H_6O_5$:	3.55	49.39
Found:	3.87	48.59

0.5 g. of the acid sufficiently exposed to sunlight was esterified by refluxing for thirty minutes with 3 cc. of methanol and 0.3 g. of conc. sulfuric acid. The methyl ester crystallised out and was recrystallised from ethyl acetate. It formed colourless rhombs and melted at 237° with decomposition.

	H	C
Anal. Calcd. for $C_9H_{10}O_5$:	5.08	54.52
Found:	4.86	54.00

The mixed melting point of this methyl ester and the photochemically changed methyl ester showed no depression.

Summary

2-Furanacrylic acid gave 1,4-pentadien-3-one-1,5-dicarboxylic acid in a fairly good yield by treatment with aqueous hydrogen peroxide containing hydrochloric acid. This acid underwent the same photochemical change by direct sunlight as its methyl ester.

This acid was reduced to γ-ketopimelic acid by aluminium amalgam, and oxidised to fumaric and oxalic acids by potassium permanganate. It is assumed that the two double bond have the trans structure. The phenylhydrazones of the acid and the methyl ester were obtained.

The Scientific Research Institute, Tokyo

The Visible Absorption Spectra and Binding Energy of Quinhydrone-Type Molecular Compounds

By Hiroshi TSUBOMURA

(Received February 17, 1953)

Introduction

Although quinhydrone and homologous molecular compounds have been well known for many years, the nature of the intermolecular binding force has not yet been thoroughly clarified. Recently, some interesting results concerning this problem have been obtained. Osaki and Matsuda[1] have, through the analysis of the x-ray pattern of quinhydrone crystal, determined the structure of this compound. K. Nakamoto[2] observed the dichroism of the visible absorption spectra of quinhydrone crystal, and found that "the spectrum by the light with the electric vector abundant with the parallel component to the benzene ring is more bathochromic and hyperchromic than the one with the electric vector abundant with the perpendicular component to the benzene ring". Seki and others[3] determined the heat of formation of quinhydrone from its component-molecules as 5.39 kcal./mol. by the measurements of the heat of solution and the vapor pressure. This would be the first reliable experimental data of the binding energy of this compound.

The present author has determined the heat of association of quinhydrone and some homologues in dilute solutions by measuring quantitatively the absorption spectra of the solutions of quinone and the compounds which combine with it (in this research, hydroquinone, dimethylhydroquinone and phenol, hereafter called B compounds) in various concentrations and temperatures. The visible absorption spectra of these systems in various concentrations were measured by L. Michaelis and S. Granick. They treated the results with the theory of chemical equilibrium and reported that the molecular compounds in solutions are in a dimeric form, $Q_1 \cdot B_1$, without regard to their compositions in the solid state. However, they had no intention of deriving the heat of association from these measurements, though the determination of these values is, in principle, possible.

In the second part of this paper, a structure of these molecular compounds will be proposed on the basis of some experimental knowledge concerning these compounds. On this assumed structure, the origin of the binding force and the visible absorption spectra of these molecular compounds are discussed.

Part I. The Determination of the Heat of Association in Solution by the Measurements of the Visible Absorption Spectra

Principle of the Experiment

The principle of deriving the experimental equilibrium constant of association and the molecular extinction coefficient of the molecular compound is the same as that which was employed by Benesi and Hildebrand.[4] Namely, if we designate the total molar concentration of quinone and a B compound by c^0_Q and c^0_B, the extinction coefficient of the molecular compound by d_X, and its molecular extinction coefficient by ε_X, then the linearity relation

$$c^0_Q/d_X = 1/(K \cdot \varepsilon_X \cdot c^0_B) + 1/\varepsilon_X \qquad (1)$$

(1) Osaki and Matsuda, *Acta Cryst.* (to be published). Their results were quoted in Nakamoto's paper (ref. (2)).
(2) K. Nakamoto, *J. Am. Chem. Soc.* **74**, 1738 (1952).
(3) S. Seki, *Kagaku*, **22**, 416 (1952). Detailed information will be published in the near future in this bulletin.
(4) H. A. Benesi and J. H. Hildebrand, *J. Am. Chem. Soc.*, **71**, 2703 (1949).

holds between (c^0_Q/d_X) and $(1/c^0_B)$, if the equilibrium is expressed by the formula $Q+B \rightleftarrows QB$ and if $c'_Q \ll c^0_B$. We found that equation (1) really holds for all molecular compounds we investigated, agreeing with Michaelis' results. Then, we can calculate the equilibrium constant K and the molecular extinction coefficient ε_X using the least square method.

Since quinone, unfortunately, has absorption in the visible region, it is necessary to select some wave lengths which are most suitable for the experiment, i. e., wave lengths, in which the absorption of the molecular compound is sufficiently strong and the absorption of quinone is negligibly small. In the case in which the absorption of quinone is not small enough to be ignored even in the most suitable region of wave length, d_X was calculated by the formula

$$d_X = d_{obs} - d'_Q - d^0_B \qquad (2)$$

where d^0_Q and d'_B are the absorption of the total quinone and the B compound present in the solution including those which are associated. These d^0_Q and d^0_B were calculated from the molecular extinction coefficients of these compounds in a free state and their concentrations in each ternary system.* Of course, we should use d_Q and d_B that are the absorption of free quinone and the B compound present in the system instead of the d^0_Q and d^0_B. However, the small magnitude of d^0_Q and d^0_B as compared to d_X and the small degree of association of the molecular compounds reasonably permit the approximation.

The heat of association ΔH can be determined from the equilibrium constants at two different temperatures by use of the following formula

$$\Delta H = -RT_1 \cdot T_2/(T_1-T_2) \cdot \ln K_1/K_2 \qquad (3)$$

Experimental

Spectrophotometric measurements were made with the Beckman spectrophotometer, Model DU.

The solvent used should have the following properties:

1. Its absorption in the visible region is negligible.
2. It dissolves considerable amounts of the compounds under the investigation.
3. It has no particular influence on the association of the molecular compounds.

Cyclohexane was used as a solvent which generally fulfills these conditions. However, only for the case of quinone-hydroquinone system, 0.05M. aqueous solution of hydrogen chloride was used, since hydroquinone is quite insoluble in cyclohexane. It is known that hydroquinone dissolved in water is a little unstable under the contact of air. However, we can believe that this compound remained unchanged in such a dilute acid as above mentioned during the spectrophotometric measurements, because it was verified that the ultraviolet absorption spectrum of this compound in such a solution did not change at all for at least 30 hours.

The method of purification of cyclohexane and phenol was described elsewhere.[6] Quinone was synthetized by the oxydation of hydroquinone by sodiumbichromate,[7] and recrystalized several times out of benzene (m. p. 114—115°C). Hydroquinone was recrystalized from mixtures of benzene and methanol (m. p. 172—173°C). Dimethylhydroquinone was recrystalized from methanol (m. p. 56.0—56.2°C). The ultraviolet absorption spectra of all these compounds were checked before experiment and identity of them with the results described in literatures was confirmed.

During the measurement of absorption, the constancy of the temperature of the samples was maintained by use of a thermospacer equipped in the spectrophotometer (±1°C). Stoppered cells, which were 1 cm in width, were used.

Results

The approximate ranges of the concentrations of quinone and the B compounds in each spectrophotometric measurements were given in Table 1. These ranges of concentration were chosen so that the extinction coefficients of the ternary systems at the optimum wave lengths lie between 1 and 2. In order to apply Eq. (1), the concentration of the quinone were always made below 10% of that of the B compounds. This also decreases the error due to the visible absorption of quinone.

Table 1

	concn. of quinone	concn. of B
1	0.0033 M	0.05—0.46 M
2	0.0045 M	0.06—0.4 M
3	0.003 M—0.007 M	0.15—1.2 M

1: quinone-hydroquinone system
2: quinone-phenol system
3: quinone-dimethylhydroquinone system

For the purpose of testing the accuracy of the values derived, the same experiments were made for more than two wave lengths. The results were shown in Table 2. Since in the cases of the quinone-phenol and quinone-dimethylhydroquinone systems the attempt to derive ε_X's for the higher temperatures was unsuccessful, ε_X's for the lower temperatures were used in the calculation of K's for the higher temperatures, by the assumption that there is no great difference between ε_X's foe these two temperatures respectively. Although the values given in this table

* In this calculation, it was assumed that the absorption spectra of quinone and the B compounds are not shifted from those in a free state. This assumption is necessary, but, strictly speaking, is not in general true. For example, hydrogen-bonding between quinone and a B compound may cause a slight shift of their spectra.

(5) H. Tsubomura, *J. Chem. Soc. Japan*, **73**, 920 (1952).
(6) Organic Syntheses, **1**, 469.

Table 2

The ε_1, K_1 and the ε_2, K_2 correspond to the data for lower and higher temperatures respectively

B compound	wave length (in mμ)	ε_1	ε_2	K_1	K_2	K_1/K_2	ΔH (kcal./mol.)
hydroquinone	500	630	730	1.01	0.49	2.1	4.8
	520	510	600	1.10	0.46	2.4	5.7
phenol	330	1180	1180	1.23	0.71	1.7	4.4
	350	1110	1110	1.11	0.57	1.9	5.0
	400	850	850	1.06	0.56	1.9	5.0
dimethyl-hydroquinone	380	340	340	0.51	0.30	1.7	4.2
	390	310	310	0.69	0.43	1.6	3.8
	400	355	355	0.61	0.43	1.4	2.7

Table 3

B compound	solvent	K_1 (t°C)	K_2 (t°C)	K_1/K_2	ΔH (kcal./mol.)	λ_{max} (mμ)	ε_{max}
hydroquinone	0.05 M HCl aq. solution	1.06 (20°)	0.48 (49°)	2.2	5.2	440	890
phenol	cyclohexane	1.13 (16°)	0.61 (39°)	1.9	4.8	315	1200
dimethyl-hydroquinone	cyclohexane	0.60 (25°)	0.39 (49°)	1.6	3.5	413	370

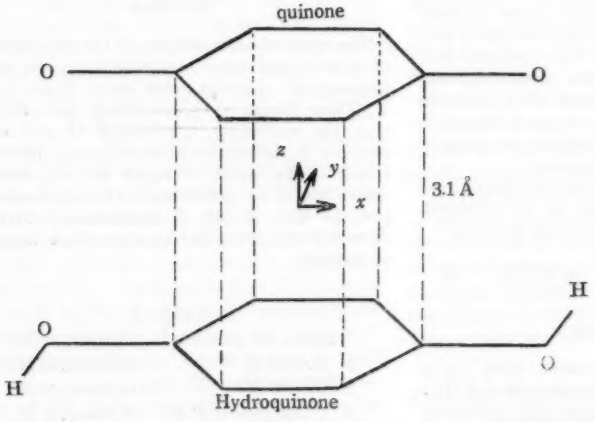

Fig. 1.

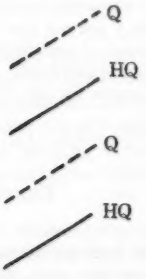

Fig. 2

are not perfectly accurate, it may be regarded that they show us the general trends of the binding energies and the absolute intensities of the visible absorption of these molecular compounds. The average values of K_1, K_2, K_1/K_2 and ΔH, with λ_{max} and ε_{max} which were obtained from the measurements of the whole spectra were given in Table 3.**

Detailed discussion on these results will be given in the second part of this paper with the theoretical treatment of these molecular compounds.

** It is to be noted here that we should be careful in comparing the heat of association of quinone-hydroquinone system with that of quinone-phenol system because these two were measured in different solvents.

Part II. Theory of the Intermolecular Binding Energies and the Electronic States of Quinhydrone and Homologous Molecular Compounds

The molecular structure of quinhydrone and homologues

As previously mentioned, quinhydrone and homologous molecular compounds in dilute solutions are of the form $Q_1 \cdot B_1$. We assume the structures of these associated molecules as those in which two benzene rings are piled up so that one ring is situated just above the other and the planes of these two rings are parallel. For example, the structure of quinhydrone is assumed as given in Fig. 1.

The basis of this assumption is as follows: The

occurance of a new visible absorption in these molecular compounds shows that there is considerable electronic interaction between molecules. Therefore, the structure of the molecular compound must be assumed in such a way as to make an electronic interaction between molecules possible. The structure shown in Fig. 1 will correspond to the strongest electronic interaction and smallest steric repulsion between two component-molecules. On the other hand, the X-ray analysis of Osaki and Matsuda shows that, in the quinhydrone crystal, the quinone and hydroquinone molecules are piled up one upon another in a way shown in Fig. 2; this structure differs from the one shown in Fig. 1 in that the benzene ring of, e. g., quinone is not situated just above the benzene ring of, e. g., hydroquinone. It may be conceived that this deformation is caused by the complicated interacting forces between every atom in the crystal. However, in a dilute solution, where the quinhydrone molecules are separated from each other, there is no reason for the centers of the two benzene rings not to lie on a common normal.

Here, a note on the binding state of the hydrogen atom in quinhydrone should be given. M. Davies[6] measured the infrared absorption spectra of quinhydrone crystal in the 3 μ region and found a peak at 3.10 μ corresponding to the hydroxyl stretching mode. Applying Badger's rule, he was lead to the conclusion that the hydroxyl bond distance is about 1.0Å, which is nearly the same as that of alcohol. According to his results, it is reaonably accepted that the two hydrogen atoms in quinhydrone are definitely bonded to the oxygen atoms, and it is improbable that a peculiar valency state exists in which the hydrogen atoms are equally bonded to the two molecules. In other words, quinhydrone is made up of quinone and hydroquinone molecules which are mutually perturbed.

The nature of the binding energies of quinone and the B compounds

It can be definitely concluded that hydrogen bonding is not a substantial cause of the binding of quinone and the B compounds, from the fact that some compounds which have no group acting as a proton donor, e. g., dimethylhydroquinone, can also combine with quinone.

If we assume the structures of the molecular compounds to be as shown in Fig. 1, it will be clear that a hydrogen bond is unable to form between two component-molecules. For the hydroxyl group in a normal hydroquinone or phenol lies in the plane of benzene ring and, therefore, is nearly perpendicular to the line connecting the two oxygen atoms of quinone and hydroquinone or phenol. It is evident that in such a structure a hydrogen bond cannot be formed, since this bond is believed to be mainly electrostatic. If the hydrogen atom of hydroquinone elevates itself from the plane of the ring, hydrogen bond would be formed. However, in this case the conjugation of the lone pair electron of oxygen with the benzene π-electrons which give rise to a considerable stabilization of the hydroquinone molecule would be destroyed. Of course, it is supposed that there are hydrogen-bonded quinone and hydroquinone or phenol molecules in a dissolved state. However, the hydrogen bond will probably be formed between molecule-pairs which, different from those of which molecular compound is composed, are situated in such a manner as shown in Fig. 3. We can suppose that the electronic interaction

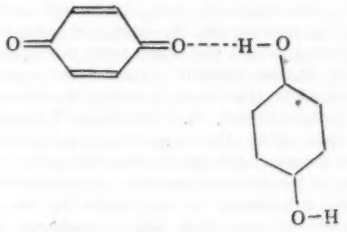

Fig. 3.

between these hydrogen-bonded molecules is negligibly small, and therefore the visible absorption spectra cannot arise from them. As the heat of association given in Table 3 is derived from visible absorption spectra, and the formation of a hydrogen bond is supposed not to disturb that of quinhydrone, we may conclude that the energy of the hydrogen bond is not included in the heat of association given in Table 3.

Briegleb and others[9] have laid stress on the so-called "Dipolinduktions-effekt" in interpreting the association of aromatic nitro-compounds and aromatic hydrocarbons. They insisted that this dipole-induction effect, together with the dispersion force which is an intermolecular binding force working more or less between every pair of molecules, are the main causes of binding in these molecular compounds. It seems, however, that this theory cannot fully explain the intermolecular binding force of quinhydrone.

The author calculated roughly the energy contribution of the dipole-induction effect for quinhydrone based on the molecular structure shown in Fig. 1. It consists mainly of the force between the dipole of the carbonyl group of quinone (about 3.8 *D*) and that of hydroquinone induced by it, and is estimated as about -1 kcal./mol. On the other hand, the interaction between permanent dipoles of quinone and hydroquinone is estimated to be about $+0.8$ kcal./mol., and almost cancels the energy of attraction of the dipole-induction effect. Also, there seems to be no reason why

(7) M. Davies, *J. Chem. Phys.*, **8**, 577 (1940).

(8) G. Briegleb, "Zwischenmolekulare Kräfte und Molekülstruktur", Ferdinand Enke, Stuttgart, 1937, p. 104.

the dispersion force between quinone and the *B* compounds should be particularly greater than those between others which are known to make no molecular compounds.* Moreover, the dipole-induction effect, or other electrostatic interaction cannot explain the change of the absorption spectra with the formation of the molecular compounds.

Theory of electronic interaction

The measurements of the static dielectric polarization of benzene-iodine mixtures,[10] or other similar systems[11] strongly suggest that the intermolecular binding of these molecular compounds is of some kind of a coordination linkage, that is, the molecular compounds are made up of two molecules, one of which has a low ionization potential and the other has a strong electron affinity, and an electron of the former is partially transferred to the latter, forming an intermolecular covalent bond. R. S. Mulliken[12] formulated this idea using the quantum-mechanical resonance theory and explained the absorption spectra of the molecular compounds. In order to test whether this theory is applicable to the quinhydrones or not, the author made a semi-quantitative treatment of the electronic states of these molecular compounds using molecular orbital method, and compared the results with absorption data.

To proceed the theoretical analysis, it is first necessary to know the electronic states of free quinone and the free B compounds. Among the electronic orbitals of quinone and B compounds, only π-orbitals are important here because the intermolecular interaction between the σ- and inner shell orbitals of quinone and the *B* compounds are far smaller than those between π-orbitals. First, the quinone-hydroquinone system is discussed.

Quinone-hydroquinone system

The π-molecular orbitals of quinone and hydroquinone constructed by the linear combination of $2p\pi$-AO's of carbon and oxygen atoms have been calculated by Nagakura and Kuboyama[13] with a simple LCAO method, using resonance integrals and coulomb integrals which are suitably made self-consistent.** The energy levels of the MO's derived by them are given in Fig. 4. Quinhydrone belongs to the symmetry group C_{2v} in our assumed structure, and therefore there are four

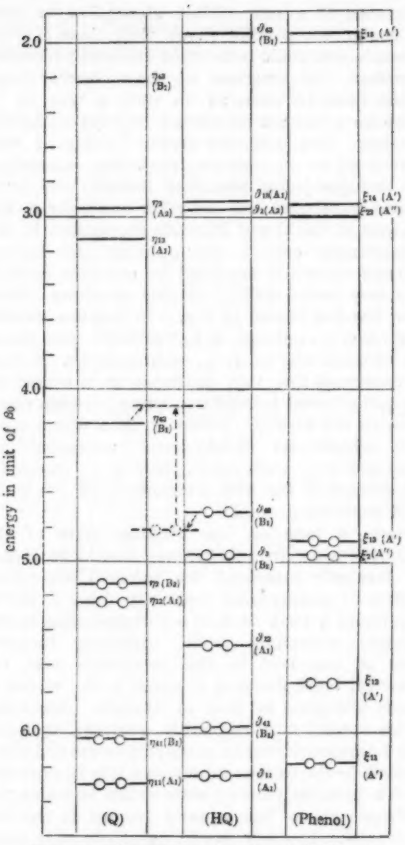

Fig. 4.—The energy levels of MO's of quinone, hydroquinone and phenol

irreducible representations A_1, A_2, B_1 and B_2.[14] The names of the irreducible representations to which each MO belongs are also given in Fig. 4. It is to be noted that the MO's of quinone and hydroquinone are very much alike since these are constructed by AO's which are similar in position as well as in number, the only difference between these two molecules being that an oxygen atom of hydroquinone has two π-electrons while that of quinone has but one. As a result, the MO of hydroquinone denoted as ϑ_{42} in Fig. 4 is a filled orbital, while the corresponding MO of quinone denoted as η_{42} is an empty one, and this difference gives slight modifications of all MO's of the one molecule as compared to the latter. Now, it can be supposed easily from experimental evidences that, relatively speaking, hydroquinone has a low ionization potential and quinone has a

* Here, we regard the dispersion force as expressible in the formula of $U=-I_1 \cdot I_2/(I_1+I_2) \times (\alpha_1 \cdot \alpha_2) \times 3/2R^6$.

(9) F. Fairbrother, *J. Chem. Soc. (London)*, **1948**, 1051.

(10) J. Weiss and H. Kronberger, *J. Chem. Soc. (London)*, **1942**, 245.

(11) R. S. Mulliken, *J. Am. Chem. Soc.*, **74**, 811 (1952).

(12) S. Nagakura and A. Kuboyama (*unpublished results*).

** The same method was used in the calculation of the energy levels of furan, pyrrole and thiophen. See, "S. Nagakura and T. Hosoya, This Bulletin, **25**, 179 (1952)".

(13) Here the notations are the same as those used by Eyring et al. See, "Eyring, Walter and Kimball, Quantum Chemistry, Appendix VII". The operation σ_v is taken as the reflection in the plane including four oxygen atoms.

strong electron affinity. This corresponds to the fact that the difference between the energies of ϑ_{12} and η_{12} is small. (See, Fig. 4). In addition, these two orbitals belong to the same irreducible representation in the over-all symmetry of the molecular compound. From these facts, it can be seen that an intermolecular conjugation between ϑ_{12} and η_{12} (which results an partial migration of an electron that is originally occupying ϑ_{12} to η_{12}) is easily produced. And, in the first approximation, only the consideration of this conjugation is sufficient in the treatment of the intermolecular conjugation as a whole.

The reason for this is given briefly as follows: Since migration is possible only between two MO's belonging to the same irreducible representation, we can see that the following intermolecular migrations of electrons from hydroquinone to quinone may be possible,

$$\vartheta_{12}\rightarrow\eta_{12},\ \vartheta_{11}\rightarrow\eta_{12},\ \vartheta_{12}\rightarrow\eta_{13},\ \text{etc.}$$

But these migrations are thought to be far less possible than that of $\vartheta_{12}\rightarrow\eta_{12}$, because in such cases the energy difference between MO's are much greater than that between ϑ_{12} and η_{12}. Next, we should note that intermolecular conjugations may occur between two filled orbitals of hydroquinone and quinone, e. g., ϑ_3 and η_3, ϑ_{12} and η_{12} etc. However, such conjugations between filled orbitals produce no effect but an increase of total electronic energy, which, as Parr and Mulliken have pointed out,[14] is attributable to the exchange repulsion between molecules.

Now we can set up the total electronic wave function of quinhydrone in the ground state as an anti-symmetrized product of one-electron MO's.

$$\Psi_g = n_g(18!)^{-1/2}\sum_{p}(-1)^p \mathrm{P}\,\eta_{11}(1)\eta_{11}(2)\eta_{12}(3)\eta_{12}(4)$$
$$\cdots\cdots\vartheta_{11}(9)\vartheta_{11}(10)\vartheta_{12}(11)\vartheta_{12}(12)\cdots\cdots$$
$$\phi_g(17)\phi_g(18)\times\alpha_1\beta_2\alpha_3\beta_4\cdots\cdots\alpha_{17}\beta_{18} \quad (4)$$

$$\phi_g(\nu) = a_0\vartheta_{12}(\nu) + b_0\eta_{12}(\nu) \quad (5)$$

Since a complete treatment of the MO's including eighteen electrons is extremely difficult, we are ought to be satisfied by a simple approximation in which the energy of the migrating electrons is expressed as

$$E(\nu) = \int \phi(\nu) H_\nu \phi(\nu) d\tau_\nu \quad (6)$$

Here, H_ν is the total hamiltonian for the migrating electron including the kinetic energy operator of an electron, the potentials of atomic cores and other electrons. Then, the minimization of $E(\nu)$ leads to the secular equation,

$$\begin{vmatrix} W_{12}-E & \beta \\ \beta & W'_{12}-E \end{vmatrix} = 0 \quad (7)$$

where W_{12} and W'_{12} are the coulomb integrals of the MO ϑ_{12} and η_{12}, respectively, and β is the resonance integral over them. Solving (7), we get the lower and upper roots, E_g and E_e;

$$E_{g,e} = (W_{12}+W'_{12})/2 \pm \{(\Delta W/2)^2+\beta^2\}^{1/2} \quad (8)$$

in which, $\Delta W = W'_{12}-W_{12}$. a_0 and b_0 can be immediately calculated from E_g. We get another wave-function ϕ_e corresponding to the upper level, E_e. This is approximately given by the following formula.

$$\phi_e = b_0\vartheta_{12} - a_0\eta_{12} \quad (9)$$

As is shown lately, a_0 is nearly one and b_0 is far smaller than a_0. Hence, it can be said that ϕ_g is much alike to ϑ_{12} and ϕ_e is much alike to η_{12}. Therefore, if we assign the visible absorption of quinhydrone to the transition from ϕ_g to ϕ_e, it has the character of an intermolecular charge-transfer spectra and agrees with Nakamoto's experimental results (ref. (2)). Other transitions of this molecular compound which have the electric moment normal to the benzene rings cannot be found in this region of wave length.

Next, we will calculate the transition moment of this transition. The total electronic wave function of quinhydrone in the singlet excited state is given in a way similar to (4).

$$\Psi_e = n_e(18!)^{-1/2}\sum_{p}(-1)^p \mathrm{P}\eta_{11}(1)\eta_{11}(2)\eta_{12}(3)\eta_{12}(4)$$
$$\cdots\cdots\vartheta_{11}(9)\vartheta_{11}(10)\vartheta_{12}(11)\vartheta_{12}(12)\cdots\cdots$$
$$\phi_g(17)\phi_e(18)\times\alpha_1\beta_2\alpha_3\beta_4\cdots\cdots$$
$$(2)^{-1/2}(\alpha_{17}\beta_{18}-\alpha_{18}\beta_{17}) \quad (10)$$

The transition moment μ is, for definition, given by

$$\mu = e\int \Psi_e^*(\sum_{\nu=1}^{n} x_\nu)\Psi_g d\tau \quad (11)$$

As a result of calculation, μ is approximately given by

$$\mu \fallingdotseq e a_0^2 b_0 R/\sqrt{2} \quad (12)$$

in which R being the distance between two molecules. From (8), we can see that a_0^2 and b_0 depend on β and ΔW. Since resonance integrals are in many cases proportional to the corresponding overlap integrals, we calculated the overlap integral between ϑ_{12} and η_{12} in order to know the magnitude of β. This can be expanded in terms of overlap integrals between AO's and can be easily calculated. If we use Slater type AO's with screening constants $z_c=3.25$, $z_o=4.55$, the result was 0.043. Then, we calculate β from the resonance integral β_0 and the overlap integral s_0 between two adjacent carbon atoms of benzene in the following way,***

(14) Parr and Mulliken, *J. Chem. Phys.*, **19**, 1273 (1951).

*** Such a procedure is often used in the calculation of the resonance integrals between two π-orbitals. Though we are here dealing with resonance integrals between two σ-orbitals, the situation is conceivable to be nearly the same.

Table 3

(The unit of W's is in β_0)

ΔW	$\Delta E(=E_e-W'_{42})$	a_0	b_0	μ_{calc}	E_e-E_f	f_{obs}	μ_{obs}
$\beta=0.2\ \beta_0$							
0.5	0.070	0.945	0.331	2.94 D	0.64 (6800 Å)	0.014	1.14
0.7	0.055	0.963	0.265	2.49 D	0.81 (5370 Å)		
0.9	0.044	0.978	0.216	2.13 D	0.99 (4390 Å)		
1.1	0.035	0.985	0.172	1.73 D	1.17 (3720 Å)		
$\beta=0.1\ \beta_0$							
0.9	0.012	0.992	0.119	1.22 D	0.92 (4740 Å)		

$$\beta=\beta_0\times s/\varepsilon_0$$

we get $\beta=0.17\ \beta_0$. It was suggested by Mulliken and others that the overlap integral between bonded atoms or molecules is supposed to be greater than that which is calculated from the Slater AO's. Therefore, in this case, we tentatively assume that β is the order of $0.20\ \beta_0$. The estimation of ΔW is also difficult. But, fortunately, the variation of this does not influence the transition moment significantly. We estimated that it lies in a region from 0.5 to $1.0\ \beta_0$*, and calculated various a_0, b_0 values using various ΔW in this region. From these values, the transition moment μ can be calculated. On the other hand, experimental oscillator strength was calculated from the absorption data in solution using the following formula,

$$f_{obs}=(nc^2m/N\pi e^2)\times 10^{8}\int\varepsilon d\nu^{(15)}\fallingdotseq 0.1875\times 10^{-8}n\varepsilon_{max}\cdot\Delta\nu \quad (13)$$

in which n is the index of refraction of the solution and $\Delta\nu$ is the distance between two points in the absorption curve at which the intensity is half the maximum value. Applying the Lorentz-Lorenz correction to this,[16] we can get f_{obs} in gaseous state, and from it the μ_{obs} can be calculated. The calculated and experimental μ's are given in Table 3. The transition energy depends mainly on ΔW, and the value of ΔW which gives a transition energy most close to the experimental one is seen to be $0.9\ \beta_0$. For reference, the oscillator strengths using $\beta=0.10\ \beta_0$ are also given using $\Delta W=0.9\ \beta_0$. These results show that the charge transfer spectra proposed here may have sufficiently strong oscillator strength to be correlated with the values experimentally obtained.

Although it is dangerous to refer to the total π-electronic energy of the molecular compound from the simple MO theory, it can be supposed that this intermolecular conjugation between filled and unfilled MO's will produce a decrease of electronic energy. If this is true, such a decrease of electronic energy by intermolecular conjugation will be the most characteristic part of the intermolecular binding energy of these molecular compounds.

Other quinhydrone-type molecular compounds

The π-electronic state of dimethylhydroquinone is quite similar to that of hydroquinone. Hence, we can expect that the π-electronic interaction between quinone and dimethylhydroquinone is also quite similar to that of quinone-hydroquinone system. From the experimental results shown in Part I., it can be seen that the molecular compound of dimethyl hydroquinone has a considerably lower absorption intensity and binding energy than that of hxdroquinone. This can be understood in the following way. The intermolecular distance of this molecular compound is supposed to be made larger than in the case of hydroquinone because the methyl group will considerably increase the steric repulsion between molecules. The resonance integral between ϑ_{12} and η_{42} will become smaller owing to the large intermolecular distance, and this will decrease the intensity of the charge transfer spectra and the charge transfer force.

In order to discuss the case of quinone-phenol molecular compound, we should know the electronic state of phenol. The author calculated the LCAO MO energy levels of phenol by use of the same method as was adopted in the calculation of quinone and hydroquinone. The energy levels obtained are given also in Fig. 4. We assume that the symmetry group of quinone-phenol molecular compound is C_{1h} (see, ref. (14)), that is, it has only one plane of symmetry (xz plane in Fig. 1). The names of the irreducible representations to which the MO's of phenol belong in the overall symmetry of the molecular compound are given in Fig. 4. On the other hand, the irreducible representations of the MO's of quinone written in Fig. 4 are transformed in this case in the following way,

$$A_1,\ B_1 \rightarrow A',\quad A_2,\ B_2 \rightarrow A''.$$

As a result, the highest filled MO of phenol, ξ_{13}, and the lowest unfilled MO of quinone, η_{42}, belong to the same irreducible representation in the C_{1h}

* The ΔW calculated as the energy difference between η_{42} and ξ_{43} in Fig. 4 is $0.5\beta_0$. On the other hand, the electron affinity for η_{42} orbital was calculated to be about 8.0 ev., with a method similar to that employed by Sklar[16] in the calculation of the electron affinity of benzene ring of substituted benzenes. This corresponds roughly to $\Delta W=1.0\ \beta_0$.

(15) A. L. Sklar, *J. Chem. Phys.*, **7**, 992 (1939).

symmetry of the molecular compound. From the stand-point analogous to that in the former discussions, we may conclude that, in this molecular compound, the conjugation between ξ_{13} and η_{42} is predominant. By the calculation of the AO coefficients of the MO's of phenol, we can see that the AO coefficients of ξ_{13} are very much like those of ϑ_{42} in hydroquinone and therefore it is conceivable that the overlap integral between ξ_{13} and η_{42} is of nearly the same magnitude as that between ϑ_{42} and η_{42}. The calculated value of the former integral is really 0.040, in close agreement with the latter. Hence, we may expect that the resonance integral between ξ_{13} and η_{42} is also as large as that between ϑ_{42} and η_{42}. The ionization potential of phenol is supposed to be larger than that of hydroquinone, because the energy level of the highest filled orbital of phenol is lower than that of hydroquinone. Hence, ΔW in quinone-phenol system is expected to be larger than that of quinone-hydroquinone system. The change of ΔW, however, does not influence the absorption intensity seriously as was previously stated. Therefore, we deduce that the absorption intensity of quinone-phenol system is of the same order of magnitnde with that of quinone-hydroquinone system. Also, the charge transfer force as a contribution of the binding energy in this molecular compound is expected to be the same as quinone-hydroquinone system. However, as the change of ΔW directly changes the transition energy, we should expect that the peak wave-length of quinone-phenol system will be shorter than that of quinone-hydroquinone system. These considerations agree with experimental results.

Summary

The absolute intensities of the visible absorption spectra and the binding energies of quinhydrone-type molecular compounds have been determined by the measurements of their absorption intensities in solutions. The visible absorption spectra of these molecular compounds can be explained as the charge-transfer spectra of the π-electrons of quinone and the B compounds. The intensity of these charge-transfer spectra can be calculated roughly by setting up linear combination of the lowest unfilled MO of quinone and the highest filled MO of the B compound, and the results agree qualitatively with the experimentally derived absorption oscillator strengths. This charge-transfer resonance is thought to be the most characteristic part of the intermolecular binding energy in these molecular compounds.

The author's sincere thanks are due to Prof. K. Kozima for his encouragement, and to Prof. S. Nagakura and Mr. A. Kuboyama who permitted the author to use the results of their calculation and the spectrophotometer of their laboratory.

Tokyo Institute of Technology,
Meguroku, Tokyo

The Separation of Isotopes by Countercurrent Gaseous Exchange Column. II. Experimental Tests of the Theory

By Kunihiko KIGOSHI

(Received February 18, 1953)

In order to test the theory developed in part 1, the isotope separation of carbon by the countercurrent gaseous exchange column was carried out by hot wire type thermal diffusion column. The isotopes used for this experiments are C^{12} and C^{14}, and the gaseous species for the exchange reaction are carbon dioxide and carbon monoxide. Taylor and Bernstein[1] had performed similar experiments on the separation of C^{13} and C^{12} but we need thorough investigation of this experiment and reliable data on the over-all separation factors for various filament temperatures.

Equilibrium constants for many isotopic exchanges have been studied by Urey and his co-workers[2]. The results of their calculation and the theory on the gaseous exchange column enable us to predict the possibilities of the high efficient isotope separations by the gaseous chemical exchange method.

(1) B. B. Bernstein and T. I. Taylor, *J. Chem. Phys.*, **16**, 903 (1948).

(2) H. C. Urey, *J. Chem. Soc.*, 562 (1947); H. C. Urey and L. J. Greiff, *J. Am. Chem. Soc.*, **57**, 321 (1935).

Experimental Apparatus

Figure 1 is an illustration of the apparatus arrangement. The exchange column was constructed by a water jacketed glass tube of 12.7 mm. in diameter and 150 cm. long. The filament used in the experiments was a platinum wire of 0.7 mm. diameter and it was hung from the top of the column. The centering of the filament was made by five spacers of a small piece of nichrome wire. At the bottom of the column a 70 g. weight was attached to the end of the filament to keep the filament taut. Electrical contact was made by a steel rod (13 cm. long) which was attached to the weight keeping the contact to the mercury pool at the bottom of the column. Constant electric power supply for filament heating was obtained using a ballast tube which has a plateau of characteristic curve between 28~40 volt with 8.5 amp. Power regulation was made by two autotransformers F. T and S. T in Figure 1. When the voltage applied to the ballast tube was adjusted to proper value we could obtain an almost constant power supply for filament heating within the input voltage variations between 90~100 volt.

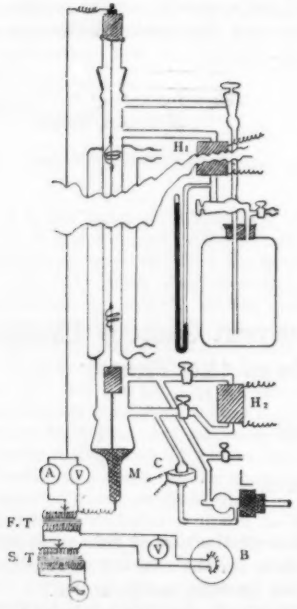

Fig. 1.—Experimental apparatus, H_1; electric furnace for circulation, H_2; Zn-reducer, C; gas circulation pump, M; mercury pool, L; Lauritsen electroscope, B; ballast tube, F. T. and S. T; autotransformers, A; ammeter, V; voltmeter

A top gas reservoir was a glass bottle of 22 l which was connected to the top of the column by two glass tubings. One of these was heated by an electric furnace in order let the gas in the reservoir flow to the top of the column. Flow velocity was measured in the preliminary experiments and we found that it was about 200 cc. per minute. To the bottom reservoir a zinc reducer was attached for reducing carbon dioxide to carbon monoxide. Temperature of the reducer was maintained to 400°C. by an electric furnace which was regulated by an automatic temperature regulator. The volume of the bottom gas reservoir was 250 cc. including the reducer and the ionization chamber of the Lauritsen type electrometer.

Carbon dioxide generated from sodium carbonate and sulfuric acid was introduced into the previously evacuated apparatus through two gas washing bottles with water. The active isotope C^{14} of two or three microcuries was previously mixed into the sodium carbonate used for the gas generation. It has been found by Brandner and Urey[3] that the water vapour or hydrogen is good catalysis for the isotopic exchange reaction between carbon dioxide and carbon monoxide. Increase of reaction velocity reduces the temperature T_b. Therefore we can expect the increase of separation factor by the presence of these gases. To saturate the water vapour in the bottom reservoir a little amount of water was introduced on the mercury pool. In all essential respects the details of operation of the separation column were the same as have been described by Bernstein and Taylor[1].

Measurements of Isotopic Ratio C^{14}/C^{12}

A concentration of C^{14} was measured by Lauritsen type electrometer having an ionization chamber of 160 cc. content. The gas of the bottom reservoir was circulated through the ionization chamber by a magnetically operated gas circulation pump with the flow velocity 30 cc. per minute. Ionization current produced by β-rays from C^{14} depends not only on the concentration of C^{14} but also the composition of gases in the ionization chamber. Therefore we have to know the relation between concentration of C^{14} and ionization current produced in the various mixtures of gases. Results on the measurements of ionization current of the Lauritsen electrometer at various compositions and pressure are represented in Figure 2. In these experiments the concentration of C^{14} was maintained constant (about 6 μc./mol.) and ionization current was expressed in div./sec. Pressure-ionization current curves for carbon dioxide and carbon monoxide showed similar variation. We obtained the similar curves for the mixtures of both gases although these were not represented in Figure 2. The linear dependences of ionization current on the composition of the mixture of two different gases are represented by curves 3 and 4 in Figure 2.

(3) J. D. Brandner and H. C. Urey, *J. Chem. Phys.*, **13**, 351 (1945).

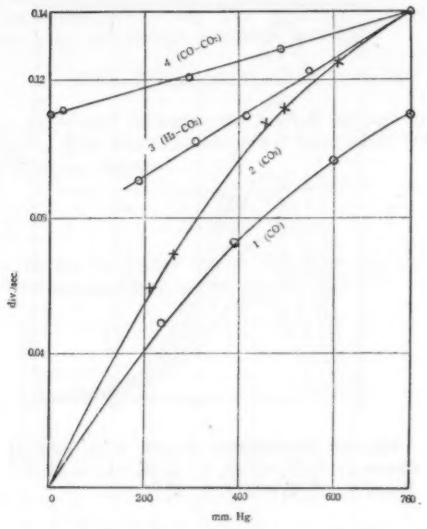

Fig. 2.—Pressure and composition dependence of ionization current with constant amount of C^{14}, Curve 1; pure CO, abscissa is total pressure. 2; pure CO_2, abscissa is total pressure. 3; H_2-CO_2 mixture, abscissa is partial pressure of CO_2 (total pressure is 760 mm. Hg.). 4; CO-CO_2 mixture, abscissa is partial pressure of CO_2 (total pressure is 760 mm. Hg.).

If we measure ionization current and pressure and composition of the samples using Figure 2 we can easily obtain the ionization current which would be observed if pure carbon dioxide is introduced under the standard pressure in the ionization chamber with the same amount of active isotope. The corrected ionization current thus obtained may be regarded to be proportional to C^{14} concentration, because a linear dependence of the ionization current on C^{14} concentration holds in a wide range of the concentration[4].

High content of hydrogen was observed in the bottom reservoir at the initial stage of the separation process. However after a few hours' operation, the hydrogen content in the bottom reservoir became less than 0.5%, therefore the corrections to the measured activities were made only for carbon monoxide contents in the ionization chamber.

Results

Some of the typical changes of C^{14} concentration at the bottom reservoir are shown in Figure 3. We may see that the continuous operation of about fifty hours is ample time to obtain the equilibrium state. The estimation of the initial isotopic transport τ_0 was made by the initial increase of the heavy isotope in the bottom reservoir. The values of initial isotopic transport and over-all separation in the equilibrium states for various filament temperatures are tabulated in Table 1.

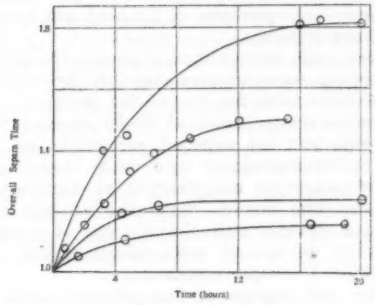

Fig. 3.—Dependence of over-all separation on time

Table 1

Run	$c_1(0)$	$c_1(Z)$	P mm.Hg.	T_2 °C.	S	τ_0/ν ×10⁷mol./sec. Obs.	Calc.
11	85.7	14.2	715	680	1.16	0.9~1.1	0.97
12	80.4	20.4	780	800	1.24	1.5~1.8	1.14
13	68.6	11.8	780	900	1.29		1.35
14	54.0	13.4	750	1100	1.64	2.2~2.5	1.90
15	93.0	30	755	650	1.19		0.95
16	75.0	24.2	746	1170	1.82	3.4~4.5	2.23
17	52	15	750	1130	1.68		2.05
18	85	21	772	1030	1.52	1.8~2.4	1.68
19	65.7	17.5	756	715	1.18	1.0~1.6	0.99
20	52.9	10.6	755	510	1.15		0.92

Values of isotopic transport, over-all separation and experimental conditions at final equilibrium states

$c_1(0)$ = CO% in the bottom reservoir,
$c_1(Z)$ = CO% in the top reservoir,
P = total pressure in the column,
T_2 = filament temperature,
S = over-all separation,
τ_0 = initial transport of C^{14} along the column,
ν = C^{14} concentration at the initial state

The filament temperature was measured by the thermal expansion of the filament. A linear expansion coefficient of 1.00×10^{-5} cm./cm., deg. for platinum wire was used for this measurement. This expansion coefficient was obtained from the measurements on the expansion of our platinum filament without any spacers. A platinum wire with 50~100g. weight at the end was hung outside the column and the temperature of electrically heated platinum wire was measured with optical pyrometer. The observed linear expansion coefficient was independent of the amount of weight

(4) F. C. Henriques, Jr., and C. Margnetti, *Ind. Eng. Chem.*, Anal. Ed., **18**, 417 (1946).

and was in accordance to other observations[5]. The uniformity of the temperature along the column was examined by optical pyrometer and we found almost uniform heating except the small regions (about 10 cm.) near the spacers at which the temperature was lower than other parts, but it did not exceed 100°C. Therefore the difference between measured temperature and maximum temperature of filament was ignored in our experiments.

Occasionally compositions of gases in the bottom and the top reservoirs were examined by ordinary gas analysis using few cc. of the samples. The bottom gas always contained 50~90 percent carbon monoxide and the required corrections on the activity measurements were made according to the measured gas compositions as described in the preceding section. Since the samples were small compared with the amount of gases in reservoirs, we ignored their effects on the time variation of isotopic concentration.

From the change of composition of the top reservoir we could obtain the net transport τ_1 of carbon monoxide along the tube. Observed value was $\tau_1=2.9\pm0.5$ cc./min. The results were insufficient in accuracy for the determination of τ_1. Perhaps the errors of the measurements were derived from the non-uniformity of gases in the top reservoir. Then in order to obtain an accurate value of transport we undertook the preliminary experiments. A well stirred bottom gas reservoir of two liters was filled by carbon monoxide at the initial states. The variations of the composition in this reservoir were measured during two or three hours' operations with the filament temperatures between 700 and 1000°C. We obtained $\tau_1=3.3\pm0.2$ cc./min. for these filament temperatures. The results were also not accurate enough to obtain a dependence of τ_1 on the filament temperature, but rather good compared with the results from the top gas analysis; therefore we used $\tau_1=3.3$ cc./min. in our latter treatment.

Discussion of Results

In the theoretical consideration, the over-all separation of our experiments was given by the formula (51) in part 1. In this formula H_b/H was estimated by equation (54) which was valid only in the extreme case $r_2/r_1\to0$, but this approximation did not yield good results in the cases of our experiments. Therefore we had to use the original form of γ instead of the expression of γ described in equations (41). An exact expression of γ had been given by Furry and Jones[6] and the results of numerical calculation of γ for $r_1/r_2=18.2$, $T_2/T_1=10/3$, 11/3, 4, 13/3, 14/3 and 5 are illustrated in Figure 4. We can estimate H_a and H_b by the numerical integrations of the following expressions.

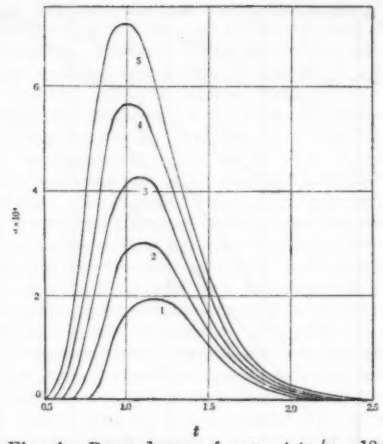

Fig. 4.—Dependence of γ on t ($r_1/r_2=18.2$) Curve 1; $T_2/T_1=10/3$, 2; $T_2/T_1=11/3$, 3; $T_2/T_1=4$, 4; $T_2/T_1=13/3$, 5; $T_2/T_1=5$

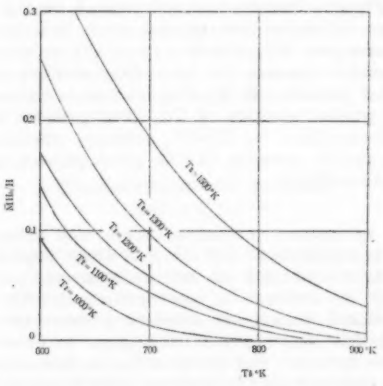

Fig. 5.—Dependence of $\overline{M}H_b/H$ on T_b

$$H/\overline{M}=a\int_{t_1}^{t_2}\alpha_t\frac{\gamma}{t}dt \qquad (1)$$

$$H_b=a\int_{t_b}^{t_2}\gamma\frac{d\alpha}{dt}dt \qquad (2)$$

where $a=2\pi(\rho^2g/\eta)_1\cdot r_1^4t_1^3\exp(2t_1^3)$, and α_t is thermal diffusion constant for the mixture of carbon dioxide and carbon monoxide. We used $\alpha_t=0.10$ which was obtained from the experimental data of Kitagawa and Wakao[7]. Expression (1) had been derived by Furry and Jones and expression (2) was obtained from equations (41) and (43) in part 1.

The results of numerical calculation of $\overline{M}H_b/H$ are graphically represented in Figure 5. Where

(5) Randolt and Börnstein, "Physik.-Chem. Tab. Eg III c" p. 2212.

(6) W. H. Furry and R. C. Jones, *Phys. Rev.*, **69**, 459 (1946).

(7) H. Kitagawa and M. Wakao, *J. Chem. Soc. Japan*, **62**, 100 (1941).

we assumed $T_1=300°K$, we neglected the temperature dependence of α_t. The equilibrium constant α for the isotopic exchange reaction

$$C^{14}O+C^{12}O_2 \rightleftarrows C^{12}O+C^{14}O_2 \qquad (3)$$

was calculated following the method adoped by Urey[2]. The results of numerical calculation of equilibrium constant

$$\alpha^{14}=\alpha=\frac{[C^{12}O][C^{14}O_2]}{[C^{14}O][C^{12}O_2]}$$

are shown in Figure 6 with the same constant α^{13} for the equilibrium between C^{12} and C^{13}.

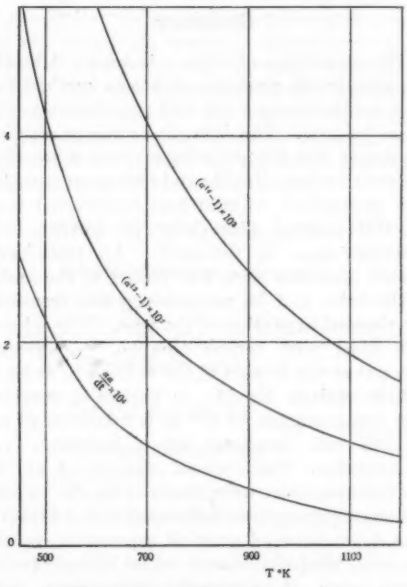

Fig. 6.—Temperature dependences of equilibrium constants $\alpha(=\alpha^{14})$, α^{13}, and $d\alpha/dT$

Our experiments were performed with the isotopic mixture which contains minute quantity of the heavy isotope C^{14} in the natural isotopes of carbon. Therefore the equilibrium constant α may be regarded as an isotopic ratio $\alpha=[C^{14}O_2]/[C^{14}O]$ at the equilibrium (3).

The over-all separation S was estimated by the following expression derived in part 1.

$$-\ln S=\ln\frac{\nu(Z)}{\nu(0)}=\left[1-\alpha(T_b)+\frac{D_2-D_1}{\bar{D}}\frac{\bar{M}H_b}{H}\right]\times\frac{\tau_1 Z}{B_c+B_d}+\frac{D_2-D_1}{\bar{D}}\frac{\bar{M}H_b}{H}(c_1(Z)-c_1(0)) \qquad (4)$$

where $\nu(Z),\nu(0)=$ fractional molar concentration of C^{14} at the top and the bottom of the column, D_1, D_2=self diffusion coefficient of carbon monoxide and carbon dioxide, $\bar{D}$=mean value of D_1 and D_2, Z=column length, and $c_1(Z)$, $c_1(0)$=fractional molar concentration of carbon monoxide at the top and the bottom of the column. A value of $(D_1-D_2)/\bar{D}=0.461$ was obtained from the self diffusion coefficients of carbon dioxide and carbon monoxide[3]. If an appropriate value of T_b is assumed, we may obtain over-all separation S using the experimental data on the value of transport (τ_1) of carbon monoxide along the tube and the concentrations of carbon monoxide in the top and the bottom reservoirs at a final equilibrium state. Assuming $T_b=600$, 700, 750, 800, 850, and 900°K., the numerical evaluation of expression (4) was performed, and obtained the values of $\ln S$ as functions of filament temperature T_2 are illustrated in Figure 7. In these calculations B_c and B were obtained by substituting into equations (40) and (47) the following numerical data,

$\rho=1.46\times10^{-3}$	$T_1=300°K.$
$\eta=165\times10^{-6}$	$r_1=0.635$
$\bar{D}=0.141$	$r_2=0.035$
$\bar{M}=36$	$c_1(0)-c_1(Z)=0.7$

In practice, $c_1(0)-c_1(Z)$ changed in each experimental case, but the second term of equation (4) did not exceed 5% of the total value; therefore the variation of $c_1(0)-c_1(Z)$ was ignored in our treatment.

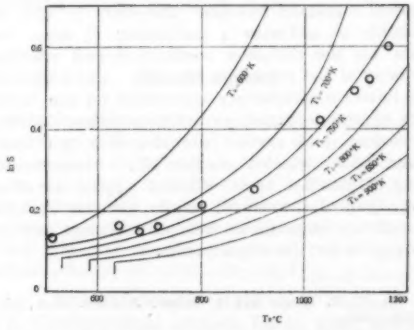

Fig. 7.—Dependence of calculated and observed over-all separation on the filament temperature

In Figure 7 we plotted $\ln S$ obtained from the experimental values of Table 1. Perhaps an appreciable error would be introduced concerning the temperature measurements of the filament. However within limits of error, observed over-all separations coincide with the calculated values for $T_b=750°K$ as illustrated in Figure 7. The observed over-all separations in the cases of low filament temperatures were rather large compared with the expected values. These discrepancies between experimental values and theoretical values may be attributed to the neglect of isotopic

(8) J. H. Jeans, "The Dynamical Theory of Gases" (1925) p. 321.

enrichment by the ordinary thermal diffusion in the theoretical treatment of this report.

The theoretical estimation on the isotopic transport is made by equation (45) in part 1. Since there is no isotopic concentration gradient along the column at the initial state, an initial transport can be obtained putting $d\nu_1/dz=0$, then we have,

$$-\tau_0=(\tau_1)_{t=0}=\left[(1-\alpha(T_b))\tau_1+c_1c_2H_b\frac{D_2-D_1}{\bar{D}}\right]\nu_1$$

Using equation (2) in part 1, it becomes

$$-\tau_0=\left[1-\alpha(T_b)+\frac{D_2-D_1}{\bar{D}}\frac{\bar{M}H_b}{H}\left(1+\frac{B_c+B_d}{\tau_1}\frac{dc_1}{dz}\right)\right]\nu_1\tau_1. \qquad (5)$$

The substitutions of the values of $\bar{M}H_b/H$ for $T_b=750$°K. and of other constants corresponding to the experimental conditions in equation (5) yielded calculated initial isotopic transports tabulated in Table 1. On account of the difficulties in the determination of the initial slopes of curves such as in Figure 3, we can not draw any detailed conclusion from the small discrepancies between calculated and observed values in Table 1, but these experimental evidences support our theoretical interpretation.

At the cylindrical region of the column at T_b°K., we assumed that both variations of the isotopic composition by exchange reaction and by diffusion process maintain balance. Therefore it will be possible to estimate a parameter T_b from the data on the diffusion coefficients and reaction velocity of the exchange reaction. Unfortunately we have no satisfactory knowledge on the kinetics of isotope exchange reaction between carbon monoxide and carbon dioxide, although there have been detailed studies[3][9]. However we may construct a most efficient apparatus using the obtained theoretical results, because T_b takes a constant value for an isotopic exchange reaction employed for the experiments.

(9) T. H. Norris and S. Ruben, *J. Chem. Phys.*, **18**, 1595 (1950).

The high efficiency of the isotope separation in our experiments at the elevated filament temperatures was caused by the high value of $\bar{M}H_b/H$ in expression (4). On the similar base it is supposed that the rise of cold wall temperature brings high over-all separation factor. The elevation of the temperature in the whole tube results in decreasing of t_b—the lower limit of integral (2)—with respect to the curves of γ. A steep increase of γ with the decrease of t also yields a steep increase of $\bar{M}H_b/H$ by the elevation of the tube temperature, because a range of integration of H_b depends on t_b as was shown by expression (2).

Summary

The separation of carbon isotope C^{14} by the countercurrent gaseous exchange method has been studied using a hot wire type thermal diffusion column. The isotopic exchange reaction employed for the experiments was a reaction between carbon dioxide and carbon monoxide. The separation column was constructed with a water-jacketed glass tube of 150 cm. long and 12.7 mm. in diameter. An electrically heated platinum wire was placed at the center of the tube, and its temperature was measured by thermal expansion of the wire. The column was filled with carbon dioxide. A converter was put at the bottom of the column in order to reduce carbon dioxide to carbon monoxide. The concentration of C^{14} at the bottom of the column was measured by a Lauritsen type electrometer. The over-all separations at the equilibrium states were observed for the various filament temperatures between 570 and 1170°C. The dependence of over-all separation on the filament temperature and initial isotopic transports were in reasonable agreement witd theoretical estimates.

Department of Physics and Chemistry, Gakushuin University, Mejiro, Tokyo

On the Ring-Opening Reactions of the Furan Compounds. II. The Synthesis of γ, ζ, ι-Triketobrassylic Acid from Difurfurylideneacetone

By Hiroshi MIDORIKAWA

(Received February 21, 1953)

It had already been found that furfurylideneacetone yields γ, ζ-diketocaplyric acid[1] by refluxing with alcoholic hydrochloric acid. By a similar furan ring opening, γ, ζ-diketosebacic acid was synthesized from δ-furfurylidenelevulinic acid.[2] In the present report, γ, ζ, ι-triketobrassylic acid was obtained from difurfurylideneacetone by the same procedure. This reaction is illustrated below.

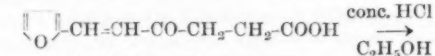

δ-furfurylidenelevulinic acid

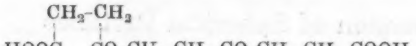

γ, ζ-diketosebacic acid

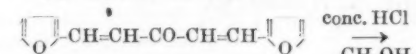

difurfurylideneacetone

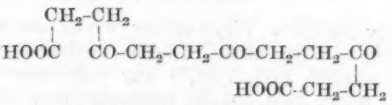

γ, ζ, ι-triketobrassylic acid

This acid gave an oily matter when combined with phenylhydrazine.* The semicarbazone and the hydrazone of this acid did not crystallize out. It was readily esterified by refluxing with alcohol and sulfuric acid. In the case of difurfurylidene-methyl-ethyl ketone (I), difurfurylidenecyclohexanone (II) and furfurylidenediethyl ketone (III), the similar ring opening reaction did not take place with the same procedure as δ-furfurylidene levulinic acid and difurfurylidene acetone.

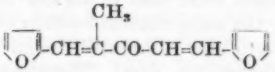

I

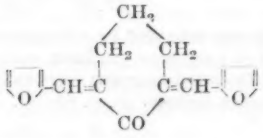

II

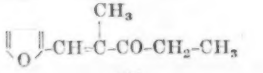

III

These furfurylidene ketones have a branched chain at the carbon atom between the furfurylidene and the carbonyl goups. It seems that the ring opening is hindered by the presence of the branched chain.

Experimental

Difurfurylideneacetone.—20 g. furfural and 6 g. acetone were dissolved in 270 cc. water, and 30 g. 10% aqueous caustic soda solution was introduced at once. After stirring for four and a half hours, the reaction was over. Then, neutralised with sulfuric acid, it was left overnight and solidified. Yield, 20g.. It was recrystallized from ligroin; yellow prisms; m. p. 60—1°; lit.[3] m. p. 60—1°.

γ, ζ, ι-Triketobrassylic Acid.—A mixture of 13 g. difurfurylidene acetone, 130 cc. conc. hydrochloric acid and 200 cc. methanol was refluxed on the water-bath for three hours. The reaction mixture was evaporated on the water-bath to remove hydrogen chloride, water being repeatedly added to it. The residue was extracted with a sufficient quantity of boiling water, and the extract was concentrated on the water-bath, after being decolorized with active charcoal. On cooling, colorless foliated crystals separated out from it, and were recrystallized from water. Yield, 1.5 g.; m. p. 168—9°; readily soluble in water, methanol and acetic acid on heating; insoluble in benzene, chloroform, acetone and ether.

(1) E. A. Kehrer and P. Igler, *Ber.*, **32**, 1177 (1899).
(2) E. A. Kehrer and E. Hofacker, *Ann.*, **294**, 167 (1897).
* Kehrer and Hofacker had reported that the diphenylhydrazone of γ, ζ-diketosebacic acid is difficult to crystallize.
(3) L. Claisen and A. C. Ponder, *Ann.*, **223**, 146 (1884).

	C	H
Anal. Calcd. for $C_{13}H_{18}O_7$:	54.52	6.33
Found:	54.59	6.23

Esterification of γ, ζ, ι-Triketobrassylic Acid. —0.5g. of the acid was boiled in a mixture of 2 cc. methanol and 0.1 cc. conc. sulfuric acid for thirty minutes. On cooling the reaction mixture, the methyl ester was separated out. It was recrystallized from water. Yield, 0.4 g.; colorless needles; m. p. 92—3°.

	C	H
Anal. Calcd. for $C_{15}H_{22}O_7$:	57.29	7.06
Found:	57.20	7.20

0.3 g. of the acid was esterified by refluxing with 2 cc. ethanol and 0.1 cc. conc. sulfuric acid for thirty minutes. The ethyl ester was recrystallized from water; colorless leaflets: m. p. 63—4°.

	C	H
Anal. Calcd. for $C_{17}H_{26}O_7$:	59.61	7.63
Found:	59.66	7.36

Difurfurylidenecyclohexanone, difurfurylidene-methyl-ethyl ketone and furfurylidene diethyl ketone were synthesized by the same method as difurfurylidene acetone.

Summary

The γ, ζ, ι-triketobrassylic acid which is a new triketo-dicarboxylic acid was obtained from difurfurylidene acetone by the ring opening.

The similar ring opening did not take place in difurfurylidene cyclohexanone, difurfurylidene-methyl-ethyl ketone and furfurylidene-diethyl ketone which have a branched chain at the carbon atom between the furfurylidene and the carbonyl groups. It seems that the ring opening reaction is hindered by the presence of the branched chain.

The Scientific Research Institute Tokyo

The Dielectric Constant of Dispersion of Spherical Particles

By Masaji KUBO and Sankichi NAKAMURA

(Received February 23, 1953)

The dielectric constant of emulsions and suspensions and the magnetic permeability of compressed powders have been studied theoretically and experimentally in view of their scientific as well as of their technical importance. Many empirical and theoretical equations have been proposed for disperse systems composed of two different phases. Almost all the empirical formulas assume that some function of dielectric constant ε changes linearly with the volume fraction ϕ.

$$f(\varepsilon)=\phi_1 f(\varepsilon_1)+\phi_2 f(\varepsilon_2) \qquad (1)$$

where suffixes denote the two components constituting the heterogeneous system. The following functions have been proposed.

$f(\varepsilon)=\varepsilon$ (2)
$f(\varepsilon)=1/\varepsilon$ (3) } Wiener's limiting formulas

$f(\varepsilon)=\log\varepsilon$ (4) Lichtenecker

$f(\varepsilon)=(\varepsilon-1)/(\varepsilon+2)$ (5) Clausius-Mosotti

$f(\varepsilon)=(\varepsilon-1)/(\varepsilon+u)$ (6) Wiener

Here u is a constant dependent on the form of the particles. Since earlier works on the problem have already been reviewed by Heymann[1] and Voet,[2] our references to such works need not be comprehensive. The Wiener's limiting formula (2) applies strictly to such heterogeneous systems, in which each single part of the components is cylindrical in shape with the generating line of the cylindrical surface parallel to the electric vector, while the formula (3) to systems in which all the boundary surfaces between the phases are planar and perpendicular to the field. To be sure, the actual heterogeneous systems of interest are very different from these limiting cases. In fact we may expect for instance that an oil-in-water emulsion has a different dielectric constant from that of a water-in-oil emulsion with the same volume fraction of the oil. In fact Goto and Koizumi[3] found that such was actually the case. Therefore we should reject the additive rule of the form (1)

(1) E. Heymann, *Kolloid-Z.*, **66**, 229 (1934).
(2) A. Voet, *J. Phys. Coll. Chem.*, **51**, 1037 (1947).
(3) R. Goto and N. Koizumi, *Rep. Inst. Chem. Research, Kyoto Univ.*, **18**, 121 (1949); R. Goto, *Rev. High Molecules*, **5**, 47 (1951).

and derive a theoretical formula taking into account the non-equivalence of the dispersion medium and the disperse phase. Such an attempt has already been made by Wiener[4] and by Bruggeman.[5] The original paper by Wiener was not available to the writers. His formula for the dielectric constant of a dispersion of concentration ϕ in volume fraction is

$$\frac{\varepsilon-\varepsilon_0}{\varepsilon+2\varepsilon_0}=\frac{\varepsilon_1-\varepsilon_0}{\varepsilon_1+2\varepsilon_0}\phi \qquad (7)$$

for spherical particles of dielectric constant ε_1 dispersed in a medium of dielectric constant ε_0. Piekara[6] derived the same formula with the aid of Wiener's proportionality postulate. That is, he calculated the dielectric constant of dispersion of spherical particles in vacuum and assumed that the same equation holds for a dispersion in a homogeneous medium if in the original equation ε and ε_1 are substituted by $\varepsilon/\varepsilon_0$ and $\varepsilon_1/\varepsilon_0$ respectively. This procedure lacks an adequate theoretical justification. In addition he employed Mosotti's inner field, which has nothing to do with dispersions of particles of greater size than molecular dimensions. Bruggeman proposed the following formula.

$$\frac{\varepsilon_1-\varepsilon}{\varepsilon_1-\varepsilon_0}\left(\frac{\varepsilon_0}{\varepsilon}\right)^{1/3}=1-\phi \qquad (8)$$

He employed Rayleigh's formula,[7] which gave the dielectric constant increment due to the introduction of spherical particles arranged regularly at the lattice points of a simple cubic lattice into a homogeneous phase. Then he ignored higher terms of ϕ. The result is equivalent to that derived from the assumption of Wiener's proportionality postulate, the difference between his theory and Wiener's being that instead of using Mosotti's inner field he integrated a differential equation containing $d\varepsilon/d\phi$. Hence it is not surprising that these two formulas give an identical value for $d\varepsilon/d\phi$ at $\phi=0$.

The present writers have taken a different method of approach avoiding the use of the Wiener's proportionality postulate and obtained an entirely different theoretical formula. The basic assumptions underlying the writers' derivation are as follows. Each particle of the disperse phase is spherical in shape. The radius of the sphere is very small compared with the dimension of the whole heterogeneous system, enabling us to ignore the effect of boundary of the whole system. But it is very great in comparison to the molecular dimensions so that the disperse phase and the dispersion medium can be considered to be homogeneous media characterized by their respective dielectric constants alone. The particles are assumed to have no net charge. If the particles are not so finely dispersed, the effect of polarization will be more important than that of charges at the boundary surfaces. The system may be polydisperse, i. e., the radius of the particles may not be uniform. For the time being, let us assume that all the particles have a radius a.

Suppose a dispersion containing n particles of disperse phase per unit volume. The volume fraction ϕ is given by

$$\phi=\frac{4\pi}{3}a^3n. \qquad (9)$$

Let us imagine $\Delta\nu$ spheres of radius a in unit volume. The number of spheres is so small that the distance between them is very great compared with the radius a. Take out the matter in the spheres and substitute it with a medium of dielectric constant ε_1. If such substitution were made on a homogeneous medium of dielectric constant ε, we could give an expression for the dielectric constant increase. We assume that the same formula for the dielectric constant change is approximately valid for the result of substitution applied on an already existing dispersion containing n particles per unit volume. This means that the heterogeneous system can well be represented by a homogeneous system of the same dielectric constant. Actually the system under consideration is not perfectly static, i. e., the particles already present are moving with respect to the newly inserted spheres. Hence the averaging may be justified to a certain extent. The assumption would be exact if the particles already present were much smaller in size than those introduced. In our case, however, the representation of a heterogeneous system by an average homogeneous phase is an approximation. It will be worthwhile to mention that Brinkman[8] applied the same idea to the theory of viscosity of concentrated suspensions and solutions and obtained a good viscosity formula.

When a sphere of dielectric constant ε_1 is introduced into a homogeneous medium of dielectric constant ε subjected to a uniform

(4) O. Wiener, *Abh. Königl. sächs. Ges. Wiss. Math. Phys. Kl.*, **32**, 509 (1912).
(5) D. A. G. Bruggeman, *Ann. Physik*, (5) **24**, 636 (1935).
(6) A. Piekara, *Kolloid-Z.*, **59**, 12 (1932).
(7) Rayleigh, *Phil. Mag.*, (5) 34, 481 (1892).
(8) H. C. Brinkman, *J. Chem. Phys.*, **20**, 571 (1952).

electric field E_0, the field is distorted in such a way[9] that outside the sphere, its effect is equivalent to a dipole at the center pointing to the field direction, which we shall call x-direction, with its moment equal to

$$m=\frac{\varepsilon_1-\varepsilon}{\varepsilon_1+2\varepsilon}a^3E_0. \tag{10}$$

The potential outside the sphere is given by

$$V=-E_0x+\frac{m}{r^2}\cos\theta \tag{11}$$

where r is the distance between the dipole and the point P in question and θ is the angle between r and the x-direction. On the other hand the sphere is uniformly polarized with a modified field given by

$$F=\frac{3\varepsilon}{\varepsilon_1+2\varepsilon}E_0. \tag{12}$$

Outside the sphere the x-component of the field due to a dipole m is given by

$$\begin{aligned}F_x&=\left(-\frac{\partial V_m}{\partial r}\right)\cos\theta-\left(-\frac{1}{r}\frac{\partial V_m}{\partial\theta}\right)\sin\theta\\&=\frac{m}{r^3}(3\cos^2\theta-1)\end{aligned} \tag{13}$$

where V_m denotes the dipole potential given by the second term in the right-hand side of equation (11). The x-component of the induced moment in a volume element at P is

$$\begin{aligned}&\chi F_x r^2\sin\theta dr d\theta d\phi\\&=\frac{(\varepsilon-1)m}{4\pi r^3}(3\cos^2\theta-1)r^2\sin\theta dr d\theta d\phi\end{aligned} \tag{14}$$

where χ denotes the electric susceptibility or polarizability per unit volume. If we integrate (13) over θ from 0 to π, and over r from a to infinity, the integral over θ vanishes,

$$\int_0^\pi(3\cos^2\theta-1)\sin\theta d\theta=0 \tag{15}$$

while that over r becomes infinity.*

$$\int_a^\infty\frac{dr}{r}=\Big|\ln r\Big|_a^\infty. \tag{16}$$

From the physical point of view, it is unlikely that the effects of volume elements far from the center of the sphere are appreciable. Let us assume that the dipole field smaller than a certain value F_c can contribute to the induced moment only in a negligible magnitude. Since the dipole field is given by

$$\begin{aligned}F_m&=\left[\left(-\frac{\partial V_m}{\partial r}\right)^2+\left(-\frac{1}{r}\frac{\partial V_m}{\partial\theta}\right)^2\right]^{1/2}\\&=\frac{m}{r^3}(3\cos^2\theta+1)^{1/2}\end{aligned} \tag{17}$$

the integration over r should be extended to

$$b=\left(\frac{m}{F_c}\right)^{1/3}(3\cos^2\theta+1)^{1/6}. \tag{18}$$

Therefore the increase of moment due to the introduction of the sphere is

$$\begin{aligned}\Delta M_{\text{out}}&=\iiint\chi F_x r^2\sin\theta dr d\theta d\phi\\&=\iiint\frac{(\varepsilon-1)m}{4\pi r^3}(3\cos^2\theta-1)r^2\sin\theta dr d\theta d\phi\\&=\frac{\varepsilon-1}{2}m\int_0^\pi(3\cos^2\theta-1)\left[\int_a^b\frac{dr}{r}\right]\sin\theta d\theta.\end{aligned} \tag{19}$$

Owing to the logarithmic form of (16) and the relation (15), the constant b does not affect the integral. In other words the absolute value of the ambiguously chosen F_c is not important. Then we have

$$\begin{aligned}\Delta M_{\text{out}}&=\frac{\varepsilon-1}{2}m\int_0^\pi(3\cos^2\theta-1)\frac{1}{6}\\&\quad\times\ln(3\cos^2\theta+1)\sin\theta d\theta\\&=\frac{\varepsilon-1}{2}m\frac{1}{6}\int_{-1}^1(3x^2-1)\ln(3x^2+1)dx.\end{aligned} \tag{20}$$

The integration by parts gives

$$\begin{aligned}\Delta M_{\text{out}}&=-(\varepsilon-1)m\int_0^1\frac{x^4-x^2}{3x^2+1}dx\\&=-(\varepsilon-1)m\left|\frac{x^3}{9}-\frac{4x}{9}+\frac{4\sqrt{3}}{9\times3}\arctan\sqrt{3}\,x\right|_0^1\\&=\frac{\varepsilon-1}{3}m\left(1-\frac{4\pi}{9\sqrt{3}}\right)\\&=\frac{(\varepsilon_1-\varepsilon)(\varepsilon-1)}{3(\varepsilon_1+2\varepsilon)}ca^3E_0\end{aligned} \tag{21}$$

where

$$c=1-\frac{4\pi}{9\sqrt{3}}=0.1939. \tag{22}$$

---

(9) Cf. R. Becker, "Theorie der Elektrizität". I. Teubner, Leipzig and Berlin, 1933, p. 77.

* Higasi[10] in his theory of the solvent effect on dipole moments considered that the product of the two integrals vanishes.

(10) K. Higasi, *Sci. Pap. Inst. Phys. Chem. Research*, **28**, 284 (1936).

The increase of moment inside the sphere is obviously

$$\Delta M_{\text{in}}=\left(\frac{\varepsilon_1-1}{4\pi}F-\frac{\varepsilon-1}{4\pi}E_0\right)\frac{4\pi a^3}{3}$$
$$=\frac{(\varepsilon_1-\varepsilon)(2\varepsilon+1)}{3(\varepsilon_1+2\varepsilon)}a^3E_0. \quad (23)$$

Hence for $\Delta\nu$ such spheres far apart from each other, the increase of polarization is

$$\Delta P=(\Delta M_{\text{out}}+\Delta M_{\text{in}})\Delta\nu$$
$$=\frac{(\varepsilon_1-\varepsilon)[(2+c)\varepsilon+(1-c)]}{3(\varepsilon_1+2\varepsilon)}a^3E_0\Delta\nu. \quad (24)$$

The increase of the dielectric constant of the whole system is therefore

$$\Delta\varepsilon=\frac{4\pi\Delta P}{E_0}$$
$$=\frac{(\varepsilon_1-\varepsilon)[(2+c)\varepsilon+(1-c)]}{(\varepsilon_1+2\varepsilon)}\left(\frac{4\pi a^3}{3}\right)\Delta\nu. \quad (25)$$

By the removal of $\Delta\nu$ spheres of the initial dispersion of concentration ϕ, followed by substitution with the medium of disperse phase, we take out $\phi\Delta\nu$ particles on the average and add $\Delta\nu$ particles anew. Hence the increase in the number of particles of the disperse phase is

$$\Delta n=(1-\phi)\Delta\nu. \quad (26)$$

Combining these two equations, we have

$$\frac{\Delta\varepsilon}{\Delta n}=\frac{(\varepsilon_1-\varepsilon)[(2+c)\varepsilon+(1-c)]}{(\varepsilon_1+2\varepsilon)(1-\phi)}\left(\frac{4\pi a^3}{3}\right) \quad (27)$$

or

$$\frac{\varepsilon_1+2\varepsilon}{(\varepsilon_1-\varepsilon)[(2+c)\varepsilon+(1-c)]}d\varepsilon=\frac{d\phi}{1-\phi}, \quad (28)$$

Therefore

$$\int_{\varepsilon_0}^{\varepsilon}\frac{\varepsilon_1+2\varepsilon}{(\varepsilon_1-\varepsilon)[(2+c)\varepsilon+(1-c)]}d\varepsilon=\int_0^{\phi}\frac{d\phi}{1-\phi} \quad (29)$$

where ε_0 denotes the dielectric constant of the pure dispersion medium. The integration can be evaluated immediately and we have

$$\frac{3\varepsilon_1}{(2+c)\varepsilon_1+(1-c)}\log\frac{\varepsilon_1-\varepsilon}{\varepsilon_1-\varepsilon_0}$$
$$-\frac{(2+c)\varepsilon_1-2(1-c)}{[(2+c)\varepsilon_1+(1-c)](2+c)}\log\frac{(2+c)\varepsilon+(1-c)}{(2+c)\varepsilon_0+(1-c)}$$
$$=\log(1-\phi) \quad (30)$$

where the base of the logarithm may be either e or 10. This equation gives the relation between ε and ϕ, if ε_0 and ε_1 are known. It will be remarked that in this derivation the radius a of particles has been eliminated completely. Therefore the absolute value of the radius is trivial and the uniformity of the particle size is not a necessary condition for the derivation of this equation. For conducting particles we may put $\varepsilon_1=\infty$. Then we have

$$-\frac{1}{2+c}\log\frac{(2+c)\varepsilon+(1-c)}{(2+c)\varepsilon_0+(1-c)}$$
$$=\log(1-\phi). \quad (31)$$

This relation is applicable to metal sols of spherical particles.

Equations in magnetostatics are similar in form to those in electrostatics. If magnetic permeabilities are approximately equal to unity, the second term of the left-hand side of the equation (30) vanishes. This condition is satisfied for dia- or paramagnetic solid powder in air. Then the following simple relation holds for the magnetic permeability μ

$$\frac{\mu_1-\mu}{\mu_1-\mu_0}=1-\phi. \quad (32)$$

That is, the magnetic permeability of a heterogeneous system changes linearly with the volume fraction. Linearity holds also between the magnetic susceptibility and the volume fraction. This relation is used for the measurement of the magnetic susceptibilities of solids by the powder method.

A comparison of the relation (30) with the Bruggeman's formula will be of interest. If we substitute E_0 in the first line of (23) by F, a procedure which is not justified of course, and let $\Delta M_{\text{out}}=0$ or $c=0$, we have

$$\frac{\varepsilon_1+2\varepsilon}{3\varepsilon(\varepsilon_1-\varepsilon)}d\varepsilon=\frac{d\phi}{1-\phi} \quad (33)$$

instead of (28). Integration gives

$$\log\frac{\varepsilon_1-\varepsilon}{\varepsilon_1-\varepsilon_0}-\frac{1}{3}\log\frac{\varepsilon}{\varepsilon_0}=\log(1-\phi) \quad (34)$$

which is identical with the Bruggeman's formula (8).

Though at first sight our theoretical formula and those by Wiener and Bruggeman seem to cover the whole volume fraction range from 0 to 1, the volume fraction of a disperse phase can never be higher than $\pi/3\sqrt{2}=74.0\,\%$. It is expected that these theories will become inadequate when the volume fraction approaches this limiting value.

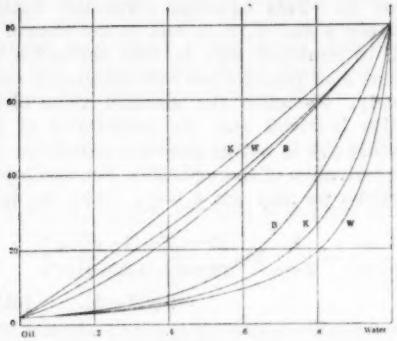

Fig. 1.—The dielectric constants of an oil-in-water type emulsion (upper three curves) and a water-in-oil type emulsion (lower three curves) after the theories of Wiener (W), Bruggeman (B) and the present writers (K)

As an example we have drawn in Figure 1 the dependence of dielectric constant upon the volume fraction for dispersions of water-in-oil and oil-in-water types, taking the dielectric constants of water and oil to be equal to 80 and 2 respectively. For comparison, curves from the formulas of Wiener and Bruggeman are also given. It will be seen that though the functional forms of the three theoretical formulas are entirely different, the curves are similar to each other in their general trend. Namely, the dielectric constant of an oil-in-water type emulsion is higher than that of the water-in-oil type emulsion of the same volume fraction. The curve for the oil-in-water type emulsion is slightly convex to the abscissa, while the deviation from linearity is considerable for the water-in-oil type emulsion. These theoretical conclusions are in conformity with experiments.[11] Most of the experiments which have hitherto been made[12] deal with dilute dipsersions, in which the disperse phase has higher dielectric constant than that of the dispersion medium. In this case the three theories give nearly coincident results. Up to the present, the Bruggeman's formula has been tested and is supposed to be fairly satisfactory. A quantitative comparison of the three theoretical formulas will be made in the succeeding paper.

Summary

The dielectric constant of the dispersion, in which spherical particles of dielectric constant ε_1 are dispersed in a medium of dielectric constant ε_0, has been worked out theoretically without employing Wiener's proportionality postulate. The following equation has been derived for the relation between the dielectric constant ε of the dispersion and the volume fraction ϕ of the disperse phase.

$$\frac{3\varepsilon_1}{(2+c)\varepsilon_1+(1-c)}\log\frac{\varepsilon_1-\varepsilon}{\varepsilon_1-\varepsilon_0}-\frac{(2+c)\varepsilon_1-2(1-c)}{[(2+c)\varepsilon_1+(1-c)](2+c)}\log\frac{(2+c)\varepsilon+(1-c)}{(2+c)\varepsilon_0+(1-c)}=\log(1-\phi)$$

where $c=1-4\pi/9\sqrt{3}$

Chemical Department, Faculty of Science, Nagoya University, Nagoya

(11) R. Goto and N. Koizumi, loc. cit.
(12) A. Voet, loc. cit. F. Wachholtz and A. Franceson, *Kolloid-Z.*, **92**, 158 (1940); A. Piekara, Ibid., **49**, 97 (1929); **58**, 283 (1932).

Heterogeneous Structure of Rayon. III. Peeling-off by Heterogeous Nitration

By Saburo OKAJIMA, Shigeru HAYAMA and Kiyoshi WATANABE

(Received March 5, 1953)

In the preceding papers[1] the authors studied the conditions of peeling-off the rayons by heterogeneous acetylation and reported some results obtained by applying this method for several types of rayons. The results are very interesting but it requires too long acetylation up to some hundred to one thousand hours at 60°C. and the reaction is followed by remarkable degradation of cellulose, which will

(1) S. Okajima, S. Hayama and K. Kobayashi, This Bulletin, **25**, 271, 275 (1952).

be a disadvantage in some cases.

As is well known, the ordinary nitration of cellulose proceeds very smoothy with little degradation, but the reaction velocity is too large to be used for our present purposes. Furthermore the ordinary nitration is said not to be fiber-heterogeneous. But according to S. Watanabe,[2] the nitration in organic diluents proceeds with moderate speed and in the case of the natural fibers the reaction seems to be fibrillar-heterogeneous under appropriate conditions. Therefore this type of nitration is very interesting also for our study and some peeling-off examination was made by nitration.

In this report the conditions under which the nitration proceeds fiber-heterogeneously with moderate speed are described and the radial distributions of the orientation degrees in some rayons obtained by this method are compared to those obtained previously by heterogeneous acetylation.

Conditions of Fiber-heterogeneous Nitration

Using a HNO_3—$(CH_3CO)_2O$—CCl_4 system as the nitration bath, the conditions in which a fiber-heterogeneous nitration proceeded with moderate speed was determined. Pieces of an ordinary viscose rayon on the market were extracted with ether and hot water (60°C.)as described previously, and were used as the samples by drying in vacuum immediately before nitration. After nitration for various hours at room temperature the samples were washed with CCl_4 and then thoroughly with water (60°C.) and air dried.

The reaction type varies with the composition of the acid mixture, which was examined by observing the nitrated products under a polarization microscope. If the reaction is fiber-heterogeneous the nitrated sheath of each filament can be clearly recognized, as the birefringence of the cellulose differs remarkably from that of the nitrocellulose.[3] And moreover when such a fiber is swollen in the acetone-water mixture (2:1) only the nitrated sheath swells and a clear demarcation appears between the nitrated and unreacted parts of celluloses and after dissolving away with pure acetone, a slender core remains, which shows some lateral striations as does the original fiber. A permutoid reaction does not indicate such a behavior and the fiber swells homogeneously. Therefore the reaction type can easily be distinguished by such tests.

As to the conditions, dilution ratio DR, nitric acid ratio NAR and bath raio BR are defined as follows:

DR: Weight of $HNO_3+(CH_3CO)_2O$/Weight of CCl_4,

NAR: Weight of HNO_3/(Weight of $HNO_3+(CH_3CO)_2O$),

BR: Weight of the total acid mixture/Weight of the cellulose.

The reaction velocity is dependent on these factors, and the conditions are selected in such a way that the nitration is completed in about 7 hours at room temperature.

The results are summarized in Tables 1 and 2, according to which the following facts are seen: (1) DR has little effect on the type of reaction and the velocity within such experiments. (2) NAR are very effective and at 55% NAR the reaction is too speedy to be followed and at 45% it is too slow. (3) NAR affects also the type of reaction; at 55% NAR the fiber extracted with acetone becomes slender but the lateral striations disappear, and the nitration is of slight permutoid.

Table 1

Effect of the Bath Composition, $T=20°C$.

Exp. No.	DR	NAR(%)	t (hr.)	Reaction type
1	1/5	50	2	F. H.*
2	1/10	50	2	F. H.
3	1/10	50	15	Completely reacted
4	1/5	55	0.5	F. H.
5	1/5	55	1	Completely reacted
6	1/5	45	22	F. H. but the reaction is too slow

* Fiber-heterogenous

Table 2 indicates the effect of AR, according to which the yarn reacts too rapidly at AR=1/2.5 and the optimum value is 1/5~1/10.

Table 2

Effect of DR and BR, T=13°C. and NAR=50%.

Exp. No.	DR	BR	t (hr.)	Type of reaction
1	1/2.5	230	3	Completely reacted
2	1/5	200	3	F. H.
3	1/10	182	3	F. H.
4	1/15	178	3	F. H.
5	1/20	175	3	F. H.
6	1/10	182	8	Nearly completely reacted

To summarize, the best conditions for our purpose are as follows:

DR=1/5~1/20,

NR=50%,

providing $t=0$~7 hrs and T=15~20°C.

Peeling-off by Nitration

The conditions of nitration used for peeling-off is now determined; it is applied to some rayon samples. Those results are summarized in the following tables and figures, where the notations used are the same as described previously unless being noted specially.

(2) S. Watanabe, *J. Soc. Chem. Ind. Japan*, **45**, 832 (1942), **47**, 561 (1944).

(3) Ambronn und Frey, "Polarisationsmikroskop", 1926, S. 169; K. Kanamaru, *Helv. Chim. Acta*, **18**, 1429 (1934).

Table 3

Viscose Rayon V–1

(1) NAR=50%, DR=1/10, BR=180, T=18°C.

Not denitrated. * indicates the value after denitration.

t, hr	5/61	10/60	25/60	1	2	3-20/60	4-40/60	7
$W'/W-1$, %	4.1	6.0	9.2	14.2	21.8	26.0	41.1	55.0
L_T/W, %	3.1	5.1	8.7	14.2	21.4	30.7	44.5	55.7
N, %	1.01	1.74	2.54	3.68	5.28	6.11	8.40	10.05
$x/3(N)$, %	4.0	7.0	10.6	16.0	24.2	29.3	44.3	57.2
$x/3$, %	4.9	7.2	11.0	17.0	28.2	31.2	49.3	66.0
P_r, %	1.6	2.6	4.4	7.4	11.4	16.8	25.5	33.4
$\Gamma \cdot 10^3$	21.5	—	18.2	17.5	16.0	16.2	—	—
$\Gamma \cdot 10^3$**	20.4	21.2	19.6	17.0	17.1	16.2	16.5	16.3

(2) NAR=50%, DR=1/10, BR=150, T=18°C.

Not denitrated.

t, hr	5/60	10/60	25/60	1	2	3-30/60	5-15/60	7-20/60
$W'/W-1$, %	4.4	5.7	8.2	13.2	19.3	28.4	36.2	53.5
L_T/W, %	6.5	5.4	7.5	8.2	—	26.8	34.3	—
N, %	1.27	1.49	2.38	3.42	4.50	6.60	7.70	9.25
$x/3(N)$, %	5.0	5.9	9.9	14.8	20.0	32.7	40.1	51.3
$x/3$, %	5.3	6.8	9.8	15.8	23.2	34.1	42.2	64.2
P_r, %	2.6	2.7	3.8	4.3	—	14.4	19.0	—
$\Gamma \cdot 10^3$	—	—	—	—	—	—	—	—

Table 4

Cuprammonium Rayon C

(1) NAR=50%, DR=1/10, BR=220, T=18.5°C.

Not denitrated. * indicates the values after denitration.

t, hr	5/60	10/60	25/60
$W'/W-1$, %	24.9	39.2	69.0
L_T/W, %	20.2	36.6	72.5; 77.2*
N, %	5.78	8.94	12.34
$x/3(N)$, %	27.3	49.0	79.5
$x/3$, %	29.9	47.0	82.8
P_r, %	10.8	20.4	47.5; 52.2*
$\Gamma \cdot 10^3$	—	—	— 28.1*

(2) NAR=50%, DR=1/15, BR=212, T=16°C.

Not denitrated.

t, hr	5/60	9/60	15/60	26/60	42/60
$W'/W-1$, %	6.3	13.8	19.3	29.0	38.3
L_T/W, %	3.4	4.8	12.8	25.8	36.0
N, %	2.17	3.39	4.64	7.15	8.70
$x/3(N)$, %	8.9	14.6	20.8	36.2	47.2
$x/3$, %	7.6	16.6	23.2	34.8	46.0
P_r, %	1.7	2.4	6.5	13.6	20.0
$\Gamma \cdot 10^3$	—	—	—	—	—

(3) NAR=46%, DR=1/10, BR=154, T=14°C.

Denitrated. L_T/W* indicates the values before denitration.

t, hr	3/60	6/60	12/60	24/60	50/60	30/60**	35/60***
$W'/W-1$, %	3.1	6.1	9.2	15.4	21.8	39.0	42.8
L_T/W*, %	0.0	0.0	1.9	10.3	19.3	35.6	37.3
L_T/W, %	2.6	4.8	—	15.4	23.8	40.6	42.0
N, %	1.06	1.95	2.52	3.75	5.55	7.97	9.25
$x/3(N)$, %	3.3	8.0	10.3	16.7	26.1	42.1	51.1
$x/3$, %	3.7	7.3	11.0	18.5	26.2	46.8	51.4
P_r, %	1.3	2.4	—	8.0	12.7	22.9	23.8
$\Gamma \cdot 10^3$	31.4	31.8	—	31.3	30.8	30.4	29.9

** NAR=56%, DR=1/10, BR=220, T=2°C.

*** NAR=60%, DR=1/10, BR=220, T=2°C.

Table 5

Tire cord T

(1) NAR=50%, DR=1/10, BR=220, T=12°C. Denitrated. L_T/W^* indicates the values before denitration.

t, hr	40/60	1	1-20/60	1-40/60	2
$W'/W-1$, %	16.2	22.8	29.0	38.3	46.0
L_T/W^*, %	14.2	21.7	28.1	35.8	42.5
L_T/W, %	17.2	—	—	38.8	45.5
N, %	4.11	5.73	6.64	8.56	9.30
$x/3(N)$, %	18.1	27.1	33.0	46.2	51.3
$x/3$, %	19.4	27.4	34.8	46.0	55.2
P_r, %	9.0	11.1	15.5	21.6	26.2
$\Gamma \cdot 10^5$	33.6	—	—	32.7	32.0

(2) NAR=50%, DR=1/10, BR=220, T=10°C. Denitrated. L_T/W^* indicates the values before denitration.

t, hr	10/60	30/60	1-40/60	3-30/60
$W'/W-1$, %	5.6	10.2	20.1	53.1
L_T/W^*, %	3.1	7.9	19.4	53.0
L_T/W, %	5.5	10.1	—	56.1
N, %	1.54	2.66	4.81	9.26
$x/3(N)$, %	6.1	11.2	21.9	51.3
$x/3$, %	6.7	12.2	24.1	63.7
P_r, %	2.8	5.1	—	33.7
$\Gamma \cdot 10^5$	33.7	33.7	—	30.6

(3) NAR=50%, DR=1/10, BR=220, T=14°C. Denitrated. L_T/W^* indicates the values before denitration.

t, hr	55/60	1-50/60	2-20/60	3
$W'/W-1$, %	26.6	56.9	71.1	85.2
L_T/W^*, %	24.8	55.8	73.4	—
L_T/W, %	27.7	—	76.0	—
N, %	5.91	9.92	11.28	—
$x/3(N)$, %	28.1	56.1	67.9	—
$x/3$, %	31.9	68.3	85.3	—
P_r, %	15.0	33.5	51.0	—
$\Gamma \cdot 10^5$	33.2	—	30.4	—

Some of the previous samples are used also here in order to compare the acetylation and nitration results.

The notation in the above tables are defined below:

t: Duration of nitration, hr.
W: Weight of the sample used for nitration, g.
W': Weight of the nitrated yarn, g.
L_T/W: Extracted portion (by acetone) of the nitrated yarn. The percentage is expressed on the cellulose base.
N: Nitrogen content (%) of the nitrated yarn, determined with Lunge nitrometer.
P_r: Peeled-off portion of the single filament, expressed on the percentage of the original diameter.

Experimental Results

(1) Nitration.—In Fig. 1 the weight increase W'/W is plotted against the nitrogen content of the nitrated yarn, where the curve is the theoretical relation. The observed points of cuprammonium yarn (×) are on the theoretical curve, but the highly nitrated products of the other two samples (○ and ▲) deviate upward from the relation. The cause is not yet clear but this is certainly because the nitrogen content which is obtained is too low; of course in the case of the cuprammonium yarn it is said to be correctly obtained. Then it can be said, at least, that no part of the nitrated yarn disperses away in the nitration bath as the yarn does during acetylation, and then $\log(W'/W-1)$ versus $\log t$ is expected to be linear. Fig. 2 shows that this is the case.

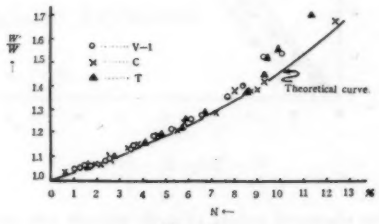

Fig. 1.

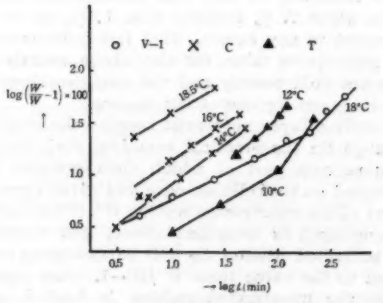

Fig. 2.

The knick points are seen on the relations of $V-1$ and T, but none on that of C. This relates probably to the existence of the skin, which will be studied precisely in the future.

The temperature coefficient of the nitration reaction is considerable.

(2) The weight of the peeled-off portion.—If the nitrated OH is x mols per 162 g of cellulose, W'/W is expressed by the following function of x.

$$W'/W-1=45/162 \cdot x$$

Assuming now that all the NO_2-groups are concentrated to the nitrated shell to constitute

trinitrocellulose[1] and this triester is extracted by acetone to give L_T, then L_T/W must be $x/3$. These relations are shown in Fig. 3, where $W'/W-1$ is plotted on the abscissa instead of $x/3$. x can be also calculated from the observed values of N %, which is given in Table 3~5 by $x/3(N)$, but this value which is obtained seems to be too low and the discussion is now ommitted here.

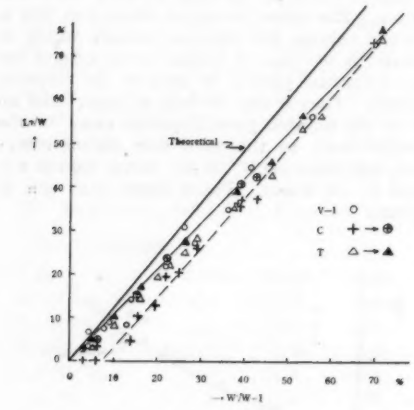

Fig. 3.

The observed points of each sample are on the separate lines, but they are all smaller than the corresponding theoretical values. It is worth while especially to note that the cuprammonium rayon whose N % is lower than 1.5% can not be extracted to any extent. This fact indicates that the assumption taken for the above calculation does not hold exactly and the next consideration can be given for one of the reasons.

A diffuse layer may exist between the trinitrocellulose (in the practical meaning) shell and the cellulose core, part of which then remains unextracted on the cellulose core and gives a greater value of the unextracted residue W', if the residue is considered as described above, and therefore the extracted portion L_T will be smaller as compared to the value from $W'/W-1$. And indeed when the unextracted residue is treated with NH_4SH alcoholic solution, L_T/W approaches to the theoretical; In the figure the point △ of T and + of C shift to the corresponding values is indicated by ▲ and ⊕ respectively.

These corrected points belong to a line which starts from the origin, but the inclination of the line differs from that of the theoretical line. This means that the part of the diffuse layer remains undissolved and the amounts increase as the nitration proceeds because the layer as it diffuses, becomes broader and broader toward the center of the filament.

Of course acetone dissolves not only trinitrocellulose but also lower nitrates, so the above consideration is a first approximation. But in this case L_T/W calculated from W'/W must be still larger.

Radial Distribution of Γ

The thickness of the peeled-off shell, P_r, was calculated from the values of L_T/W, where the extracted yarn with acetone was followed by the complete denitration with NH_4SH alcoholic solution, which was prepared by the well known method.[1]

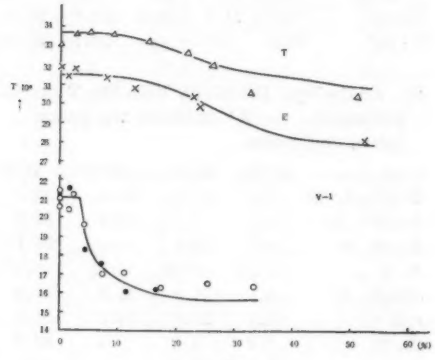

→ P_r

Fig. 4.

The intrinsic double refraction, Γ, of the peeled-off core was measured as described in the preceding paper. The double refraction of the extracted filament changes but slightly by denitration (cf. Fig. 4, ○ and ● of V—1 are the values before and after the denitration respectively) but the treatment is necessary to obtain the reasonable value of P_r, as the surface layer of the core contains some low substituted nitrocellulose before denitration.

The relation of Γ and P_r are shown in Fig. 4, where P_r of V—1 is exceptionaly calculated from L_T/W before denitration. Even in this case Γ is the double refraction after denitration. The observed points are plotted in the figure, where the curves are the relation taken from the second report of this series, obtained by the acetylation method. In the cases of the tire cord and cuprammonium rayons Γ of the original filaments differs tolerably from the corresponding values of the previous measurements, so the previous curves are shifted upwards in the figure so that the origins coincide in both measurements. This discrepancy of Γ is probably caused by the fact that the composition of the immersion liquids used for the present measurement of the refractive indices differs from those of the previous one. In the case of V—1 the same liquid compositions

(4) J. Chédin, *Kolloid. Z.* **125**, 65 (1952).

(5) Dorée, "The Method of Cellulose Chemistry", 1933, P. 227.

were used and such a phenomenon is not observed and therefore the correction is unnecessary.

Then the observed points nearly agree with the previous curves in all cases. So now it is proved that the nitration method is also suitable for the peeling-off and it is superior in some cases, where the speedy reaction with no degradation is required. Such examples will be reported in the near future.

The cost of this research has been defrayed by the Grant in Aid for Fundamental Scientific Research from the Ministry of Education, to which the authors' thanks are due.

Faculty of Engineering,
Yamagata University, Yonezawa
and
Faculty of Engineering,
Tokyo Metropolitan University, Tokyo

Vat Dyes of Pyrazoloanthrone Series. IV. Constitution and Properties of N-alkyl Derivatives of Pyrazoloanthrone Yellow[1]

By Toshio MAKI and Takashi AKAMATSU

(Received March 5, 1953)

The actual existence of the two isomers of N-alkyl derivatives of pyrazoloanthrone, 9-N-alkyl form (I) and 1-N-alkyl isomer (II), was shown in our previous report.[2] We have then pointed out the tautomerism of Pyrazoloanthrone Yellow (2, 2'-dipyrazoloanthronyl) (III $\rightleftarrows$ IV, R=H)

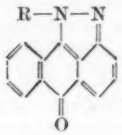

(I)

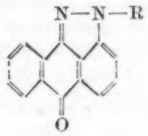

(II)

and established the constitution of the two isomers of its N, N'-dialkyl derivatives. Thus, 9-N, 9'-N'-dialkyl formula (III) has been given to the rubine red dyes and 1-N, 1'-N'-dialkyl structure (IV) to the orange isomers.[3]

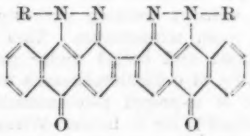

(III)

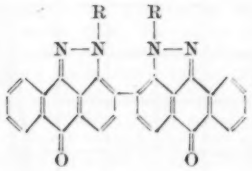

(IV)

The methyl (R=CH_3) and ethyl (R=$CH_2 \cdot CH_3$) compounds were already described in our preceding report.[3] We have now prepared hitherto unknown N, N'-di-n-propyl (III, IV, R=$CH_2 \cdot CH_2 \cdot CH_3$) and N, N'-di-n-butyl (III, IV, R=$CH_2 \cdot CH_2 \cdot CH_2 \cdot CH_3$) derivatives by the alkylation of Pyrazoloanthrone Yellow with the corresponding alkyl *p*-toluenesulfonate. In all cases rubine red vat dyes (III) of higher light fastness and orange isomers (IV) of lower light fastness were simultaneously produced, and the former dyes were the principal products (72~75% of the theory). The rubine red dyes are nearly insoluble in organic solvents, while the orange isomers so very easily soluble, that the quantitative separation of the two isomers can simply be carried out using *o*-dichlorobenzene.

	Yield (% of the theory)	
	Rubine red dyes (III)	Orange isomers (IV)
R=CH_3	75.1%	21.4%
R=$CH_2 \cdot CH_3$	74.9	23.8
R=$CH_2 \cdot CH_2 \cdot CH_3$	72.6	26.8
R=$CH_2 \cdot CH_2 \cdot CH_2 \cdot CH_3$	72.3	27.3

(1) Read before the 5th Annual Meeting of the Chemical Society of Japan on April 5, 1952.

(2) T. Maki and T. Akamatsu, *J. Chem. Soc. Japan, Ind. Chem. Section*, **54**, 281 (1951).

(3) T. Maki and T. Akamatsu, *J. Chem. Soc. Japan, Ind. Chem. Section*, **54**, 326 (1951); See also *J. C. S.*, **1952**, 1631, 1637~8.

Various coloring properties of the four principal rubine red vat dyes are compared.

Constitution (III)	Streak	Conc. H_2SO_4	Vat	On cotton	
				Shade	Light fastness
R=CH_3	Purple red	Red orange	Blue (A)	Rubine red	5~6(B)
R=C_2H_5[4]	Purple red	Red orange	Blue (A)	Rubine red	6 (A)
R=n-C_3H_7	Purple red	Red orange	Blue (C)	Rubine red	5~6(C)
R=n-C_4H_9	Purple red	Red orange	Blue (B)	Rubine red	5~6(D)

In the column of vat, (A) means easily soluble, (B) and (C) soluble with some difficulty. Under the light fastness, (A), (B), (C) and (D) denote the order of fastness. (A) is the highest among the four compounds.

More accurate comparison of the four rubine red dyeings were carried out using self recording G. E. spectrophotometer with 1% cotton dyeings (IN method) and the obtained reflectance curves (Fig. 1) were analysed according to the I. C. I. system.[5]

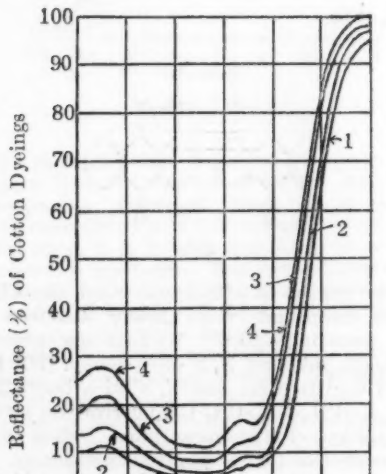

1.....(III), R=CH_3
2.....(III), R=C_2H_5
3.....(III), R=n-C_4H_9
4.....(III), R=n-C_3H_7

Fig. 1

Constitution (III)	R=CH_3	R=C_2H_5	R=n-C_3H_7	R=n-C_4H_9
Trichromatic coefficient x	0.4352	0.4252	0.3894	0.4137
Trichromatic coefficient y	0.2725	0.2609	0.2625	0.2650
Brightness Y(%)	9.16	11.47	19.46	16.07
Dominant wave-length (mμ)	495.1c	496.9c	499.2c	497.0c
Color purity (%)	41	44	36.2	40

Comparing the dominant wave-lengths it is known that the shade of the N, N'-dimethyl derivative is most reddish and that of the N, N'-di-n-propyl derivative most bluish although their differences are not very remarkable. It was unexpected that the n-butyl is less bluish than the n-propyl homologue. The shade of the N, N'-diethyl compound shows the highest color purity (i. e. most monochromatic) among the four, while lower brightness (Y) of the N, N'-dimethyl and diethyl compounds is shown due principally to their stronger dyeing powers. The order of the cotton dyeing powers is: methyl>ethyl>n-butyl>n-propyl.

Vinylon[6] fibres and cloths, to which most vat dyes are not satisfactorily applicable, can be dyed in rubine red shades by a modified IN method with these N, N'-dialkylated Pyrazoloanthrone Yellow, in which the N, N'-di-n-propyl compound gives the most clear and strong red dyeings of sufficient intensity. The washing fastness of vinylon dyeings of the *n*-propyl derivative was excellent, light fastness about 5 grade, their fastness to rubbing, however, was not very high (nearly 3 grade). The order of the vinylon dyeing powers is: n-propyl>ethyl>n-butyl>methyl.

Experimental Part

N, N'-Di-*n*-propyl Derivatives of Pyrazoloanthrone Yellow.—1.32 g. (1 mol. ratio) of Pyrazoloanthrone Yellow[3] was converted into nearly 20% paste by the usual method, heated on a water bath with 4 g. of 90% sodium hydroxide and 4 cc. of water, diluted with 62 cc. of cold water, the N, N'-disodium salt thus formed was filtered and without washing perfectly dried in vacuum at room temperature. This was then finely powdered and boiled under reflux with stirring in 26 g. of *o*-dichlorobenzene with 1.93g. (3 mol. ratio) of n-propyl p-toluenesulfonate (b. p. 4 mm. 145±3°) for 6 hours. When the hot solution was filtered and washed with alcohol and hot water the rubine red compound (III, R=$CH_2.CH_2.CH_3$) was obtained as an insoluble

(4) According to our studies this must be the true constitution of Indanthren Rubine R. See reference (3).
(5) A. C. Hardy, Handbook of Colorimetry.
(6) Polymerized vinyl alcohol partially acetallized (ca. 35%) with formaldehyde.

crystalline powder. Yield was 1.14 g. (72.61% of the theory). From the *o*-dichlorobenzene filtrate crude orange isomer (IV, R=$CH_2 \cdot CH_2 \cdot CH_3$) was collected after steam distillation. Yield was 0.42 g. (26.75% of the theory), the total yield corresponds to 99.36% of the theory.

The insoluble rubine red compound is a brown red powder, having a purple red streak, dissolves in conc. sulfuric acid with red orange color, from which by gradual addition of water successively resulted yellow-orange solution, yellow solution, yellow precipitate and at last purple red precipitate. Hydrosulfite vat, which is a little less easily soluble than other three N,N'-dialkyl derivatives, is blue, and cotton is dyed in clear purple-red shade by IN method (2% dye). When the substance was dissolved in 20 parts of 98.5% sulfuric acid and 8.2 cc. of water added dropwise with external cooling to produce 70% sulfuric acid the insoluble part (92%) was the rubine red dye of highest purity. Found: N, 10.68; Calculated for $C_{34}H_{26}O_2N_4$ (III, R=n-C_3H_7): N, 10.72 %.

The crude orange isomer, which had been obtained by steam distillation from the *o*-dichlorobenzene filtrate, was further purified by dissolving in monochlorobenzene, shaking with active coal, filtering and adding alcohol to the concentrated filtrate. It is an orange brown crystalline powder with an orange streak. Conc. sulfuric acid solution is red orange, from which orange precipitate resulted by the addition of water. From a blue hydrosulfite vat (IN) it dyes cotton red-orange of lower light fastness than the rubine red isomer. Found: N, 10.62; Calculated for $C_{34}H_{26}O_2N_4$ (IV, R=n-C_3H_7): N, 10.72%.

Vinylon fibres can be dyed by a modified IN method using dye paste. The dye bath consisted of 120 cc. of water, 3 cc. of 25% sodium hydroxide, 0.8 g. of hydrosulfite and 0.4 cc. of turkey red oil and vatted at 60° for 15 min. The fibres were dyed at 50° for 90 min. and after air oxidation, washing and acidification treated with soap solution (0.2:100) at 60° for 30 min. Sufficient intensity is obtained with 2% dye.

N,N'-Di-*n*-butyl Derivatives of Pyrazoloanthrone Yellow.—2.19 g. (1 mol. ratio) of Pyrazoloanthrone Yellow was converted into N,N'-disodium salt using 8 g. of 90% sodium hydroxide as in the case of the above n-propyl compounds. This was then as a dry, fine powder boiled with 44 g. of o-dichlorobenzene and 3.42 g. (3 mol. ratio) of n-butyl *p*-toluenesulfonate (b. p. 3.5 mm. 140~145°) for 6 hours and filtered hot. The yield of insoluble crystalline powder of the rubine red compound (III, R=$CH_2 \cdot CH_2 \cdot CH_2 \cdot CH_3$) was 1.96 g. (72.33% of the theory), while the amount of the soluble orange isomer (IV, R=$CH_2 \cdot CH_2 \cdot CH_2 \cdot CH_3$) was 0.74 g. (27.31% of the theory). The total yield was 99.64% of the theory. Their color reactions and dyeing properties are on the whole similar to those of the corresponding n-propyl derivatives. The comparison of the homologous rubine red dyes are given in the general part of this paper. The rubine red n-butyl compound of the highest purity remained insoluble (93%) by the treatment with 70% sulfuric acid. Found: N, 10.17; Calculated for $C_{36}H_{30}O_2N_4$ (III, R=*n*-C_4H_9): N, 10.18%.

The orange isomer was purified a in the case of the n-propyl compound with monochlorobenzene, active coal and alcohol and the orange brown crystalline powder thus obtained was analysed. Found: N, 10.11; Calculated for $C_{36}H_{30}O_2N_4$ (IV, R=n-C_4H_9):N, 10.18%.

Measurement of Reflectance Curves of the Cotton Dyeings.—1% IN cotton dyeings were carefully prepared using the rubine red vat dyes purified with 70% sulfuric acid. The dyes were converted into paste form before dyeing. The reflectance (%) of the cotton dyeings was measured by self recording G. E. spectrophotometer taking a similarly treated, undyed cotton cloth as the standard in order to cancel the absorption effect of the latter. The light source C of the I. C. I. system was used.

The authors express their gratitude to The Government Industrial Research Institute, Tokyo for the measurement of reflectance curves using self recording G. E. spectrophotometer.

Dyestuffs Research Laboratory,
Department of Applied Chemistry,
Tokyo University, Tokyo

A Reinvestigation of the Structure of Ethylene Oxide by Electron Diffraction

By Masato IGARASHI

(Received March 5, 1953)

Recently, Cunningham, Boyd, Gwinn, Myer, and Le Van investigated the structure of ethylene oxide by microwave spectrum,[1] and gave the results different from those of Ackermann and Mayer's earlier electron diffraction study[2] (Table 1). The difference is very large in the C—C distance. Therefore we have reinvestigated the structure by electron diffraction.

Ethylene oxide was prepared from ethylene chlorohydrin and lime. Electron diffraction photographs were obtained by the apparatus with a camera distance of about 9 cm and an electron wave length of about 0.055 Å. The maxima and minima of diffraction halos were measured by the visual method on the photographs; the q values are given in Table 2 and represented by the arrows in Fig. 1 ($q = (40/\lambda)\sin\phi/2$, where λ is the electron wave length and ϕ is the scattering angle).

A the atomic distances are equal to those of Ackermann and others, and in model B they are equal to those of Cunningham and others while in models C and D only the C—C distances are varied from those of B. The theoretical intensity curves (Fig. 1) were calculated by the well-known formula,[3]

$$I = \sum_{ij}(Z_i Z_j / r_{ij}) \exp(-a_i q_r^2) \sin(\pi q r_{ij}/10)$$

where r_{ij} is the distance between the atoms i and j, and Z_i is the atomic number of the atom i. The value of the coefficient a_{ij} was assumed to be 0.00016 for bonded hydrogen terms, 0.0004 for unbonded hydrogen terms, and zero for all the others. The theoretical values of q and their ratio to the observed values at the maxima and minima are shown in Table 2. It is clear that the models B and C fit better with the observed than the other

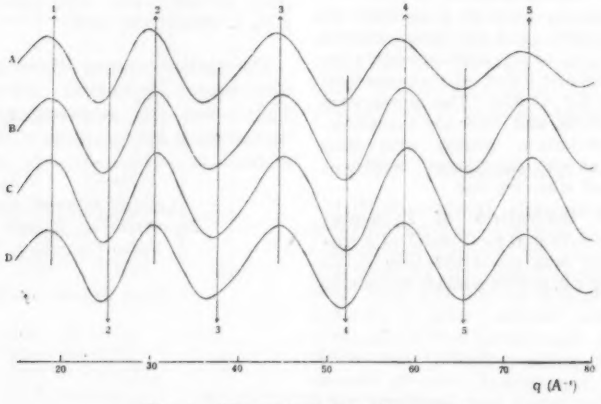

Fig. 1.—Theoretical intensity curves

The molecular models used for the correlation methods are compared in Table 1. In model models. Thus we can conclude that the C—C distance is 1.46±0.03 Å, supporting the results of the microwave spectroscopy.

(1) G. L. Cunningham, A. W. Boyd, W. D. Gwinn, and W. I. Le Van; *J. Chem. Phys.* **17**, 211 (1949); G. L. Cunningham, A. W. Boyd, R. J. Myer, W. D. Gwinn, and W. I. Le Van, ibid. **19**, 676 (1951).

(2) P. C. Ackermann and J. E. Mayer, *J. Chem. Phys.* **4**, 377 (1936).

(3) S. Spurr and V. Schomaker, *J. Am. Chem. Soc.* **64**, 2693 (1942).

Table 1

	(a) Cunningham	(b) Ackermann	(c) Models used for our study			
			A	B	C	D
C—C	1.472A	1.56±0.05A	1.56A	1.47A	1.44A	1.50A
C—O	1.436A	1.45±0.05A	1.45A	1.44A	1.44A	1.44A
C—H	1.082A	1.05±0.07A	1.05A	1.08A	1.08A	1.08A
∠H—C—H	116°41′		109.5°	116°41′	116°41′	116°41′
∠H_2—C—C	159°25′		151°	159°25′	159°25′	159°25′

Table 2

Max.	Min.	q_{obs}	q_{calc} A	q_{calc} B	q_{calc} C	q_{calc} D	q_{calc}/q_{obs} A	q_{calc}/q_{obs} B	q_{calc}/q_{obs} C	q_{calc}/q_{obs} D
1		18.9	18.2	18.6	18.7	18.5	0.962	0.983	0.988	0.978
	2	25.3	24.2	24.8	24.9	24.6	0.965	0.980	9.984	0.972
2		30.45	29.7	30.5	30.7	30.6	**0.975**	**1.002**	**1.008**	**0.998**
	3	37.6	35.8	36.7	37.1	36.5	0.952	0.976	0.987	0.971
3		44.5	44.2	44.6	44.9	44.5	**0.994**	**1.003**	**1.010**	**1.001**
	4	52.1	51.2	51.9	52.2	51.7	0.982	0.996	1.002	0.992
4		58.65	57.8	58.6	59.0	58.4	**0.986**	**0.999**	**1.006**	**0.996**
	5	65.4	65.0	65.8	66.1	65.4	0.994	1.006	1.011	1.000
5		72.6	71.6	72.6	73.2	72.3	0.986	1.000	1.008	0.996
			Average				0.979	0.996	1.002	0.992
			Average deviation				0.012	0.008	0.008	0.009

Values in Gothics were doubly weighted in computing averages.

The author wishes to express his gratitude to the late Professor H. Oosaka and to Professor A. Kotera for their kind guidance during the course of this research.

Department of Chemistry, Faculty of Science, Tokyo University of Education, Tokyo

---

4,4′-Dimethoxy-2,2′-dihalogeno-α,α′-dialkylstilbenes, Their Ultraviolet Absorption Spectra and Estrogenic Action

By Michinori ŌKI[1]

(Received March 9, 1953)

The essential features of the molecular structure favorable for the development of a strong estrogenic activity are two groups carrying active hydrogen atoms or producing such in vivo, located at an optimum distance from each other, and an optimum thickness.[2] Diethylstilbestrol, 4-HOC_6H_4CEt=CEtC_6H_4OH-4′, acquires its favorable molecular structure by virtue of the steric effect of the two ethyl groups at the α,α′-positions which force the benzene rings to rotate to a suitable extent. The smaller activity of 4,4′-dihydroxy-α,α′-dimethylstilbene (dimethylstilbestrol), 4-HOC_6H_4CMe=CMeC_6H_4OH-4′, is attributed to its thinner structure formed by the smaller steric effect of the methyl groups. It has been reported by Hudson and Walton[3] that 4,4′-dihydroxy-2,2′,α,α′-tetramethylstilbene, 4,2-

(1) Present address: Department of Chemistry, Faculty of Science, Tokyo Metropolitan University, Meguro, Tokyo.

(2) M. Ōki and Y. Urushibara, This Bulletin, **25**, 109 (1952).

(3) B. J. F. Hudson and E. Walton, *J. Chem. Soc.*, **1946**, 85.

Table 1

Estrogenic Activity of 4,4′-Dimethoxy-2,2′-dihalogeno-α,α'-dialkylstilbenes, 4,2-$CH_3OXC_6H_3CR=CRC_6H_3XOCH_3$-2′,4′.

	Substance	Melting point or Boiling point	Minimum active dose in mice
(I)	R=CH_3, X=Cl	[112—113°]	200 γ (5.9×10^{-7}mol.)
(II)	R=CH_3, X=Br	[117.5—119.5°]	200 γ (4.7× 〃)
(III)	R=CH_3, X=I	[159—160°]	500 γ (9.6× 〃)*
(IV)	R=C_2H_5, X=Cl, trans	[105.5—106.5°]	100 γ (2.7× 〃)
(V)	R=C_2H_5, X=Br, trans	[114.5—115°]	100 γ (2.2× 〃)
(VI)	R=C_2H_5, X=I, trans		200 γ (3.6× 〃)
(VII)	R=C_2H_5, X=Cl, cis	(88—89°/0.07 mm.)	1 mg.
(VIII)	R=C_2H_5, X=Br, cis	(87—89°/0.04 mm.)	1 mg.
(IX)	R=C_2H_5, X=I, cis	(108—110°/0.02 mm.)	1 mg.

* Active in 75 % animals.

Table 2

Absorption and Estrogenic Activity of 4,4′-Dimethoxy-α,α'-dialkylstilbenes, 4-$CH_3OC_6H_4CR=CRC_6H_4OCH_3$-4′.

	Substance	Melting point	$\lambda_{max.}$(mμ)	$\varepsilon_{max.}\times10^{-4}$	Minimum active dose in mice
(X)	R=CH_3	141.5—143°	247	2.85	100 γ (3.7×10^{-7}mol.)
(XI)	R=C_2H_5	121.5—123°	236	2.20	2.5 γ (0.084× 〃)

$HOMeC_6H_3CMe=CMeC_6H_3MeOH$-2′,4′, is a strong estrogen. Then it comes out that the methyl groups at 2,2′ positions may coöperate with the methyl groups at α,α'-positions to produce a molecular structure favorable for estrogenic action. As the bromine atom possesses a van der Waals radius nearly equal to that of the methyl group, it might be expected that introduction of bromine atoms into the 2,2′-positions of the 4,4′-dihydroxy-α,α'-dimethylstilbene would give also a potent estrogen, although it has been indicated that the bromine atoms in 4,4′-dimethoxy-α,α'-dibromostilbene, 4-$MeOC_6H_4CBr=CBrC_6H_4OMe$-4′, appear to have a smaller steric effect on the rotation of the benzene rings than that of the methyl groups in the corresponding α,α'-dimethyl compound.[4]

The present paper records the results of the investigations on the effect of introduction of two equal halogen atoms into the 2,2′-positions of 4,4′-dimethoxy-α,α'-dimethylstilbene and 4,4′-dimethoxy-α,α'-diethylstilbene (diethylstilbestrol dimethyl ether). The general principle of preparations, which are described in details in the Experimental Part, was as follows:

2-Halogeno-4-methoxy-acetophenone or -propiophenone, prepared from *m*-halogenoanisole and acetyl chloride or propionic anhydride, was transformed into the hydrazone. The hydrazone was oxidized to the diazomethane with yellow mercuric oxide. Treatment of the diazomethane with sulfur dioxide followed by decomposition of the resulting ring-sulfone gave the final product. Estrogenic potency was taken as an evidence for the structure of the product and as the basis for distinguishing the trans-form from the cis-form. Only the trans-form of each dimethyl compound was obtained, while in the cases of the diethyl compounds fractional distillation of the products gave geometrical isomerides.

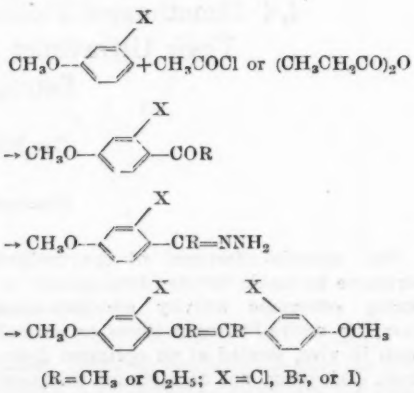

(R=CH_3 or C_2H_5; X=Cl, Br, or I)

The ultraviolet absorption curves of the trans-compounds are shown in Figs. 1 and 2. The absorption data of the parent compounds are given in Table 2. The trans-diiodo-diethyl compound (VI) was not obtained in a pure state and was not included in the

(4) M. Oki, This Bulletin, 26, 37 (1953).

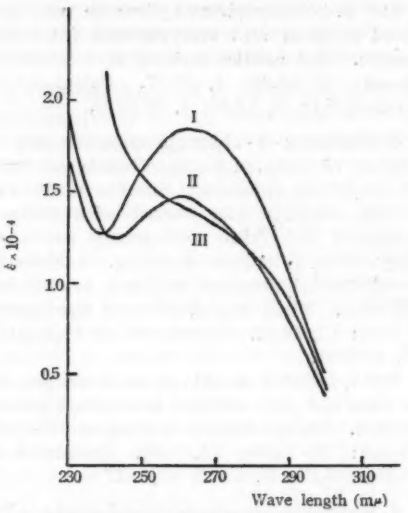

Fig. 1.—Ultraviolet absorption spectra of 4,4'-Dimethoxy-2,2'-dichloro-α,α'-dimethylstilbene ( ), 4,4'-Dimethoxy-2,2'-dibromo-α,α'-dimethylstilbene (II), and 4,4'-Dimethoxy-2,2'-diiodo-α,α'-dimethylstilbene(III)

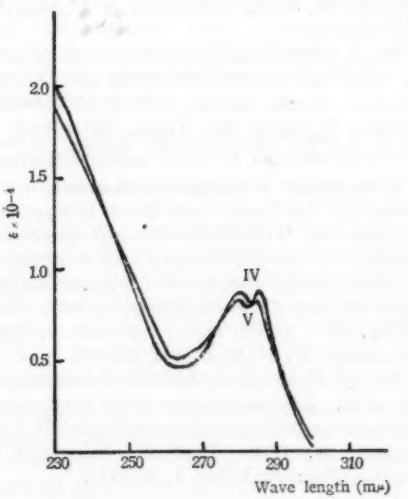

Fig. 2.—Ultraviolet absorption spetra of 4,4'-Dimethoxy-2,2'-dichloro-α,α'-diethylstilbene (IV) and 4,4'-Dimethoxy-2,2'-dibromo-α,α'-diethylstilbene (V).

absorption measurement. The dimethyl compounds and the diethyl compounds, respectively, showed absorption maxima at the same wave lengths irrespective of the kinds of halogen atoms at 2,2'-positions, although the diiodo-dimethyl compound (III) gave no maximum but a shoulder. Provided that the observed absorptions are those depending on the conjugation of the system comprising the benzene rings and the central ethylenic linkage, this may suggest that the halogen atoms at 2,2'-positions in any of the substances examined have little steric influence on the rotation degree of the benzene rings, because it would be less plausible to consider alternatively that they had definite and equal influence in spite of their different bulks. Then it may be said that the alkyl groups at α,α'-positions alone determine the rotation degree of the benzene rings, and the 2,2'-dihalogeno-compounds retain the structures of the parent compounds except the halogen atoms present in place of the hydrogen atoms at 2,2'-positions.

However, it remains unexplained why the bathochromic effect of the halogen substitution is greater in the diethyl compounds than in the dimethyl compounds. The observed absorptions of the dimethyl compounds and those of the diethyl compounds might not correspond to each other, because they appear characteristically different both in the shapes and in the extinction coefficients.

The minimum active doses were determined by the vaginal smear test with ovariectomized mice, substances in camellia oil being injected subcutaneously in two portions. The results given in Table 1 indicate that the diethyl compounds are stronger than the corresponding dimethyl compounds, and, either in the diethyl or in the dimethyl series, the dichloro-compound and the dibromo-compound have nearly the same potency, while the diiodo-compound a weaker potency. The liquid isomerides of the diethyl compounds showed very weak activities, indicating that they were cis-forms. The activities of the parent compounds are given in Table 2 with the absorption data. Comparison of the activities of the dihalogeno-derivatives with those of the parent compounds shows that the halogen substitution at 2,2'-positions reduced the activity, slightly in the dimethyl series, while profoundly in the diethyl series. The reduction of the activity was probably caused, at least partly, by the fattening of the molecules by the halogen atoms, and it is quite natural to suppose that the sharp peak of activity peculiar to the optimum structure of diethylstilbestrol may be very sensitive even to a slight deformation of the structure.

Experimental Part

4-Methoxy-2-chloroacetophenone.—To a

mixture of 14.3 g. of 3-chloroanisole, prepared from 3-methoxybenzenediazonium chloride and cuprous chloride,[5] and 16.0 g. of anhydrous aluminum chloride in 30 c.c. of carbon disulfide, 7.9 g. of acetyl chloride were gradually added with good stirring and cooling. The reaction mixture was left to stand for 30 minutes at room temperature and then gently boiled for 30 minutes. The upper carbon disulfide layer was decanted off. After treated with ice and hydrochloric acid (20 c.c.), the mixture was extracted with benzene. The benzene solution was washed with 10% aqueous sodium hydroxide and then with water, dried over calcium chloride, and distilled under a reduced pressure. 4-Methoxy-2-chloroacetophenone distilled over at 139–141° (10 mm.) and solidified on cooling. Recrystallization from petroleum ether gave colorless needles melting at 26–27°. Yield 11.5 g. (62% of the theory). Found: Cl, 19.15. Calculated for $C_9H_9O_2Cl$: Cl, 19.20%.

The 2,4-dinitrophenylhydrazone was obtained in yellowish orange needles melting at 181–183°, when recrystallized from ethyl acetate. Found: N, 15.58; Cl, 9.56. Calculated for $C_{15}H_{13}O_5N_4Cl$: N, 15.36; Cl, 9.72%.

4-Methoxy-2-bromoacetophenone.—Obtained in the same way as 4-methoxy-2-chloroacetophenone by using 18.7 g. of 3-bromoanisole, prepared from 3-methoxybenzenediazonium bromide and cuprous bromide.[6] 4-Methoxy-2-bromoacetophenone distilled at 149–151°(8 mm.) or 163–166°(15 mm.). It solidified on cooling in a refrigerator to large prisms melting below the room temperature (23°). Yield 13.5 g. (59% of the theory). Found: Br, 34.72. Calculated for $C_9H_9O_2Br$: Br, 34.89%.

The 2,4-dinitrophenylhydrazone was obtained in reddish yellow needles melting at 193–194°, when recrystallized from ethyl acetate. Found: N, 13.67; Br, 19.76. Calculated for $C_{15}H_{13}O_5N_4Br$: N, 13.69; Br, 19.53%.

4-Methoxy-2-iodoacetophenone.—Synthesized in the same way as described for 4-methoxy-2-chloroacetophenone from 23.4 g. of 3-iodoanisole, prepared by the decomposition of 3-methoxybenzenediazonium chloride in an acidic potassium iodide solution.[7] 4-Methoxy-2-iodoacetophenone distilled at 168—170° (9.5 mm.) or 158—159° (6 mm.) and was recrystallized from petroleum ether. Colorless needles melting at 68—70°. Yield 15.8 g. (55% of the theory). Found: I, 45.52. Calculated for $C_9H_9O_2I$: I, 45.97%.

(5) F. Leverdin and F. Eckhard, *Ber.*, **32**, 2626 (1899).
(6) Cf. H. R. Snyder and Z. Wicks, Jr., "Organic Syntheses", Vol. 24, p. 22.
(7) A. Baeyer and V. Villiger, *Ber.*, **35**, 3026 (1902).

The 2,4-dinitrophenylhydrazone was prepared as usual and recrystallized from ethyl acetate. Red needles melting at 108.5—109°. Found: N, 12.40; I, 27.87. Calculated for $C_{15}H_{13}O_5N_4I$: N, 12.28; I, 27.82%.

4-Methoxy-2-chloropropiophenone.—A mixture of 14.3 g. of 3-chloroanisole and 30.0 g. of anhydrous aluminum chloride in 50 c.c. of carbon disulfide was treated with 10.5 g. of propionic anhydride analogously as in the preparation of its lower homolog. 4-Methoxy-2-chloropropiophenone distilled at 152–153° (12 mm.). Yield 12.2 g. (61% of the theory). Found: Cl, 18.02. Calculated for $C_{10}H_{11}O_2Cl$: Cl, 17.85%.

The 2,4-dinitrophenylhydrazone was prepared as usual and recrystallized from ethyl acetate-alcohol. Orange leaflets melting at 168–169°. Found: N, 15.55; Cl, 9.50. Calculated for $C_{16}H_{15}O_5N_4Cl$: N, 15.45; Cl, 9.77%.

4-Methoxy-2-bromopropiophenone.—Prepared in the same way as 4-methoxy-2-chloropropiophenone, 18.7 g. of 3-bromoanisole being used instead of 3-chloroanisole. 4-Methoxy-2-bromopropiophenone distilled at 146–147° (6 mm.). Yield 15.7 g. (65% of the theory). Found: Br, 32.94. Calculated for $C_{10}H_{11}O_2Br$: Br, 32.88%.

The 2,4-dinitrophenylhydrazone was prepared as usual and recrystallized from ethyl acetate-alcohol. Orange leaflets melting at 154–155°. Found: N, 13.51; Br, 19.68. Calculated for $C_{16}H_{15}O_5N_4Br$: N, 13.76; Br, 19.62%.

4-Methoxy-2-iodopropiophenone.—Prepared in the same way from 23.4 g. of 3-iodoanisole. 4-Methoxy-2-iodopropiophenone distilled at 158–162°(6 mm.) and solidified on cooling. Recrystallization from petroleum ether gave colorless plates melting at 61–63°. Yield 17.3 g. (58% of the theory). Found: I, 43.86. Calculated for $C_{10}H_{11}O_2I$: I, 43.75%.

The 2,4-dinitrophenylhydrazone was prepared as usual. Recrystallization from ethyl acetate gave orange-yellow needles melting at 161-162°. Found: N, 12.78; I, 28.23. Calculated for $C_{16}H_{15}O_5N_4I$: N, 12.56; I, 27.94%.

4-Methoxy-2-chloroacetophenone-hydrazone.—A solution of 4-methoxy-2-chloroacetophenone (5.0 g.) and hydrazine hydrate (1.6 g.) in hot propyl alcohol (5 c.c.) was refluxed for 5 hours on an oil bath. Crystals separating on cooling were collected and recrystallized from alcohol. Colorless needles melting at 138–139°. Yield 0.2 g. (4% of the theory). Found: N, 14.22; Cl, 18.09. Calculated for $C_9H_{11}ON_2Cl$: N, 14.10; Cl, 17.85%. On standing it decomposed probably to an azine.

All the ketones described above gave poor yields of hydrazones even when heated with hydrazine hydrate in ethanol for 5 hours.

4,4'-Dimethoxy-2,2'-dichloro-α,α'-dimethylstilbene (I).—A suspension of 3.0 g. of the above hydrazone and 5.5 g. of yellow mercuric oxide in 30 c.c. of petroleum ether was shaken for 8 hours at 12–16°. The resulting red solution containing the diazomethane was filtered from solids. To the filtrate cooled in ice-water, a rapid stream of sulfur dioxide was passed until the color disappeared. The solvent was distilled off from the reaction mixture and the remainder was heated at 160–200° to complete the decomposition. The oil solidified on cooling and was purified by chromatographical separation followed by recrystallization from benzene-petroleum ether. Pale yellow needles melting at 112–113°. Yield 0.4 g. (16% of the theory). Found: Cl, 21.32. Calculated for $C_{18}H_{18}O_2Cl_2$: Cl, 21.03%.

4-Methoxy-2-bromoacetophenone-hydrazone.—Treatment of the ketone (13.5 g.) with hydrazine hydrate (3.5 g.) in propyl alcohol gave difficultly crystallizable hydrazone, which was directly used in the next reaction. On long standing at a cool place it solidified and was recrystallized from alcohol. Colorless needles melting at 88–90°. Found: N, 11.60; Br, 32.98. Calculated for $C_9H_{11}ON_2Br$: N, 11.48; Br, 32.74%.

4,4'-Dimethoxy-2,2'-dibromo-α,α'-dimethylstilbene (II).—A suspension of the above crude hydrazone and yellow mercuric oxide in petroleum ether was treated in an analogous way as described for the dichloro-compound (I). Recrystallization from benzene-petroleum ether gave 4,4'-dimethoxy-2,2'-dibromo-α,α'-dimethylstilbene in pale yellow needles melting at 117.5–119.5°. Yield 0.3 g. (3% of the theory). Found: Br, 37.73. Calculated for $C_{18}H_{18}O_2Br_2$: Br, 37.51%.

4-Methoxy-2-iodoacetophenone-hydrazone.—Prepared in the same way. The crystalline product obtained in colorless needles melting at 158–160° after recrystallization from benzene-petroleum ether was not the expected hydrazone. The major part of the product was an oil and used in the next step without purification.

4,4'-Dimethoxy-2,2'-diiodo-α,α'-dimethylstilbene (III).—Prepared from the above crude hydrazone in the same way as the dichloro-compound (I). Chromatographical separation followed by recrystallization from benzene-alcohol or ethyl acetate gave pale yellow plates melting at 159–160°. Yield 0.03 g. from 3.0 g. of the crude hydrazone (1% of the theory). Found: I, 49.12. Calculated for $C_{18}H_{18}O_2I_2$: I, 48.80%.

4-Methoxy-2-chloropropiophenone-hydrazone.—Prepared in the same way as the acetophenone-hydrazones. The oily hydrazone was used without purification.

4,4'-Dimethoxy-2,2'-dichloro-α,α'-diethylstilbene (IV) (VII).—Prepared in the same way as the corresponding dimethyl compound (I). Five hours' shaking was sufficient for oxidation. Distillation of the product gave a pale yellow oil boiling at 125–145° (0.5 mm.) and another yellow viscous oil boiling at 210–220° (0.5 mm.). Redistillation of the former gave a colorless oil boiling at 88–89° (0.07 mm.). Found: Cl, 19.52. Calculated for $C_{20}H_{22}O_2Cl_2$: Cl, 19.41%. The latter fraction solidified on standing at a cool place for a long time and was recrystallized from alcohol. Colorless prisms melting at 105.5–106.5°. Found: Cl, 19.53. Calculated for $C_{20}H_{22}O_2Cl_2$: Cl, 19.41%. Yield 0.8 g. of the liquid compound and 1.5 g. of the solid isomeride from 10.0 g. of the starting ketone (25% of the theory).

The estrogenic activities showed that the liquid compound was the cis-form and the solid the trans-form. The same holds good for other diethyl compounds described below.

4-Methoxy-2-bromopropiophenone-hydrazone.—Obtained as an oily substance and used without purification.

4,4'-Dimethoxy-2,2'-dibromo-α,α'-diethylstilbene (V) (VIII).—Prepared from the above crude hydrazone. Distillation of the product gave a pale yellow oil boiling at 135–140°(0.3 mm.) and a yellow viscous oil boiling at 190–205°(0.25 mm.). The former was refined to a colorless oil boiling at 87–89°(0.04 mm.). Found: Br, 35.02. Calculated for $C_{20}H_{22}O_2Br_2$: Br, 35.19%. The higher boiling fraction solidified on standing at a cool place for a long time and was recrystallized from alcohol. Colorless prisms melting at 114.5–115°. Found: Br, 35.23. Calculated for $C_{20}H_{22}O_2Br_2$: Br, 35.19%. Yield 1.2 g. of the liquid cis-isomeride and 1.7 g. of the solid trans-isomeride from 10.0 g. of the starting ketone (31% of the theory).

4-Methoxy-2-iodopropiophenone-hydrazone.—Obtained as an oily substance and used without purification.

4,4'-Dimethoxy-2,2'-diiodo-α,α'-diethylstilbene (VI) (IX).—Synthesized from the above hydrazone. Distillation of the product gave a yellow oil boiling at 65–120°(0.03 mm.)

and a residue. The distillate was refined to a colorless oil boiling at 108–110°(0.02 mm.). Found: I, 46.58. Calculated for $C_{20}H_{22}O_2I_2$: I, 46.74%. The residue did neither distil even at 200°(0.0005 mm.) nor solidify. It was fractionated through an alumina column in benzene solution and the solvent was evaporated in vacuo. A heavy viscous oil. Found: I, 45.82. Calculated for $C_{20}H_{22}O_2I_2$: I, 46.74%. Yield 1.3 g. of the cis-isomeride and 2.0 g. of the trans-isomeride from 10.0 g. of the starting ketone (33% of the theory).

Ultraviolet absorption spectra. — They were recorded with a Beckman Model DU photoelectric quarz spectrophotometer in 95% ethanol. The length of solutions was 5 mm. and the concentrations were 0.02 to 0.05 millimol per litre.

The author wishes to thank Professor Y. Urushibara for his kind guidance. Thanks are also due to Mr. F. Ueno of the Teikoku Hormone Manufacturing Co., Ltd., Kawasaki, for the bio-assays and to the Ministry of Education for the Grant in Aid for Fundamental Scientific Research.

Department of Chemistry,
Faculty of Science, Tokyo University.

Radiometric Determination of Small Amounts of Thallium

By Tomitaro ISHIMORI

(Received March 17, 1953)

In 1940, a method of gravimetric determination of thallium which is based on the quantitative precipitation of thallium as $[Co(NH_3)_6](TlCl_6)$ was first reported by G. Spacu and A. Pope.[1] They determined about 100 mg. thallium by their method.

In 1949, examining this method carefully, Y. Murakami[2] improved it slightly and ascertained its excellent selectivity. According to this author an amount of thallium as small as 5 mg. could be determined precisely. In this paper, a new method of radiometric determination of smaller amounts of thallium, i. e. 3 mg. —0.5 microg. thallium is proposed.

This method consists in the precipitation of thallium by radioactive hexammine cobaltic trichloride which is labelled with cobalt-60 and the measurement of radioactivity of the precipitate which is due to the radioactive cobalt combined with hexachlorothallic ion as hexammine cobaltic ion. As the precipitation of thallium with hexammine cobaltic trichloride is highly selective, the method will be applied in various cases. However, the presence of radioactive thallium will disturb the determination. Therefore, for example, the determination of thallium contents in radioactive minerals will not be successful.

Further, it must be added that another method of radiometric determination of microamounts of thallium had been reported by H. Moureu et al.[3] in 1944. Their method is based on the formation of radioactive thallium iodide.

Experimental Part

(1) **Apparatus.**—Chemical procedures are operated in a microbeaker. For the filtration of the precipitate a filter-tube with a layer of sintered glass is used. The filtering surface is covered with fibres of filter paper, suspended in the water, by sucking up through the tube.

For the measurement of radioactivity, a Lauritsen electroscope made by the Scientific Research Institute, Tokyo, and a Geiger-Müller counter with a scaler of 32 which is prepared by Prof. T. Sasaki, Kyushu University, are used.

(2) **Reagents.** — Stock solution of thallium nitrate is prepared by dissolving thallous nitrate (Merck reagent), and standardised by the Spacu's method. Diluting this stock solution, a series of standard solutions (acidified slightly with nitric acid) is prepared.

Solution of potassium chlorate: 1 g. potassium chlorate is dissolved in 15 cc. distilled water.

Solution of hexammine cobaltic trichloride: According to the amounts of thallium to be determined, either the solution of the precipitant (A) or that of (B) is used.

Solution of the precipitant (A): 0.05 *M* aqueous solution of the hexammine cobaltic trichloride which is prepared by the Biltz's method[4] from 10 g. cobalt chloride containing about 2.5 mg. cobalt-60 chloride. This solution is used for the

(1) G. Spacu und A. Pope, *Z. Anal. Chem.* **120**, 322 (1940).
(2) Y. Murakami, This Bulletin **22**, 206 (1949).
(3) H. Moureu, P. Chovin and R. Daubel, *Chem. Abst.* **40**, 1752 (1946); *Compt. rend.* **219**, 127 (1944).
(4) H. Biltz, "Übungsbeispiel aus der anorg. Experimentalchemie", Leipzig, **1913**, s. 165.

determination of 3.1—0.034 mg. thallium.

Solution of the precipitant (B): About 0.05 *M* aqueous solution of the hexammine cobaltic trichloride which is prepared as above from 0.5g. cobalt chloride containing about 5 mg. cobalt-60 chloride. This solution is used for the determination of less than 30 microg. thallium.

(3) **Procedure.**—A known quantity of a thallium solution is taken from a burette into a microbeaker. 0.5 cc. of 1% ammonium chloride, 1—2 drops of hydrochloric acid (1:1) and 3—5 drops of potassium chlorate solution are added to the beaker. Thallium is oxidised to the thallic state by gentle boiling on a hot plate. When the volume of the liquid is reduced to less than one half, the beaker is removed from the hot plate and cooled on standing. The total volume of the solution must be 0.5—2 cc. Then 2—5 drops of the radioactive hexammine cobaltic trichloride reagent are added, until the solution is coloured orange red. If the amount of thallium present is less than about 30 microg., the precipitate is scarcely seen or is not seen at all. In such cases, it is preferable to leave it overnight. In other cases, the precipitate is formed immediately and it is necessary to leave it only for a short time. The precipitate formed as above is filtered with the above-mentioned filter-tube, and washed four times with small portions of 2% hydrochloric acid. Filtrate and washings are discarded. About 1 cc. of 3% hydrogen peroxide and a few drops of acetic acid are added to the beaker which contains the precipitate and filter-tube. After dissolving the precipitate by heating on a water bath, the solution is poured into a glass dish through the filtertube by suction. Several times the filter-tube and the inside of the beaker are rinsed with small portions of distilled water. All these washings are transferred into the glass dish. The combined solution in the glass dish is evaporated up on a water bath. After cooling, the radioactivity of the glass dish which contains the residue is measured.

(4) **Measurement of Radioactivity.**—Measured radioactivity of each specimen which is corrected for the natural leaks or natural counts is represented by divisions per minute (d/m), or counts per minute (c/m). The specimen obtained from 1.55 mg. Tl by using the solution of precipitant (A) is reserved as the standard of radioactive $[Co^*(NH_3)_6][TlCl_6]$. Shortly after the measurement of the radioactivity of each specimen, the radioactivity of the standard, $(d/m)_s$ or $(c/m)_s$ is measured in the condition of the same geometry. The ratio $(d/m)/(d/m)_s$ or $(c/m)/(c/m)_s$ is not affected by the variation of the sensitivity of the Lauritsen electroscope or the Geiger-Müller counter and the decay of the radioactivity of cobalt-60. So far as the reagent of the same bottle is used, the specific activity of the reagent is constant and the ratio $(d/m)/(d/m)_s$ or $(c/m)/(c/m)_s$ will depend only on the amount of thallium.

(5) **Results Obtained.**—The results for 3.1—0.034 mg. Tl are shown in Table 1. All these results are obtained by using the solution of the precipitant (A). From the Table 1 we can see that there are no serious differences between the results obtained by Geiger-Müller counter and those obtained by Lauritsen electroscope and that the relation between the amount of thallium and the ratio $(c/m)/(c/m)_s$ is almost linear. The deviations of $(c/m)/(c/m)_s$/mg. Tl of the each experiment from the mean value of $(c/m)/(c/m)_s$/mg. Tl, 0.701, are calculated in the fourth column, and from the mean value of the deviations we can estimate the accuracy of the determination.

Table 1

Results for 3.1—0.034 mg. Tl

mg. Tl (taken)	Measured by G. M. Counter $\frac{(c/m)}{(c/m)_s}$	Measured by G. M. Counter $\frac{(c/m)/(c/m)_s}{\text{mg. Tl}}$	% Deviation	Measured by Lauritsen Electroscope $\frac{(d/m)}{(d/m)_s}$
3.100	2.196	0.708	1.0	2.184
2.790	1.853	0.664	−5.3	1.857
2.325	1.534	0.659	−5.9	1.630
2.108	—	—	—	1.468
2.015	1.411	0.700	0.0	1.329
1.721	—	—	—	1.115
1.550	1.000	0.645	−8.0	1.000
1.225	0.871	0.711	1.4	0.867
0.744	0.493	0.662	−5.6	0.505
0.482	0.347	0.719	2.6	0.360
0.449	0.300	0.668	−4.7	0.303
0.360	0.273	0.755	7.7	0.259
0.228	0.171	0.750	7.0	0.163
0.130	0.098	0.753	7.4	0.096
0.077	0.064	0.831	18.5	0.059
0.034	0.020	0.588	−16.0	0.019
0.000	0.000	—	—	0.000
mean	—	0.701	±6.5	—

Table 2

Results for 24.6—0.46 microg Tl

microg Tl (taken)	$(d/m)/(d/m)_s$	$\frac{(d/m)/(d/m)_s}{\text{microg Tl}}$	% Deviation
24.6	0.619	0.0251	−14.4
23.4	0.657	0.0281	− 4.1
21.6	0.594	0.0275	− 6.1
18.4	0.517	0.0281	− 2.7
15.4	0.465	0.0302	3.1
12.9	0.370	0.0287	− 2.1
9.08	0.226	0.0248	−15.4
5.95	0.152	0.0255	−13.0
3.85	0.117	0.0303	3.4
1.86	0.063	0.0338	15.4
1.24	0.045	0.0363	23.8
0.46	0.015	0.0326	11.3
0.00	0.000	—	—
mean	—	0.0293	±9.5

If the amount of thallium is calculated from the following equation (1), the accuracy of the method will be in the order of $\pm(6-7)\%$.

$$\text{mg. Tl} = (c/m)/(c/m)_s/0.701 \qquad (1)$$

The results for 24.6—0.46 microg. Tl obtained by using the solution of the precipitant (B) are shown in Table 2. In these cases the radioactivity is measured only by the Lauritsen electroscope. From Table 2 we can see that the linear relation between the amount of thallium and ratio $(d/m)/(d/m)_s$ is not so good and that although more than about five micrograms thallium may be calculated from the following equation (2), it is preferable to use a working curve in the determination of thallium less than about five micrograms.

$$\text{microg. Tl} = (d/m)/(d/m)_s/0.029 \qquad (2)$$

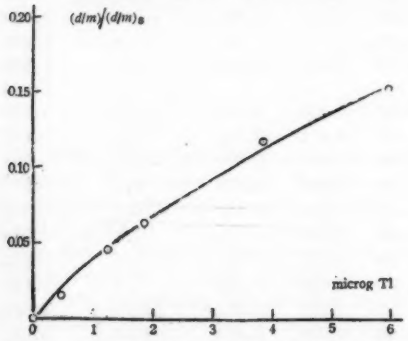

Fig. 1.—Working Curve for Determination of minute Amounts of Thallium

Fig. 1 shows the working curve for the determination of minute amounts of thallium. Roughly speaking, the error in the determination of the minute quantities of thallium is estimated about ten per cent or more.

(6) **Application.** — The method is applied to the determination of the thallium contents in volcanic rocks in the following procedure[5]:

To about 2 g. of finely divided rock powder in a platinum dish add about 8 cc. of 6N sulfuric acid and about 12 cc. of hydrofluoric acid. Evaporate to dryness and fume off the excess sulfuric acid avoiding decomposition of ferric sulfate. Take up the residue in a little water and again fume off the sulfuric acid. Treat the residue with water; warm to bring all soluble material into solution. Cool the solution and make up to about 100 ml. Reduce thallium to thallous state with hydroxylamine hydrochloride and add 5 cc. of 10% potassium cyanide and 5 cc. of 10% ammonium citrate. Adjust the *p*H to about 10 adding dilute ammonium hydroxide dropwise. Extract the mixture with four 10—15 cc. portions of 0.1% dithizone in chloroform. Combine the extracts and wash with 20—50 cc. of (1:1000) ammonium hydroxide. Separate the chloroform layer and shake the aqueous phase with a few cc. of dithizone solution to recover any thallium that may have passed into the ammonia solution. Shake the combined chloroform extracts with 10 cc. of (1:100) nitric acid and separate the chloroform layer. The aqueous layer is transferred to a microbeaker and evaporated to about 1 cc. or less. The resultant solution is treated as (3) using solution of precipitant (B).

To examine the recovery of thallium, known quantities of thallium standard solution are diluted to about 100 cc. and treated with dithizone following the above-mentioned procedure. Results are considerably low as shown in the Table 3.

Table 3
Recovery of Thallium

microg Tl (taken)	$(d/m)/(d/m)_s$	microg Tl (found) (a)	microg Tl (found) (b)	% Recovery
14.8	0.398	—	13.5	91
3.8	0.092	2.8	3.1	73—81

(a): calcd. from Fig. 1 (b): calcd. from Eq. (2)

Table 4
Thallium contents of Rocks

Sample	microg Tl (added)	$(d/m)/(d/m)_s$	microg Tl (found) (a)	microg Tl (found) (b)	%Tl
2.11 g. Liparite (Kozusima, Izu)	none	0.029	0.8	1.0	0.00005
2.04 g. 〃 (〃)	6.1	0.139	5.1	4.7	—
1.77 g. Basalt (Fuji)	none	0.003	0.1	—	0.00000

(a): calcd. from Fig. 1 (b): calcd. from Eq. (2)

The results obtained on two Japanese volcanic rocks are shown in Table 4. These values will be low from the above-mentioned results of examination of the extraction of thallium, but it will be sure that the thallium content of the liparite is in the order of $10^{-5}\%$.

Further study on the determination of thallium content of silicate rocks is to be continued.

The auther wishes to express his sincere thanks to Prof. Sinnosuke Matuura for the opportunity to carry out this investigation and to Mr. Tohru Nozaki for his assistance in the experiment.

Chemical Laboratory, Faculty of Science, Kyushu University

(5) c. f. F. J. Welcher, "Organic Analytical Reagents". Vol. 3, D. Van Nostrand Co, New York, (1949), p. 544.

The Raman Spectrum of Cyanuric Acid

By Mitsuo ITO

(Received April 6, 1953)

Introduction

From the experimental results of the ultraviolet absorption spectra, E. Agallidis and his coworkers as well as I. M. Klotz and Themis Askounis have concluded that enol-and keto-formal cyanuric acids coexist in aqueous solution in the tautomeric relation.[1],[2] In the present work, the author tried to ascertain this from the view-point of Raman spectrum, and computed further approximate force constants for both forms by simple calculations.

Experimental

For photographing Raman spectra a powerfully light-gathering spectrograph constructed by us was used. It had two dense flint prisms (height 4.5 cm, side length 6 cm), a collimator lens (diameter 9 cm., focus 45 cm.) and a camera lens (diameter 8 cm., focus 21 cm.). Two glass mercury lamps were used as the light source, placed on both sides of the wood-type Raman tube. The exposure time, on "Oriental" Hyper Panchromatic plates, ranged from 10 to 100 hours.

A sample of pure cyanuric acid, recrystallized from water three times, was dissolved in a hydrogen chloride acidic and a caustic soda alkaline solution. As the concentration of the aqueous solution at room temparature could not be made greater than about 10 %, although water seems to be the best solvent for the acid, a rather long exposure time was needed to record measurable Raman lines. During the exposure hot water was circulated continually through the outer jacket of the wood tube in order to prevent the precipitation of crystal.

Table 1 lists wave number shifts measured in the Raman spectra of both the acidic and alkaline solutions, with indications of their relative intensities and exciting mercury lines.

Discussion

As shown in Table 1, there are some Raman lines which have nearly coinciding wave number shifts, but with changing relative intensities observed in the two solutions. For example, 708 cm.$^{-1}$ measured for the alkaline solution and 715 cm.$^{-1}$ measured for the acidic solution, giving the same Raman shift within experimental error, shows a much greater intensity in the alkaline solution. Other such examples are found in the pairs of 331 and 329, 432 and 425, and 1410 and 1421 cm.$^{-1}$.

Table 1

Observed Raman lines of cyanuric acid in the acidic and alkaline solutions

Alkaline solution			Acidic solution		
Wave number shift (cm.$^{-1}$)	Exciting mercury line	Relative intensity	Wave number shift (cm.$^{-1}$)	Exciting mercury line	Relative intensity
331	e	3	329	e	1
432	e	3	425	e, k	1
456	e, k, i	1			
572	e, k, i	2			
708	e, —e, k	8	715	e, k	3
			816	e, k	3
853	e	3	853	e, k, i	6
923	e, k	3	921	e	4
1090	k, i	2			
			1371	e, k, i	2
1410	k, i	4	1421	e, k, i	2
			1636	k, i	5
			3446	e, k, i	6
			3488	e, k	4

(1) E. Agallidis, H. Fromherz and A. Hartmann, *Ber.*, **71**, 1391 (1938).

(2) I. M. Klotz and Themis. Askounis, *J. Am. Chem. Soc.*, **69**, 801 (1947).

On the other hand, there are some pairs of lines whose intensities are in the reverse ratio, that is, strong in the acidic and weak in the alkaline solution. The pairs 853 and 853, and 923 and 921 cm.$^{-1}$ belong to this type.

Such a change of relative intensities of the corresponding Raman lines can be readily understood by assuming that tha enol-and keto-formal cyanuric acids coexist in aqueous solution and that the equilibrium between them changes with the *p*H of the solution. This assumption is in agreement with and supports the result of ultra-violet absorption.[1],[2]

In caustic soda alkaline solution, cyanuric acid exists more stably in the form of cyanuric acid ion represented by formula (1) in Fig. 1, while in acidic solution the keto form represented by (11) is more stabilized. Then the Raman lines which are stronger in the alkaline solution must be due to (1), and those stronger in the acidic solution to (11). Accordingly the shifts 331, 432, 708 and 1410 cm.$^{-1}$ are attributed to (1), and those of 853, 921, 1636, 3446 and 3488 cm.$^{-1}$ to (11).

Let us consider first the frequencies of totally symmetric vibrations of the cyanuric acid ion of form (1). X-ray diffraction studies show that the symmetry in cyanuric acid crystal is D_{3h}.[3]

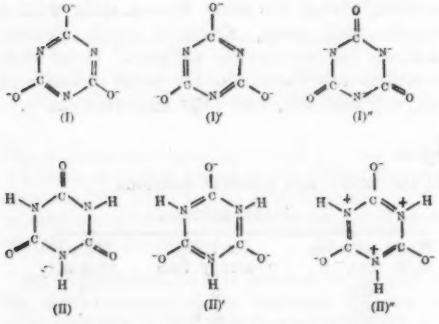

Fig. 1.—Resonance structures for cyanuric acid of enol-and keto-forms.

Assuming the same symmetry also for the ion (1), there are in all three totally-symmetric vibrations. As totally-symmetric vibrations generally appear strongly in the Raman effect,[4] it is reasonable to consider that among the four strong lines attributed by us to (1) (either one of 331 or 432, 708 and 1410 cm.$^{-1}$) the first one is probably the totally-symmetric deformation vibration of the six-membered ring, the second the totally-symmetric breathing vibration of the whole ion, and the last the totally-symmetric stretching vibration of the carbon and oxygen atoms.

On a crude assumption that cyanuric acid ion resonates only between the two Kekulè-like structures (1) and (1)′ in Fig. 1, the totally-symmetric vibration frequencies were calculated using the valence-force-field model.[4]

For the force constants the following values were used:

k (C—O) $= 5.00 \times 10^5$ dyne/cm.,[5]
k (C—N) $= 7.6 \times 10^5$ dyne/cm.,[5]
δ ($\angle$NCN) $= 0.23 \times 10^5$ dyne/cm.,[6]
δ ($\angle$CNC) $= 0.32 \times 10^5$ dyne/cm.,[6]

where k and δ refer to stretching and bending vibrations respectively. The three totally-symmetric vibration frequencies and the corresponding vibrational types are

481 cm.$^{-1}$: deformation vibration,
904 cm.$^{-1}$: breathing vibration,
and 1288 cm.$^{-1}$: stretching vibration of the c-o bonds.

These calculated frequencies, however, do not agree well with the Raman frequencies observed above, meaning that the force constants used are not suitable. An attempt was made then to derive more reasonable force constants by substituting the obsered Raman frequencies into the final equations of the frequency calculation and to interpret their meaning. For this purpose 708 and 1410 cm^{-1} were taken as the two totally-symmetric non-deformation vibrations because of their prominent intensities. For the remaining totally-symmetric frequency we may choose either 331 or 431 cm.$^{-1}$.

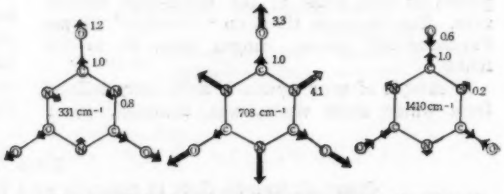

Fig. 2.—Calculated totally-symmetric vibrational frequencies and modes of the cyanuric acid ion.

If we chose 431 cm.$^{-1}$, some force constants would come out negative. Therefore we took

(3) E. H. Wiebenga and N. F. Moermann, *Z. Krist.*, **99**, 217 (1938).
(4) G. Herzberg, "Raman and infrared spectra of polyatomic molecules," Van Nostrant, N. Y., (1945).
(5) Hibben, "Raman effect and its chemical application", Reinhold, N. Y., (1939).
(6) L. Kellner, *Proc. Roy. Soc. London*, **177**, 456 (1941).

331 cm.$^{-1}$ as the frequency of the third totally-symmetric vibration. The force constants calculated on the above assumptions are

k (C—O)$=6.71\times10^5$ dyne/cm.,
k (C—N)$=5.71\times10^5$ dyne/cm..

In Fig. 2, the calculated vibrational modes are shown for each frequency.

Comparing the above force constants with those already known for other molecules, the k value for the c-o bond may be explained as the result of addition of a slight double-bond character to that of the formal single bond, and the k value for the C—N bond caused by the actual bond having a more single-bond character than the formal one-and-half-bond. Thus the cyanuric acid ion gets some resonance contribution also from the keto-ionic structure as well as from the kekulé-like structures, as shown in Fig. 1.

Next, we applied the same consideration to the keto-formal structure (II) which is stable in acidic solution. Assuming also the symmetry D_{3h} for this structure, the totally-symmetric vibrations are four in number theoretically, i. e. in addition to the three vibrational types mentioned above for the cyanuric acid ion there is one more totally-symmetric stretching vibration of the N—H bond.

With the same procedures the four totally-symmetric vibration frequencies belonging to the formula (II) in Fig. 1 were calculated, using the following force constants

k (C=O)$=11.6\times10^5$ dyne/cm.,[5]
k (C—N)$=4.85\times10^5$ dyne/cm.,[5]
k (N—H)$=6.20\times10^5$ dyne/cm.,[5]
δ ($\angle$NCN)$=0.23\times10^5$ dyne/cm.,[6]
δ ($\angle$CNC)$=0.32\times10^5$ dyne/cm.,[6]

The resulting frequencies are

353 cm.$^{-1}$: deformation vibration,
769 cm.$^{-1}$: breathing vibration,
1811 cm.$^{-1}$: stretching vibration of the C=O bond,
3346 cm.$^{-1}$: stretching vibration of the N—H bond.

These frequencies are again very different from the observed Raman values 853, 1636, etc. In order to obtain a better agreement, we must adopt a larger and a smaller force constant for the C-N and the C=O bond respectively. The binding strength of the C-N bond in thit molecule should be larger than that of the formal C-N bond, and the C=O bond of it should be weaker than in the formal C=O bond. Accordingly some amount of the resonance contribution from the ionic structures (II)′ and (II)″ in Fig. 2 may be expected.

Although it is certain that cyanuric acid takes predominantly the keto-form in the acidic solution and enol-form in the alkaline solution, respectively, only the extreme structures (I) and (II) cannot explain the facts.

For example, the reported atomic distances in crystalline cyanuric acid are 1.28 A for the C-O bond and 1.37 A for the C-N bond,[3] both of which are intermediate between the normal single and the normal double bond lengths.

This fact is also confirmed by magnetic susceptibility measurements.[7] In the case of cyanuric acid in acidic or alkaline solution the structural contribution of the enol-or the keto-form appears much more dominant than in the case of crystal, depending on the pH value of the solution.

Finally, the author wishes to express his hearty thanks to Professor S. Imanishi, and to Assistant Professor Y. Kanda for their kind guidance. He also thanks Mr. Furukawa for his assistance in the experimental part of the work.

Department of Chemistry,
Faculty of Science, University of Kyushu,
Fukuoka

(7) J. Maruyoshi, *J. Chem. Soc. Japan*, **71**, 627 (1950).

Theoretical Study on the Polarographic Limiting Currents. I. Revised Equation for the Diffusion Currents*

By Hiroaki MATSUDA

(Received April 9, 1953)

Criticism of the Revised Equations Already Reported

Recently H. Strehlow and M. von Stackelberg,[1] J. J. Lingane and B. A. Loveridge[2] and T. Kambara, M. Suzuki and I. Tachi,[3] taking the curvature of dropping mercury electrode into consideration, derived the following revised expression of Ilkovič equation representing the mean diffusion current $\bar{i}_d(\mu A)$.

$$\bar{i}_d = 607 n {}^*C D^{1/2} m^{2/3} \tau^{1/6} (1 + A D^{1/2} m^{-1/3} \tau^{1/6}) \quad (1)$$

In this equation, n, ${}^*C$, D, m and τ are the number of electrons associated with the electrode reaction, the concentration of depolarizer in the bulk of solution in millimol/l, the diffusion constant of depolarizer in cm.^{2}/sec., the rate of flow of mercury in mg./sec. and the drop time in sec., respectively; A is a coefficient of interest to be discussed.

Strehlow and von Stackelberg have obtained the value $A=17$, upon solving the so-called Stackelberg's integral equation[4] representing the "differential thickness of diffusion layer" denoted by δ.[5] It seems, however, that the conclusion $A=17$ has not a good theoretical ground owing to the error contained in the integral equation employed by them, as given below. They define the "integral thickness of diffusion layer", denoted by Δ, by the relationship:

$$\Delta = \frac{2}{{}^*C} \int_{r_0}^{\infty} ({}^*C - C) dr \quad (2)$$

and upon assuming that $4\pi r_0^2 \cdot \Delta$ is proportional to the total amount of reduction product, they derive

$$\Delta = \frac{2D}{r_0^2} \int_0^t r_0^2 \delta^{-1} dt \quad (3)$$

where t is the time. These assumptions stated by them are not right in tri-dimensional problem, although they are legitimate in unidimensional one. This can be readily seen, when we treat a stationary spherical electrode, in which the quantity $4\pi r_0^2 \Delta$ is clearly not proportional to the amount of reduction product, and thus Eq. (3) does not hold. In order to define the integral thickness of diffusion layer in such a rational way, as Eq. (3) can hold in the case of stationary spherical electrode, we should use the following equation instead of Eq. (2).

$$\Delta' = \frac{2}{{}^*C r_0^2} \int_{r_0}^{\infty} ({}^*C - C) r^2 dr \quad (4)$$

It can be shown that in the case of diffusion at a stationary spherical electrode Δ' and δ are given by

$$\Delta' = 4\sqrt{\frac{Dt}{\pi}} \left(1 + \frac{\sqrt{\pi Dt}}{2r_0}\right) \quad (5)$$

$$\frac{1}{\delta} = \frac{1}{r_0} + \frac{1}{\sqrt{\pi Dt}} \quad (6)$$

Elimination of t from Eqs. (5) and (6) leads to the relationship between Δ' and δ, which holds for the stationary electrode of spherical form; thus it is found that

$$\Delta' = \frac{4}{\pi} \frac{r_0 \delta}{r_0 - \delta} \left(1 + \frac{\delta}{2(r_0 - \delta)}\right) \quad (7)$$

If we assume that Eq. (7) holds for the diffusion at the dropping electrode, upon eliminating Δ' from Eqs. (3) and (7), we obtain the following integral equation:

$$\pi D \int_0^t r_0^2 \delta^{-1} dt = r_0^3 \left\{ 2 \frac{\delta}{r_0 - \delta} + \left(\frac{\delta}{r_0 - \delta} \right)^2 \right\} \quad (8)$$

---

* A part of this paper was read at the 5th Annual Meeting of the Chemical Society of Japan, April 4, 1952, Tokyo.

(1) H. Strehlow and M. von Stackelberg, *Z. Elektrochem.*, **54**, 51 (1950).

(2) J. J. Lingane and B. A. Loveridge, *J. Am. Chem. Soc.* **72**, 438 (1950).

(3) T. Kambara, M. Suzuki and I. Tachi, This Bulletin **23**, 219 (1950).

(4) M. von Stackelberg, *Z. Elektrochem.*, **45**, 466 (1939).

(5) The differential thickness of diffusion layer is defined as follows:

$$i = {}^*C f (\partial C / \partial r)_{r=r_0}$$

In this equation, C, r_0 and r are the concentration of depolarizer at an arbitrary point in the diffusion layer, the radius of mercury drop and the distance of any point from the center of drop, respectively.

This equation is the Stackelberg's integral equation determining the thickness δ in the case of spherical diffusion at a mercury drop expanding symmetrically. This equation has been already derived by Kambara, Suzuki and Tachi,[5] and upon solving this equation by means of an approximate calculation, they have shown the value of A to be 29.3.[6] The present author expands the quantity δ into the power series of $(m^{-1/3}D^{1/2}t^{1/6})$; i.e.

$$\delta=(D^{1/2}t^{1/2})\sum_{j=0}^{\infty}\beta_j(m^{-1/3}D^{1/2}t^{1/6}),$$

and then by comparing the means of comparison of coefficients, the β's are determined; thus Eq. (8) can be solved more precisely and the value of $A=31.2$ is obtained.

The above stated procedures are all based on the assumption that Stackelberg's integral equation, i.e. Eq. (7) showing the relationship between the differential and integral thicknesses of diffusion layer at a stationary spherical electrode, is valid even in the case of a dropping electrode. However, this assumption seems to have no theoretically concrete basis.

On the other hand, the intuitive consideration of Lingane and Loveridge[2] gave the value $A=39$. Kambara and Tachi[7] approximately solved the differential equation proposed by D. MacGillavry and E. K. Rideal[8] and the result was $A=39$; but the accuracy of this approximate calculation seems considerably inferior.

On account of these circumstances, it may be significant to consider here again the theoretical revision of Ilkovič equation. In this paper the solution of MacGillavry-Rideal differential equation by means of the method, that has been employed in the field of hydrodynamics by Th. von Kármán[9] and K. Pohlhausen[10] in order to evaluate the velocity distribution in the boundary layer, will be demonstrated and the expression for the limiting diffusion current will be shown. Further, the shielding effect of capillary will be considered theoretically. Finally, the revised Ilkovič equation representing the diffusion current in amalgam polarography will be also shown.

(6) T. Kambara and I. Tachi, This Bulletin, **25**, 284 (1952).
(7) T. Kambara and I. Tachi, This Bulletin, **23**, 225 (1950).
(8) D. MacGillavry and E. K. Rideal, *Rec. trav. chim.*, **56**, 1013 (1937).
(9) Th. von Karman, *Z. angew. Math. u. Mech.*, **1**, 233 (1921).
(10) K. Pohlhausen, ibid., **1**, 252 (1921).

Theoretical Derivation of the Revised Equation for the Diffusion Current

The movement of solution in the vicinity of mercury drop appears to be very complicated; now let us assume that the solution around the mercury drop is pushed away by the concentric expansion of drop, the volume of which increases at a constant rate. Then we can find $C(r,t)$ the concentration of depolarizer in the diffusion layer, by solving the following MacGillavry-Rideal differential equation:

$$\frac{\partial C}{\partial t}=D\frac{1}{r^2}\frac{\partial}{\partial r}\left(r^2\frac{\partial C}{\partial r}\right)-\frac{a^3}{3r^2}\frac{\partial C}{\partial r} \qquad (9)$$

where

$$a=(3m/4\pi d)^{1/3}$$

In this equation d represents the density of mercury at 25°C.

The initial and boundary conditions are clearly given by

$$C={}^*C \quad \text{for} \quad t=0,\ r>r_0;$$
$$C=0 \quad \text{for} \quad r=r_0,\ t>0;$$
$$C={}^*C,\ r^2\frac{\partial C}{\partial r}=0 \quad \text{for} \quad r\to\infty,\ t>0.$$

${}^*C$ represents here the concentration of depolarizer in the bulk of solution, and the radius of mercury drop r_0 is given by

$$r_0=at^{1/3}=\left(\frac{3}{4\pi d}\right)^{1/3}m^{1/3}t^{1/3}=0.260m^{1/3}t^{1/2}(\text{mm})$$

Upon multiplying the both sides of Eq. (9) by r^2, and integrating the equation thus obtained with respect to r from r_0 to infinity, it can be readily seen that

$$\frac{\partial}{\partial t}\int_{r_0}^{\infty}({}^*C-C)r^2dr=Dr_0^2\left(\frac{\partial C}{\partial r}\right)_{r=r_0}.$$

Since the diffusion constant of depolarizer is very small, the inhomogencity of concentration distribution occurs only in the vicinity of electrode surface; therefore, the integration interval from r_0 to infinity shown in the above equation may be replaced by that from r_0 to $\delta'(t)$, resulting in no appreciable deviation. Here, $\delta'(t)$ is a function of time, and represents the thickness of layer, in which the inhomogeneity of concentration arises, i.e. the thickness of diffusion layer. Writing

$$r=r_0+x,$$

then it is found that

$$\frac{\partial}{\partial t}\int_0^{\delta'}({}^*C-C)(r_0+x)^2dx = Dr_0^2\left(\frac{\partial C}{\partial x}\right)_{x=0} \tag{10}$$

This equation corresponds to the integro-differential equation of von Kármán in hydrodynamics; in order to solve this equation, we will at first expand the quantity ${}^*C-C$ in the power series of x; i. e.

$${}^*C-C={}^*C\frac{x}{r_0+x}\left(1+\sum_{j=1}^{l}A_jx^j\right) \tag{11}$$

When the l unknown coefficients A_j ($j=1, 2, \ldots, l$) are determined as functions of δ' and r_0 with the aid of l suitable boundary conditions, then insertion of Eq. (11) into Eq. (10) gives an ordinary differential equation of first order demonstrating δ'. Upon integrating the differential equation thus obtained, we can find δ' as a function of time, from which the proper expression for the diffusion current is derived.

(i) At first we will put $l=6$; then the following boundary conditions are found, by which A_j ($j=1, 2, \ldots, 6$) are to be determined.

$$\left.\begin{aligned}&(C)_{x=\delta'}={}^*C;\ \left(\frac{\partial C}{\partial x}\right)_{x=\delta'}=0;\\&\left(\frac{\partial^2 C}{\partial x^2}\right)_{x=\delta'}=0;\ \left(\frac{\partial^3 C}{\partial x^3}\right)_{x=\delta'}=0;\\&\left(\frac{\partial^4 C}{\partial x^4}\right)_{x=\delta'}=0;\\&\left[\frac{\partial^2\{(r_0+x)C\}}{\partial x^2}\right]_{x=0}=0\end{aligned}\right\} \tag{12}$$

The first five equations result from the fact that the concentration C in the diffusion layer should vary as continually as possible and be connected with the bulk concentration ${}^*C$ at $x=\delta'$. The last condition is obtained when the relation $r=r_0+x$ is inserted into Eq. (9) and then $x=0$ is put therein. Upon determining the coefficients A_j by the aid of conditions shown by Eq. (12), it is found that ${}^*C-C$ is given by

$${}^*C-C={}^*C\frac{r_0}{r_0+x}\left\{1-3\left(\frac{x}{\delta'}\right)+10\left(\frac{x}{\delta'}\right)^3-15\left(\frac{x}{\delta'}\right)^4+9\left(\frac{x}{\delta'}\right)^5-2\left(\frac{x}{\delta'}\right)^6\right\} \tag{13}$$

Insertion of Eq. (13) into Eq. (10) gives the following ordinary differential equation of first order, by which δ' is to be determined.

$$\frac{d}{dt}\left(\frac{3}{14}r_0^2\delta'+\frac{1}{28}r_0\delta'^2\right)=Dr_0^2\left(\frac{1}{r_0}+\frac{3}{\delta'}\right) \tag{14}$$

Now writing

$$\delta'=(D^{1/2}t^{1/2})\sum_{j=0}^{\infty}\alpha_j(a^{-1}D^{1/2}t^{1/6})^j$$

and inserting this equation into Eq. (14), we can determine α_j's by the method of comparison of coefficients; thus the solution of Eq. (14) is given by the equation in form of following power series.

$$\delta'=(D^{1/2}t^{1/2})\left\{2\sqrt{3}+\frac{4}{5}(a^{-1}D^{1/2}t^{1/6})-\frac{19}{75}\sqrt{3}\,(a^{-1}D^{1/2}t^{1/6})^2+\frac{856}{6375}(a^{-1}D^{1/2}t^{1/6})^3-\ldots\right\} \tag{15}$$

Since the diffusion current i_d is equal to the number of mols of depolarizer reaching the surface of dropping electrode in unit time multiplied by nF, it is found that

$$i_d=4\pi r_0^2\cdot nF\cdot D\left(\frac{\partial C}{\partial r}\right)_{r=r_0}=4\pi r_0^2\cdot nF\cdot D\cdot{}^*C\left(\frac{1}{r_0}+\frac{3}{\delta'}\right)$$

When the expression for δ' given by Eq. (15) is inserted into the above equation, then we obtain the following equation showing the instantaneous diffusion current, in which the usual conventional units are employed.

$$i_d=709\,n{}^*CD^{1/2}m^{2/3}t^{1/6}\{1+35.5(D^{1/2}m^{-1/3}t^{1/6})+266(D^{1/2}m^{-1/3}t^{1/6})^2-\ldots.\} \tag{16}$$

Accordingly the mean diffusion current is shown by

$$\bar{i}_d=608n{}^*CD^{1/2}m^{2/3}\tau^{1/6}\{1+31.1\,(D^{1/2}m^{-1/3}\tau^{1/6})+207(D^{1/2}m^{-1/3}\tau^{1/6})^2-\ldots.\} \tag{17}$$

(ii) In order to execute the calculation of higher order approximation, the value $l=10$ will be chosen; for the determination of A_j ($j=1, 2, \ldots, 10$) to the six boundary conditions shown by Eq. (12) the following four conditions will be added.

$$\left.\begin{aligned}&\left(\frac{\partial^5 C}{\partial x^5}\right)_{x=\delta'}=0;\ \left(\frac{\partial^6 C}{\partial x^6}\right)_{x=\delta'}=0;\\&\left(\frac{\partial^7 C}{\partial x^7}\right)_{x=\delta'}=0;\\&\left[\frac{\partial^4}{\partial x^4}\{(r_0+x)C\}\right]_{x=0}+4\frac{a^3}{D}\frac{1}{r_0^3}\left(\frac{\partial C}{\partial x}\right)_{x=0}=0\end{aligned}\right\} \tag{18}$$

The last condition can be obtained, when r in Eq. (9) is replaced by (r_0+x) and then equation thus obtained is twice differentiated with respect to x and further $x=0$ is put therein.

When the quite analogous mathematical procedures shown in the case of $l=6$ are carried out, then we find the following equation representing the instantaneous and mean diffusion current; i. e.

$$i_d=709n^*CD^{1/2}m^{2/3}t^{1/6}\{1+36.3(D^{1/2}m^{-1/3}t^{1/6}) +343(D^{1/2}m^{-1/3}t^{1/6})^2-\ldots.\} \quad (19)$$

$$\bar{i}_d=608n^*CD^{1/2}m^{2/3}\tau^{1/6}\{1+31.7\,(D^{1/2}m^{-1/3}\tau^{1/6}) +267(D^{1/2}m^{-1/3}\tau^{1/6})^2-\ldots.\}. \quad (20)$$

Although the accuracy of mathematical treatment can be increased with the increasing greater value of l, the numerical calculation thereof becomes more and more complicated. Furthermore, the comparison of Eq. (16) with (19) and (17) with (2) clearly indicates that the coefficients of the first, second and third terms, appearing in the above stated two calculations, show no considerable differences. Hence the approximate calculation with $l=10$ may be satisfactorily precise.

NOTE:—In the case of uni-dimensional diffusion, coresponding to the Ilkovič equation, the solution can, as well known, be obtained rationally; when the above developed approximate treatment is applied to this case with the value $l=10$, the following equations for the instantaneous and mean diffusion current are derived.

$$i_d=709n^*CD^{1/2}m^{2/3}t^{1/6}$$

$$\bar{i}_d=608n^*CD^{1/2}m^{2/3}\tau^{1/6}$$

Comparison of these equations with the Ilkovič equation indicates that the coefficients 707 and 607 obtained by Ilkovič are converted into 709 and 608, respectively, by the present approximate method. Therefore the above derived coefficients 709 and 608, which appear in Eqs. (16), (17), (19) and (20) showing the instantaneous and mean diffusion current, may be replaced by the values 707 and 607, respectively.

Shielding Effect of the Capillary Tube

In the above quoted mathematical treatment, it is assumed that the mercury drop hangs freely in solution and expands concentrically. In fact, however, at the upper end of drop the capillary tube exists, and accordingly the diffusion of depolarizer from the region neighbouring the upper part of drop is prevented.

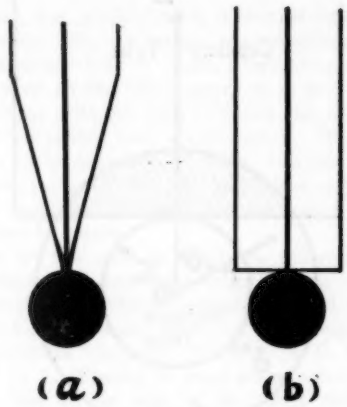

Fig. 1.

In the case of the tapering capillary tube as illustrated in Fig. 1 (a), the shielding effect of capillary may be considerably lessened; but with the capillary of thick wall as shown in Fig. 1 (b) this effect should be taken into account.

Next we will consider how the diffusion current will be affected by the shielding effect due to such a capillary as shown in Fig. 1(b). In order to treat this problem precisely, we must integrate the differential equation representing the cylindrically symmetric diffusion with the boundary conditions which are so complicated that it appears almost impossible. Hence we may be satisfied with the treatment based on the simplified model as follows.

Since the total current I, which has flowed in the time interval from $t=0$ to $t=t$, is obviously equal to the number of mols of depolarizer, which have disappeared from the solution in the same time interval, multiplied by nF, the diffusion current i_d is given by

$$i_d=\frac{dI}{dt}=nF\frac{d}{dt}\iiint_V(^*C-C)r^2\sin\theta\,dr\,d\theta\,d\varphi \quad (21)$$

where the region of integration V covers all the space in diffusion layer. In the preceding treatment, the region of integration is regarded to be the spherical shell surrounded by two spheres of radii r_0 and $r_0+\delta'$, owing to the assumption of free existence of mercury drop in solution. The upper part of this spherical shell, however, is in fact partly covered by the lower tip of capillary tube, as illustrated by the shaded portion in Fig. 2, and so the decrease in the concentration of depolarizer in this shielded part has no effect on the current

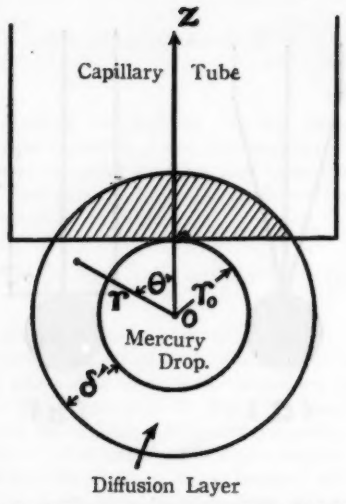

Fig. 2.—Schematic representation of shielding effect due to capillary tube.

intensity. Hence, in order to consider the shielding effect of capillary, the proper region of integration must be limited to the part of spherical shell which is really occupied by solution. Therefore, as to the three variables, r, θ and φ, the limits of integration should be $r_0 \to r_0+\delta'$, $\cos^{-1}(r_0/r) \to \pi$ and $0 \to 2\pi$, respectively. With these considerations, Eq. (21) is written in the form:

$$i_d = nF\frac{d}{dt}\int_0^{2\pi} d\varphi \int_{r_0}^{r_0+\delta'} ({}^*C-C)r^2 dr \times \int_{\cos^{-1}\frac{r_0}{r}}^{\pi} \sin\theta d\theta$$

Upon executing the calculation with the value $l=10$ after inserting the expression for ${}^*C-C$ given by Eq. (11) into the above equation, we can obtain the following equation for diffusion current.

$$i_d = 709n^*CD^{1/2}m^{2/3}t^{1/6}\{1+23.5(D^{1/2}m^{-1/3}t^{1/6}) +62.9(D^{1/2}m^{-1/3}t^{1/6})^2-\ldots.\} \quad (22)$$

Whence the mean diffusion current is found to be

$$\bar{i}_d = 608n^*CD^{1/2}m^{2/3}\tau^{1/6}\{1+20.6(D^{1/2}m^{-1/3}\tau^{1/6}) +49.0(D^{1/2}m^{-1/3}\tau^{1/6})^2-\ldots.\} \quad (23)$$

Revised Equation for the Diffusion Current in Amalgam Polarography

Next, employing the similar mathematical procedure as is already shown above, we will derive the revised Ilkovič equation showing the diffusion current observed in amalgam polarography.

Although the movement of mercury in the drop electrode seems very complicated, the diffusion process of amalgamated metal may be regarded to proceed in a spherical mercury drop expanding concentrically, provided that the rate of flow of mercury is not seriously great. Then the distribution of concentration $C_M(r,t)$ of amalgamated metal in the mercury drop is represented by the following equation.

$$\frac{\partial C_M}{\partial t} = D_M\frac{1}{r^2}\frac{\partial}{\partial r}\left(r^2\frac{\partial C_M}{\partial r}\right)-\frac{a^3}{3r^2}\frac{\partial C_M}{\partial r} \quad (r\leqq r_0) \quad (24)$$

Here, D_M is the diffusion constant (cm.²/sec.) of amalgamated metal in mercury.

Further the initial and boundary conditions are given by

$$\left.\begin{aligned} &C_M = {}^*C_M \quad \text{for} \quad t=0 \ (r<r_0);\\ &C_M = 0 \quad \text{for} \quad r=r_0 \ (t>0);\\ &C_M = {}^*C_M,\ \frac{\partial C_M}{\partial r}=0 \quad \text{for} \quad r=0 \ (t>0) \end{aligned}\right\} \quad (25)$$

where ${}^*C_M$ represents the concentration of amalgamated metal in the bulk of mercury.

Multiplying the Eq. (24) by r^2 and then integrating with respect to r from zero to r_0, it can be readily seen that

$$\frac{\partial}{\partial t}\int_0^{r_0}({}^*C_M-C_M)r^2dr = -D_M r_0^2\left(\frac{\partial C_M}{\partial r}\right)_{r=r_0}$$

Since it may be assumed that the thickness of diffusion layer $\delta'_M(t)$ is much smaller than r_0, the integration from zero to r_0 may be replaced by that from $r_0-\delta'_M$ to r_0; then putting $r=r_0-x$, we have

$$\frac{\partial}{\partial t}\int_0^{\delta'_M}({}^*C_M-C_M)(r_0-x)^2dx = D_M r_0^2\left(\frac{\partial C_M}{\partial x}\right)_{x=0} \quad (26)$$

As shown by Eq. (11), the quantity ${}^*C_M-C_M$ will be expanded into the power series of x; i. e.

$${}^*C_M-C_M = {}^*C_M\frac{r_0}{r_0-x}\left(1+\sum_{j=1}^{l}B_j x^j\right) \quad (27)$$

Then, taking $l=10$, and employing the similar boundary conditions as shown by Eqs. (12) and (18), we can determine the coefficients B_j $(j=1,2,\ldots.,10)$ as the functions of δ'_M and r_0. Next, insertion of Eq. (27) into Eq.

(26) gives then an ordinary differential equation of first order, by which δ'_M is demonstrated; upon integrating this equation, we can obtain δ'_M as a function of t. The diffusion current can be easily found therefrom, and the result is

$$i_d = -709n^* C_M D_M^{1/2} m^{2/3} t^{1/6} \times \{1 - 34.9(D_M^{1/2} m^{-1/3} t^{1/6}) + 199(D_M^{1/2} m^{-1/3} t^{1/6})^2 - \ldots\} \quad (28)$$

Further the mean diffusion current is manifested by

$$\bar{i}_d = -608n^* C_M D_M^{1/2} m^{2/3} \tau^{1/6} \times \{1 - 30.5(D_M^{1/2} m^{-1/3} \tau^{1/6}) + 155(D_M^{1/2} m^{-1/3} \tau^{1/6})^2 - \ldots\} \quad (29)$$

In the case of amalgam polarography, since the diffusion layer is built up inside the mercury drop, the shielding effect due to capillary tube is expected to be of little importance, so that it may be ignored.

Comparison with Experimental Data

(A) Mean Diffusion Current.— Recently, in order to verify the validity of the revised Ilkovič equation, many investigators have carried out precise experiments, in which the drop time and the rate of outflow of mercury are variously changed with many capillaries of different characteristics; these experiments shows that Eq. (1) holds for the drop time longer than the critical drop time. And as for the numerical value of the coefficient A appearing in the second term of Eq. (1), the experimental results can be classified into the following two cases. I. e., Lingane with Loveride[11] and L. Meites with T. Meites[12] have found the result $A=31.5\pm4.6$, in the case with reductions of several ionic species. On the other hand, von Stackelberg and his collaborators[13] have found that $A=17\pm3$ agrees well with the results; it must be noted here especially that W. Hans and W. Jensch[14] have found that $A=16.1\pm1.5$ is adequate according to their elaborated studies on the polarographic reduction of hydrogen ion. The result observed by the former group of investigators, i. e. $A=31.5\pm4.6$, is in good agreement with Eq. (20), in which the shielding effect of capillary tube is ignored, while $A=17\pm3$ observed by the latter group is in fairly good harmony with Eq. (23), in which the shielding effect is taken into consideration. Which is then more adequate of these two numerical values proposed for the coefficient A? This will be judged by many accurate experimental studies in future.

As to the case of amalgam polarography, Strehlow and von Stackelberg[1] have experimented with cadmium amalgam, and shown that Eq. (29) holds when no phenomenon of "Spüleffekt" appears. Further, R. C. Turner and C. A. Winkler[15] have also confirmed the fact that in the case of lead and cadmium amalgam Eq. (29) agrees well with the experimental findings when m is lesser than 1.2 mg./sec.

(B) Current-Time Curve.—With variable ionic species, the diffusion current-time curve during one drop-life has been investigated oscillographically by Mc Kenzie,[16] Taylor, Smith and Cooter,[17] Mac Donald and Wetmore,[18] and Kambara, Suzuki and Tachi.[3] According to these experiments, although at the last two thirds of drop-life Eq. (22) holds semi-quantitatively, the current intensity at the first one third of drop-life is found to be very small; i. e. a perfect deviation from Eq. (22) is reported. The extraordinary small current flowing in the youth of drop-life will be explained by considering some or all of the following facts, that have been ignored in the above mathematical treatment. (1) In the present calculation, it is assumed that m is constant; but it is well known that m may become considerably small in the youth of drop-life, because the back pressure due to the interfacial tension must increase with the decreasing radius of drop.[19] (2) Owing to the electrolytic reaction at the preceding drop, the succeeding drop is dipped into the solution of lower concentration of depolarizer than that of bulk; i. e. there exists at the beginning of renewed drop-life already a diffusion layer around the drop.[20] (3) At the very infancy of drop-life the diffusion layer is so thin, that the rate-determining process depends not

(11) J. J. Lingane and B. A. Loveridge, *J. Am. Chem. Soc.*, **66**, 1425 (1944); *Anal. Chem.*, **21**, 52 (1949). Cf. *Reference* (2).

(12) L. Meites and T. Meites, *J. Am. Chem. Soc.*, **72**, 3686 (1950), **73**, 395 (1951).

(13) H. Strehlow and M. von Stackelberg, *Z. Elektrochem.*, **54**, 51 (1950) H. Strehlow, O. Madrich and M. von Stackelberg, ibid., **55**, 244 (1951).

(14) W. Hans and W. Jensch, ibid. **56**, 648, (1952).

(15) R. C. Turner and C. A. Winkler, *Can. J. Chem.*, **29**, 469 (1951), *Chem. Abst.* **46**, 2421 (1952).

(16) H. A. McKenzie, *J. Am. Chem. Soc.*, **70**, 3147 (1948).

(17) J. K. Taylor, R. C. Smith and I. L. Cooter, *J. Reserch Natl. Bur. Standards*, **42**, 387 (1949).

(18) J. J. MacDonald and F. E. Wetmore, *Trans. Faraday Soc.*, **47**, 533 (1951).

(19) I. M. Kolthoff and J. J. Lingane, "Polarography" vol. 1, p. 76 (1952) Intersci. Publ.

(20) L. Airey and A. A. Smales, *Analyst*, **75**, 287 (1950).

solely on diffusion velocity and the rate of electrode process must be taken into account at the same time.[21]

(C) Ratio of the Mean Diffusion Current $\bar{i}_d$ to the Maximum Value of Instantaneous Current $i_{max.}$ — According to the Ilkovič equation, the ratio $\bar{i}_d/i_{max.}$ becomes $6/7=0.857$. On the other hand, according to the present revised equations (22) and (23) this is given by

$$\frac{\bar{i}_d}{i_{max}} = \frac{6}{7} - 2.5(D^{1/2}m^{-1/3}\tau^{1/6}) + 45(D^{1/2}m^{-1/3}\tau^{1/6})^2 - \cdots.$$

E. g., employing the numerical values given by $D=0.72\cdot10^{-5}$cm.^{2}/sec.; $m=2.305$ mg./sec.; $\tau=3.488$ sec., it is found that $\bar{i}_d/i_{max}=0.851$, while the experimental value observed by Taylor, Smith and Cooter[17] is 0.813. Thus the revised equation approaches somewhat nearer to the experimental result than the original Ilkovič equation; neverthless neither of the two theories is seen to be in complete harmony with the experiments.

(21) T. Kambara and I. Tachi, This Bulletin **25**, 135, 281 (1952); H. Matsuda, Presented at the 5th Annual Meeting of Chem. Soc. of Japan, April 1952.

Summary

In order to integrate the MacGillavry-Rideal differential equation, representing the diffusion process at the dropping mercury electrode, the present author employed the von Kármán-Pohlhausen method. Thus the following revised expression of the Ilkovič equation showing the mean diffusion current is derived, in which the shielding effect due to the capillary tube is also treated theoretically.

$$\bar{i}_d = 608n^*CD^{1/2}m^{2/3}\tau^{1/6}\{1+20.6(D^{1/2}m^{-1/3}\tau^{1/6}) + 49.0(D^{1/2}m^{-1/3}\tau^{1/6})^2 - \cdots.\}$$

The analogous treatment is also applied to the case of amalgam polarography, and the following equation for the mean diffusion current is obtained.

$$\bar{i}_d = -608n^*C_M D_M^{1/2} m^{2/3}\tau^{1/6} \times \{1-30.5(D_M^{1/2}m^{-1/3}\tau^{1/6}) + 155(D_M^{1/2}m^{-1/3}\tau^{1/6})^2 - \cdots.\}$$

The author wishes to express his hearty thanks to Dr. T. Kambara for his steady encouragement and help.

Goverment Chemical Industrial Research Institute, Tokyo

Vat Dyes of Acenaphthene Series. V. Constitution of Dibromoanthanthrone (Indanthrene Brilliant Orange RK).[1]

By Toshio MAKI and Harukichi HASHIMOTO

(Received May 19, 1953)

A brilliant reddish orange vat dye of excellent fastness (light 7~8), commercially known as Indanthrene Brilliant Orange RK, has been obtained by direct bromination of anthanthrone. Among various methods of bromination it has been acknowledged in our laboratory that only the bromination in oleum (about 8% SO_3) in the presence of a little iodine gives the best result by the application of the least amount of bromine.[2] The crude product, however, contains a small quantity of orange brown impurity and, according to our experiment, the purification can be most effectively carried out by using 92~94% sulfuric acid, in which the pure reddish orange dibromoanthanthrone is insoluble.

The constitution of the dibromoanthanthrone was hitherto not at all experimentally determined and only by assumption 4, 10-dibromo formula (II-A) has usually been suggested,[3] but sometimes the other 2, 8-dibromo structure

(1) Read before the 5th Annual Meeting of the Chemical Society of Japan on April 5, 1952.

(2) G. P. 478738, *Frdl.* **16**, 1417; See also PB 84316-3473, *FIAT* **1313**, Vol. II, 90.

(3) Rowe, "The Development of the Chemistry of Commercial Synthetic Dyes (1856~1938), 87; PB 84316-3471.

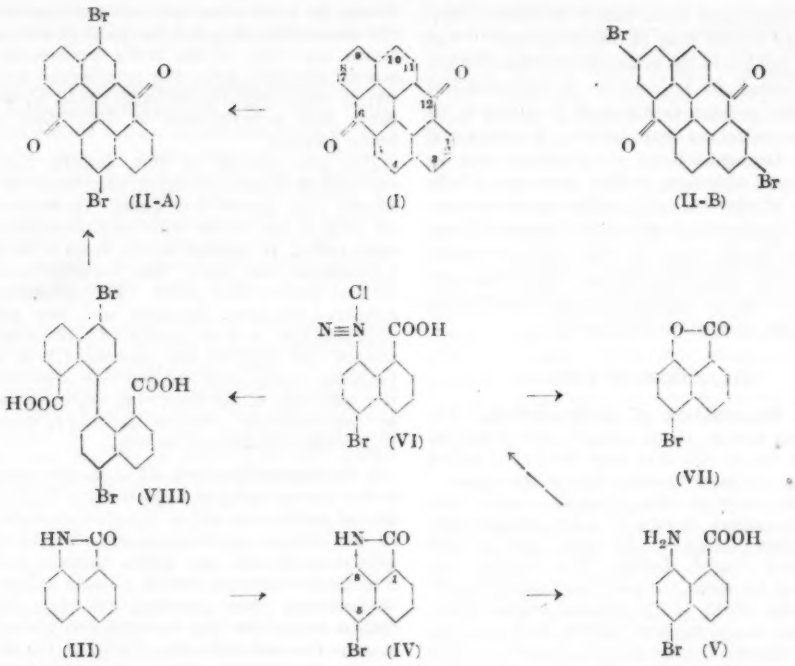

(II-B) is also adopted.[4]

We have now brominated naphthostyril (III) in acetic acid solution and found that the product is 5-bromonaphthostyril (IV) (m.p. 257°), which had been obtained by Eckstrand[5] from 5-bromo-8-nitro-1-naphthoic acid by reduction. The constitution of the bromonaphthostyril was further confirmed by converting it, after hydrolyzing the styril ring, into 5-bromo-8-hydroxy-1-naphthoic acid lactone (VII) (m. p. 193°) by diazotization and heating with dilute sulfuric acid. From this 5-bromonaphthostyril (IV) we have synthesized 4, 10-dibromoanthanthrone (II-A) via dibromodinaphthyl-dicarboxylic acid (VIII) by application of the diazo reaction and ring formation in conc. sulfuric acid analogous to the synthesis of anthanthrone from naphthostyril.[6] Our method of applying an ammoniacal solution of reduced copper sulfate and precipitated metallic copper was also useful for this diazo reaction.

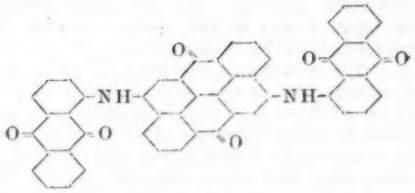

(IX)

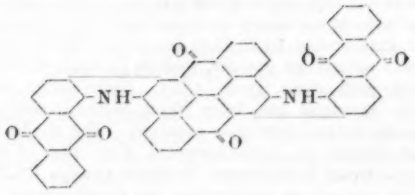

(X)

4, 10-Dibromoanthanthrone (II-A) thus synthesized is completely identical with the brilliant reddish orange dibromoanthanthrone (Indanthrene Brilliant Orange RK), which had been obtained by the direct bromination of anthanthrone. They are identical not only in their dyeings and color reactions, but in all other chemical reactivity and condensation products, for example in the formation of grayish violet di-α-anthraquinonyl-diimide

(4) *FIAT* **1313**, Vol. II, 83.
(5) Eckstrand, *J. prakt. Chem.* [2] **38**, 173, 281 (1888); *Ber.* **19**, 1136, 1139 (1886).
(6) T. Maki, H. Hashimoto and K. Kamada, *J. Chem. Soc. Japan, Ind. Chem. Section*, **55**, 483 (1952); See also PB 84316-8490; *FIAT* **1313**, Vol. II, 90.

(IX) and olive gray biscarbazole derivative (X).

Thus, as in the case of benzanthrone[7] the diphenyl residue in the molecule of anthanthrone is also found to be reactive to halogenation and in the present case p-and p'-position to the centre union are brominated. Indanthrene Brilliant Orange GK must similarly has 4, 10-dichloro structure. The formula (II-B) given in FIAT[4] is improbable as the constitution of Indanthrene Brilliant Orange RK, but may be rather that of the orange brown isomeric dibromoanthanthrone, which has been found by us as an impurity of the bromination and soluble in 90% sulfuric acid.

Experimental Part

Direct Bromination of Anthanthrone.—Anthanthrone (1.50 g., 1 mol. ratio)[6] was dissolved in 45 g. of oleum (8% SO_3) with 0.075 g. of iodine and 1.10 g. (2.8 atomic ratio, 70% of the apparent theory) of bromine was dropped down with stirring in about 30 min. at room temperature. It was then heated to 60° and kept at this temperature for 5 hours. The product was poured into ice water, the precipitate was collected, treated with 500 cc. of 1% aqueous sodium bisulfite, 500 cc. of 1% aqueous sodium carbonate and after acidification with dilute hydrochloric acid washed thoroughly with cold water. The yield of the crude product, a dark red orange powder, was 2.20 g. (96.8% of the theory). Found. Br, 38.40; calcd. for $C_{22}H_8O_2Br_2$ (II-A): Br, 34.44%. The crude dibromoanthanthrone (1 part), as a fine powder, was heated with 30 parts of 92% sulfuric acid on a water bath for 30 min. and allowed to stand over-night at room temperature. The black brown insoluble part was collected on a glass filter and when this was carried into water a brilliant red orange precipitate resulted, which was filtered and washed neutral. The yield was 72% of the crude product, corresponding to 69.7% of the theory from anthanthrone. Found: Br, 33.95; calcd. for $C_{22}H_8O_2Br_2$ (II-A): Br, 34.44%. Clear red orange powder, soluble in conc. sulfuric acid with clear green color. Hydrosulfite vat (IK) is violet red, from which brilliant reddish orange cotton dyeing is obtained. The shade of the dyeing is quite identical with that of the commercial Indanthrene Brilliant Orange RK[8].

In the above purification the concentration of sulfuric acid has unusually sensitive effect both on the yield of dye and on the shade of dyeing. Thus, the similar treatment with 94% sulfuric acid gives dibromoanthanthrone of the highest purity as the insoluble part, whose cotton dyeing is more clear and brilliant than that of the commercial dye, but the yield of the purification was 62% of the crude product. A dye almost identical with the commercial product, but of rather slightly yellowish shade, is obtained using 90% sulfuric acid in 84% yield of the crude product.

The part soluble in 90% sulfuric acid was obtained as a dark brown powder when the acid filtrate was poured into water. Its amount was ca. 14% of the crude dibromoanthanthrone. It dyes cotton in orange brown from a violet red hydrosulfite vat (IK); The solution in conc. sulfuric acid is dark green. This substance is a hitherto unknown impurity and our analysis indicates that it is an isomer of dibromoanthanthrone. We suggest the formula (II-B) as its probable constitution taking into consideration the reactivity of the remaining diphenyl residues in the molecule. Found: Br, 31.74; calcd. for $C_{22}H_8O_2Br_2$ (II-B): Br, 34.44%.

5-Bromonaphthostyril (IV).—To the solution of 5.08 g. (1 mol. ratio) of naphthostyril[6] in 51 g. of glacial acetic acid 4.55 g. (1.9 atomic ratio, 95% of the theory) of bromine, dissolved in 23 g. of glacial acetic acid, was added dropwise at 25° in 3 hours and agitated further 4 hours at the same temperature. After standing over-night the crystalline precipitate was collected and washed with water. Its yield was 6.19 g. (83.2% of the theory), m. p. 250.5~257.5° (corr.). By recrystallization from 10 parts of glacial acetic acid greenish yellow needles melting at 256.5~260.5° (corr.) were obtained. The yield was 76% of the crude product. Found: Br, 31.99; calcd. for $C_{11}H_6ONBr$ (IV): Br, 32.22%. This is identical with the 5-bromonaphthostyril (m. p. 257°) obtained by Eckstrand[5] from 5-bromo-8-nitro-1-naphthoic acid by reduction.

Conversion of Bromonaphthostyril into 5-Bromo-8-hydroxy-1-naphthoic Acid Lactone (VII).—The bromonaphthostyril (2.48 g. 1 mol. ratio), which had been obtained by the bromination of naphthostyril, was dissolved in 15 g. of 10% aqueous sodium hydroxide by heating on a water bath and diluted with 20 cc. of water. After ice cooling 0.69 g. of sodium nitrite (1 mol. ratio), dissolved in 4 cc. of water, was added to the solution and diazotized at 0° by giving 17 cc. of ice cooled 4 N hydrochloric acid and stirring further 20 min. The diazo solution was slowly poured into 100 g. of hot 20% sulfuric acid on a boiling water bath. The evolution of nitrogen gas ceased in ca. 20 min. and the color of the precipitate changed into yellow from brown. The heating was continued for further 30 min., then it was allowed to cool and the precipitate collected. Light brown powder of m. p. 182~187° (corr.), the yield was 2.24 g. or 89.9% of the theory. After crystallizing from 10 parts of glacial acetic acid 1.72 g. (76.8% of the crude product) of light brown needles melting at 191° (corr.) were obtained. By further recrystallization a sample of constant m. p. 193° (corr.) was obtained. Found: Br, 31.82; calcd. for $C_{11}H_5O_2Br$ (VII): Br 32.09%.

(7) T. Maki and Y. Nagai, *J. Soc. Chem. Ind. Japan, Suppl.* **38**, 491 B (1935); T. Maki, and T. Aoyama, *J. Soc. Chem. Ind. Japan, Suppl.* **38**, 636 B (1935); T. Maki and Y. Nagai, *Ber.* **70**, 1837 (1937); T. Maki and A. Kikuchi, *Ber.* **71**, 2031, 2036 (1938); T. Maki and A. Kikuchi, *J. Soc. Chem. Ind. Japan*, **50**, 141 (1947).

(8) The dyestuff content of the commercial Indanthrene Brilliant Orange RK (I. G.) was 75.5% and actual bromine content of this dyestuff was found to be 32.25%.

This substance was identical with 5-bromo-8-hydroxy-1-naphthoic acid lactone of Eckstrand[5] (m. p. 192°).

Synthesis of 4, 10-Dibromoanthanthrone (II-A) from 5-Bromonaphthostyril.—Two mol. ratio (5.0 g.) of copper sulfate ($CuSO_4 \cdot 5H_2O$) was dissolved in 20 cc. of water, 24 g. of 25% aqueous ammonia added and the solution was completely (rather to a faintly red color) decolorized by introduction of sulfur dioxide under ice cooling. To this solution of cuprous oxide complex, 10 g. of 25% aqueous ammonia and freshly precipitated metallic copper paste (1 mol. ratio)[9] were added.

5-Bromonaphthostyril (2.48 g., 1 mol. ratio), dissolved in 15 g. of 10% aqueous sodium hydroxide, was diazotized using 0.69 g. of sodium nitrite and 17 cc. of 4 N hydrochloric acid at 0° for 20 min., as in the case of the lactone (VII), and cooled to −5°. The diazo solution was poured into the copper solution at −5°, stirred at this temperature for 1 hour, allowed to rise in 2 hours to 20° and then stirred further 2 hours at 20°. After standing over-night the solution was filtered and dibromodinaphthyldicarboxylic acid (VIII) was precipitated from the filtrate with hydrochloric acid. Yield of a light brown powder was 1.69 g. This was dissolved without purification in 17 g. of conc. sulfuric acid, kept in a boiling water bath for 1 hour and after cooling poured into ice water. The precipitate was collected, washed neutral and heated with 300 cc. of 5% aqueous sodium carbonate in order to remove carbonate soluble impurities. The yield of dibromoanthanthrone, a dark red orange powder, was 1.41 g. or 60.8% of the theory. Further purification was carried out by heating 1 part of the finely powdered crude product with 30 parts of 92% sulfuric acid 30 min. in a boiling water bath and allowing to cool, when pure 4, 10-dibromoanthanthrone (II-A) was obtained as an insoluble precipitate. The Yield was 1.24 g. or 87.9% of the crude product. Found: Br, 33.94; calcd. for $C_{22}H_6O_2Br_2$ (II-A): Br, 34.44%.

It is a clear reddish orange powder, soluble in conc. sulfuric acid with clear green color and brilliant reddish orange cotton dyeing is obtained from a violet red hydrosulfite vat (IK). This synthetic 4, 10-dibromo compound is completely identical with the direct brominated dibromoanthanthrone in dyeings and all color reactions.

Condensation of Dibromoanthanthrone with 1-Aminoanthraquinone.[10]—One mol. ratio (1.00 g.) of the synthetic dibromoanthanthrone (Br, 33.94%), 2 mol. ratio (0.962 g.) of 1-aminoanthraquinone, 0.4 mol. ratio (0.069 g.) of precipitated cupric oxide and 2 mol. ratio (0.457 g.) of anhydrous sodium carbonate were boiled with 29.4 g. of nitrobenzene under reflux and stirring for 3 hours. Alcohol (15 g.) was added at 70° and after agitated for 30 min. the product was allowed to stand over-night. The precipitate was collected, washed with alcohol, heated with 200 cc. of dilute hydrochloric acid (1: 50) for 30 min. in a water bath, filtered and thoroughly washed with hot water. Yield was 1.534 g (94.1% of the theory). Violet gray powder, hardly soluble in organic solvents, soluble in conc. sulfuric acid with blue green color, from which violet precipitate separated by adding water. It dyes cotton grayish violet from a violet red vat (IK). The substance is completely free from bromine. Found: N, 3.49; calcd. for $C_{50}H_{24}O_6N_2$ (IX): N, 3.74%.

Dibromoanthanthrone (Br, 33.65%) obtained by the direct bromination of anthanthrone gave also quite the same di-α-anthraquinonyl-diimide (IX) both in yield and properties. Found: N, 3.57; calcd. for $C_{50}H_{24}O_6N_2$ (IX): N, 3.74%.

The carbazolation to the substance (X) was carried out by heating 1.00 g. of the diimide (IX) with 8.0 g. of anhydrous aluminium chloride and 2.0 g. of dry sodium chloride at 180° (oil bath temperature) for 6 hours and treating as usual with water and hydrochloric acid. The yield of the crude product was 1.00 g. It was then, as a dry fine powder, agitated with 10 cc. of 3.7% sodium hypochlorite solution and 5 cc. of water 1 hour at room temperature and 3 hours under reflux on a boiling water bath. The precipitate was collected, acidified with hydrochloric acid and then washed neutral. Yield was 0.94 g. Black powder, hardly soluble in organic solvents, soluble in conc. sulfuric acid with yellowish green black color, from which yellowish green black precipitate separated by the addition of water. Hydrosulfite vat (IK) is dark violet red and cotton is dyed in olive gray shade. Found: N, 3.71; calcd. for $C_{50}H_{26}O_6N_2$ (X): N, 3.76%.

The direct brominated dibromoanthanthrone gave also via the above diimide quite the same biscarbazole derivative (X) both in yield and properties. Found: N, 3.82; calcd. for $C_{50}H_{26}O_6N_2$ (X): N, 3.76%.

Dyestuffs Research Laboratory, Department of Applied Chemistry, Tokyo University, Tokyo

(9) Prepared from 2.5 g. of copper sulfate in 16 cc. of water by the addition of 0.03 cc. of turkey red oil and then 0.78 g. of zinc dust followed by decantation and washing.

(10) Compare with G. P. 485961, 487023, *Frdl.* **16**, 1422, 1424.

LETTER

A New Method of Measuring he Surface Tension of Liquids by Using the Vertical Liquid Jet

By Toshio IKEDA

(Received May 7, 1953)

Lately the present writer has derived the following theoretical approximation formula[1] for the "starting critical flow rate, V_c", the lowest flow rate necessary to change the tripping flow of the vertical jet into the laminar one:

$$V_c \doteqdot \pi r^{3/2}\sqrt{2\gamma/\rho} \qquad (1)$$

where r is the inner radius of the nozzle, γ, the surface tension of liquid, and ρ, the density of the liquid, and this formula proved to be accurate for the nozzle of the radius less than 0.05 cm. experimentally. Using this relation, one can calculate the tension of the surface that is newly developing.

Experimental Results

The liquids used were of the "chemical pure" grade. The capillary nozzle that was drawn out of a glass tube was about 10 cm. long, having the circular tube section of which inner and outer radii were 0.0375 and 0.1102 cm. respectively, and it was fixed in the direction of the gravity, joined by a short rubber tube directly to a glass siphon that was dipped into the liquid in a large glass reservoir (about 12 cm dia.).

The rate of the jet flow was regulated by changing the level of the liquid, or by sliding the reservoir upwards or downwards. The value of V_c was estimated from the volume of the liquid that ran down for ten seconds after the first development of the normal laminar jet flow, and was always accurate within 0.001 cc. per second at the room temperature.

The results are listed in Table 1. The values of γ calculated by the formula[1] and those of the static surface tensioa,[2] γ_0, for most liquids agree very well; but the reason why some anomalies, such as for water, chloroform, and carbon-tetrachloride, occur is yet to be known.

Therefore, this method could be used, if one were very careful for measuring the surface tension of liquids, the degree of accuracy here being at least 97 or 98 percent.

Department of Chemistry, the Liberal Arts Faculty, Shizuoka University.

Table 1

Liquids	Temp. °C.	ρ g./cc.	V_c cc./sec.	$\gamma_{calc.}$ dynes/cm.	γ_0 dynes/cm.
Water	15.5	0.998	0.282	88.7	73.23
Methyl alcohol	16.0	0.796	0.156	21.6	23.45
Ethyl alcohol	17.3	0.792	0.160	22.6	22.0
Aceton	19.5	0.792	0.160	22.6	23.14
Chloroform	15.6	1.50	0.110	20.2	26.9
Carbon tetrachloride	15.2	1.60	0.109	21.2	26.24
n-Hexane	16.8	0.660	0.150	16.6	17.76
Toluene	15.5	0.866	0.171	28.2	28.72
Chlorobenzene	17.2	1.108	0.159	31.2	33.84
Nitrobenzene	20.5	1.203	0.181	43.9	43.00

(1) T. Ikeda, *Reports of the Liberal Arts Faculty, Shizuoka Univ., Ser. B, No. 3*, 20 (1952).

(2) Landolt-Börnstein, "Phys. Chem. Tabellen", I, (1923) p. 208.

Eine Neue Methode zur Darstellung von Eisenrhodanidenlösung mit dem Kationenaustauschenden Harze

Von Masatoshi FUJIMOTO

(Eingegangen am 18. April, 1953)

Um eine chlor- und ammonium- (oder einwertigen metall-) ionenfreie Lösung von Eisenrhodaniden darzustellen, hat der Verfasser mit einem kationenaustauschenden Harze folgendes Experiment ausgeführt.

Die hier angewandte Darstellungsmethode beruht auf den zwei folgenden Reaktionen.

$NH_4SCN + HR \rightleftharpoons HSCN + NH_4R$ (Ionenaustausch),

$xHSCN + Fe(OH)_3 \rightleftharpoons H_{x-3}Fe(SCN)_x^{3-x} + 3H_2O$ (Neutralisierung bzw. Komplexbildung): HR (NH_4R) bedeutet ein kationenaustauschendes Harz von H- (NH_4-) Form und x, die Integrale, 3, 4, 5, und 6.

Der Versuch wird folgenderweise durchgeführt

1. Darstellung von Eisenhydroxyd—Auf gewöhnlicher Weise, d. h., aus einer Lösung des Eisensesquichlorides und verdünntem Ammoniakwasser, stellt man einen Niederschlag des Eisenhydroxydes dar und wäscht auf einem aschenfreien Filtrierpapier mit heissem destilliertem Wasser völlig aus, bis mit Silbernitrat keine Chlorionen in 5–10 ccm. des Filtrates nachgewiesen werden.

2. Darstellung der Rhodansäure durch Kationenaustausch—Man stellt eine Säule[1] des kationenaustauschenden Harzes (HR) auf, wodurch eine ungefähr 0.1- bzw. 0.3 M. wässerige Lösung des Ammoniumrhodanides stöchiometrisch in die freie Rhodansäure (HSCN) übergeführt wird.

3. Darstellung von Endprodukt—Die so hergestellte wässerige Lösung von freier Rhodansäure wird sofort auf den in einem Trichter (Abb. I) befindlichen Eisenhydroxydniederschlag hinzugefügt.—Sobald die Rhodansäure auf den Niederschlag zu tropfen beginnt, färbt sich die in C angesammelte Lösung schwarzblutrot.

Als Beispiel wird folgendes gezeigt

Mit einer Säule von Amberlite IR-120 (HR, 30 Maschen, 10 ccm. und 16 cm. lang), aus 50 ccm. von 0.15 M. Lösung des Ammoniumrhodanides und 5 ccm. von 0.42 M. Lösung des Eisensesquichlorides, hat der Verfasser eine klare schwarzrote wässerige Lösung von Eisenrhodanid gewonnen, in welcher nur kleinste Menge der Chlorionen (nach der Oxydation mit heisser konzentrierter Salpetersäure mit Silbernitrat geprüft) und der Ammoniumionen (mit Nesslerschem Reagens nachgewiesen) enthalten war.

Laboratorium der analytischen Chemie, Chemisches Institut der wissenschaftlichen Fakultät, Tokyo Universität, Tokyo.

(1) Vgl. H. Kakihana, Dieses Bulletin **22**. 242 (1949).